Study of Light Hypernuclei by Pionic Decay at JLab

M. Christy, C. Keppel, M. Kohl, Liguang Tang (*spokesperson*), L. Yuan (*spokesperson*), L. Zhu
Department of Physics, Hampton University, VA 23668, U.S.A.

N. Grigoryan, S. Knyazyan, A. Margaryan (*spokesperson*), L. Parlakyan, S. Zhamkochyan, H. Vardanyan
Yerevan Physics Institute, 375036 Yerevan, Armenia

O. Hashimoto, S.N. Nakamura (*spokesperson*)
Department of Physics, Tohoku University, Sendai, 98-77, Japan

P. Baturin, W. Boeglin, P. Markowitz, J. Reinhold (*spokesperson*)
Department of Physics, Florida International University, Miami, FL , U.S.A.

P. Bosted, K. de Jager, R. Ent, H. Fenker, D. Gaskell, T. Horn, M. Jones, J. LeRose (*spokesperson*), G. Smith, W. Vulcan, S.A. Wood
Thomas Jefferson National Accelerator Facility, Newport News, VA 23606, USA

E. Cisbani, F. Cusanno, S. Frullani, F. Garibaldi (*spokesperson*), M.L. Magliozzi
Istituto Nazionale di Fisica Nucleare, Sezione di Roma, Gr. Coll. Sanita', Viale Regina Elena 299, Rome, Italy

Ed.V. Hungerford
Department of Physics, University of Houston, Houston, TX 77204, U.S.A.

L. Majling
Nuclear Physics Institute, Academy of Sciences of the Czech Republic, Prague, Czech Republic

B. Gibson
Los Alamos National Laboratory, Los Alamos, U.S.A.

T. Motoba
Laboratory of Physics, Osaka Electro-Comm. University, Osaka, Japan

B. Hu, J. Shen, W. Wang, X. Zhang, Y. Zhang
Nuclear Physics Institute, Lanzhou University, China

D. Androic, M. Furic, T. Petkovic, T. Seva
Departments of Physics & Applied Physics, University of Zagreb, Croatia

A. Ahmidouch, S. Danagoulian, A. Gasparian
Department of Physics, North Carolina A&T State University, Greensboro, NC 27411, U.S.A.

G. Niculescu, I. Niculescu
Department of Physics, James Madison University, Harrisonburg, VA 22807, U.S.A.

M. Iodice
Istituto Nazionale di Fisica Nucleare, Sezione di Roma Tre, I-00146 Roma, Italy

G.M. Urciuoli
Istituto Nazionale di Fisica Nucleare, Sezione di Roma1, Piazza A. Moro, Rome, Italy

R. De Leo, L. Lagamba, S. Marrone
Istituto Nazionale di Fisica Nucleare, Sezione di Bari and University of Bari, I-70126 Bari, Italy

H.J.Schulze
Istituto Nazionale di Fisica Nucleare, Sezione di Catania, I-95123 Catania, Italy

J. Feng, Y. Fu, J. Zhou, S. Zhou
Department of Physics, China Institute of Atomic Energy, China

Y. Jiang, H. Lu, X. Yan, Y. Ye, P. Zhu
Department of Modern Physics, University of Science & Technology of China, China.

Abstract

We propose to use high precision monochromatic π^-'s from the unique two body mesonic weak decay of hypernuclei to investigate light Λ-hypernuclei with a variety of (Z, A) combination through identification of hyperfragments from strongly produced hypernuclear continuum (quasi-free production) in (e, K^+) electro-production. Technically, the combination of the CEBAF beam properties (intensity, structure, and minimized emittence), well defined momentum transfer direction in electro-production of Λ-hypernuclei, and the existing high precision spectrometer systems for K^+ tagging and decay π^- detection, makes the proposed experiment unique in obtaining information that may be impossible to obtain by other means and are needed to fully understand the YN interaction and to correctly describe nuclear matter with a strangeness degree of freedom. The high precision π^- spectroscopy allows us to (1) observe and determine precisely the Λ binding energies of ground states for a variety of light hypernuclei (hyperfragments) ranging from few body s-shell hypernuclei to numerous p-shell hypernuclei, (2) simultaneously investigate charge symmetry breaking (and Coulomb effect) by the differences of Λ binding energies for multiple mirror pairs, (3) search for long lived isomeric states through Λ-hypernuclei, (4) determine the neutron drip line limit with the insertion of a Λ particle (such as that through the study of heavy hyper-hydrogen), and (5) study of changes of nuclear structure and medium modification of baryons by measuring the lifetimes of possible isomeric states. These results include a unique set of bases with high precision for selection of correct theoretical models.

Though the resolution is limited, the most recent FINUDA result on π^- spectroscopy demonstrated that the principle and the concept of such an experiment are feasible. High resolution is essential for the success of this program with potential for new discoveries and findings. Currently, such an experiment can only be performed by CEBAF at JLab. There are three options for the experimental configuration: (1) Splitter and HKS coupled with HES in Hall A; (2) Septum and HRS coupled with Enge in Hall A; and (3) Splitter and HKS coupled with Enge in Hall C. All equipment are existing. Although option (1) is considered to be the best, it requires a relocation of the HKS and HES from Hall C to Hall A.

The proposal requests approval of its Phase I experiment with option (2) configuration in Hall A and ^{7}Li target. In addition, we request approval to transfer the previously approved 5 days test beam (PR08-012/PAC33) from Hall C to Hall A so that a feasibility test run with ^{7}Li target and a parasitic run with water target can be carried out during the Hall A hypernuclear experiment which is currently considered to be the last experiment in Hall A for the 6 GeV period.

1. Introduction

Since the first discovery of hypernuclei some fifty years ago in cosmic ray emulsion studies, hypernuclear physics, especially Λ-hypernuclei, has been used as an important way to extend the investigation of ordinary nuclear physics pertaining only nucleons (proton and neutron) to a new dimension with a new degree of freedom, toward a unified descriptions of the B-B interaction and structures of baryonic matter. A substantial gain in knowledge has been achieved by continued experimental and theoretical efforts. However, problems remain and can only be resolved by better precision, new techniques, new findings/discoveries, and improved theoretical understanding.

A fundamental YN interaction model was constructed based on our understanding of the NN interaction and the extremely limited YN scattering data. It relies on structure studies of the A=3~5 few body hypernuclei to verify its correctness. Extended theoretical and experimental investigations on more complicated hypernuclear structure with a wide range of charge (Z) and mass (A), different production mechanisms, and decays, are intended to understand the nature of the YN interactions and, in particular, the role of the Λ (with its known features in free space) in the strongly interacting many body medium. Study of light Λ hypernuclei plays a crucial role overall in hypernuclear physics.

The most influential data for A=3~5 systems came from emulsion experiments. One should note that none of the current leading YN models consistently agrees with experimental results for all measured few body systems in terms of Λ binding energies of ground states and first excited states. The questions for theory are how good is the current theoretical understanding of the YN interaction and how reliable are the current few body calculations. In terms of the experimental data, question is the reliability of the emulsion data analysis given the level of complications in terms of calibration and event recognition. Despite the remaining inconsistency puzzle, emulsion results are still considered to be the best or, more correctly speaking, the only available information on the ground state Λ binding energies for most of the few body hypernuclei as well as some of the p-shell ones which could not be produced directly by other production mechanisms in the past. Until now, the ground state Λ binding energies of most of the light hypernuclei ($A \leq 15$), except the drip line hypernuclei, come primarily from emulsion measurements of decades ago.

The right models for ΛN and Λ-nucleus interactions must be able to describe optimally the Λ binding energies and separations of the ground state and the low lying excited states as well as their spin/parity. Poor statistics and insufficient energy resolution made it impossible to carry out more detailed studies by emulsion experiments. The ground state spin/parity of many light hypernuclei is either not known or unconfirmed. Many puzzles remain unresolved. For instance, only 16 events were recognized and assigned to be from the ${}^{7}_{\Lambda}$He hypernucleus but are spread over various excited energies, i.e. no distinct peak could be seen. Thus, the ground state Λ binding energy could not be given by emulsion data (analysis of decay) until the recent observation of the ground state in the directly electro-produced mass spectroscopy from the JLAB E01-011(HKS) experiment. However, no low lying excited states were seen. Therefore, this system remains a puzzle and the debate about the existence of hypernuclear isomeric states may continue.

All the important observations of the excited states of light hypernuclei have come from high resolution γ transition spectroscopy, especially the measurements achieved in recent years by the HYPERBALL program (experiments done at KEK-PS and BNL-AGS). With excellent energy resolution, the observed transitions provide valuable information on hypernuclear structure leading to understanding of the spin dependent terms of the Λ-nucleus interaction. Most of the observed transitions appear surprisingly well described by simple shell model configurations. However, the latest results from $^{10}_{\Lambda}$B and $^{11}_{\Lambda}$B indicate that problems or puzzles remain; something new must be added, and additional information that may have to come from different observations is clearly needed. It is unclear if current puzzles arise from the existence of isomeric hypernuclear states that have never been clearly identified or whether the spin order assignment for the ground states is incorrect. One clear disadvantage for the γ spectroscopic program is that no ground state Λ binding energy could be determined. On the other hand, limited by the primary production reactions, either (K, π), (π, K), or (γ, K), only a handful of light hypernuclei could be produced and studied, far fewer than in emulsions which utilize weak or other observable decays from various subsequent fragmentations (hyper-fragments) from initially produced hypernuclei.

Mass spectroscopy programs were developed based on accelerator and modern counter technologies. They have significant advantages in terms of production rate, statistics, and the capability of observing states with a Λ in various orbits in a large mass range. In addition, governed by the difference in momentum transfer thus the formation probability, production reactions can selectively produce hypernuclei with different spins. Although the resolution has been greatly improved from a few MeV (experiments at CERN, BNL, and KEK) to a few hundred keV (experiments at JLAB), which enables one to measure deeply bound configurations with various spin-orbits and shell levels with improved binding energy precision, the resolution is still not sufficient to resolve the issues associated with ground-state doublets, low lying states separated only by a few hundred keV, and to confirm the spin order, which are quite essential. Discrepancies between experiments on mass spectroscopy and theory in terms of binding energies and cross sections are commonly seen.

Overall, experimental data on Λ-hypernuclei from emulsions, γ spectroscopy, and mass spectroscopy has led significant gains in knowledge in understanding the baryon strangeness in nuclear medium, thus beginning to uncover the secret of the YN interaction. However, some key ingredients appear still missing or undetermined. Theoretical studies have emphasized the importance of Λ-Σ coupling and ΛNN three body forces. They remain to be investigated in light hypernuclear systems which may not be produced easily by conventional primary reactions. Therefore, new findings and high precision data on key light hypernuclei are critically needed.

Since the 1970s, the development of the translational invariant shell model in an attempt to interpret substitutional hypernuclear states (core particle hole - Λ particle) has led to an important prediction: large yield of hyperfragments. When the mass of a hypernuclear state lies above a certain nuclear breakup threshold, the system breaks up into a lighter hypernucleus plus nuclear fragment(s). This mechanism has been successfully used to produce hypernuclei that are not easily produced directly from primary reactions (see later discussions). On the other hand, it also means that a variety of light hypernuclei can be formed from the Λ quasi-free continuum following strong nuclear cascade processes (Λ recapture followed by nucleon emission or fragmentation), including drip line hypernuclei. The quasi-free Λ can be viewed as a Λ beam

that strikes the residual nucleus in either a "virtual" process or a real re-scattering process from an independent target nucleus. It is a rich source for light hypernuclei with wide range of (Z, A). Accessing them directly from the continuum by using the currently available experimental techniques and facilities is either impossible or extremely difficult. Therefore, it has been ignored, except for a few applications in experiments that study hypernuclear weak decays. The only way to access these light hypernuclei, primarily their ground states, from the primarily produced continuum is through mesonic weak decay ($\Lambda \rightarrow \pi^- + p$) inside the nuclear medium, which has an energy release below that due to Fermi motion. This in-medium decay features high sensitivity to the spin/parity structure and dynamics of the ground state hypernucleus, and thus may provide crucial information that we do not have yet. However, high resolution and high initial yield of the continuum are the keys to studying π^- spectroscopy from the continuum.

The successful JLAB hypernuclear electroproduction programs in both Hall A and C not only established solid mass spectroscopy programs with much improved resolution and precision, but also unveiled an extremely important opportunity which is so unique that it may be achievable only by the experimental program at JLAB. The essential keys are (1) high yield of the continuum characterized by electro-production, (2) removal of the dominating background from the quasi-free Λ mesonic decay, and (3) high resolution (<200keV/c FWHM). The features of the CEBAF beam at JLAB combined with the well established and well understood experimental equipment and technique make such a program possible. To overcome the complication of spectroscopy mixing from multiple hypernuclei, the program must take a phased approach, starting from the lightest target. The well understood physics and spectroscopy will then become a solid reference for the next phase from which more complicated spectroscopy and physics can be extracted. The physics outcome will be rich and should lead to important new findings for hypernuclear physics in the near future. Overall, the major physics investigations and goals come from the following areas:

(1) Precise determination of Λ binding energies of a variety of ground state light hypernuclei;
(2) Determination and confirmation of ground state spin/parity;
(3) Direct measurement of Λ binding energy differences from multiple mirror pairs of light hypernuclei at ground state to investigate CSB and Coulomb effect;
(4) Searching for the neutron drip line limit of light hypernuclei – heavy hyper-hydrogen;
(5) Searching for evidence of the existence of isomeric hypernuclear states; and
(6) Studying impurity nuclear physics – B(E2) measurement and medium effect of baryons – B(M1) measurement through lifetimes.

Combining with information gleaned from other high precision hypernuclear studies, such as γ spectroscopy (EM level transitions) and mass spectroscopy (shell orbits and couplings), the nature of the YN and Y-nucleus interactions may be finally understood.

To avoid lengthy and perhaps disorienting descriptions of the physics motivation, the production of light hypernuclei from the quasi-free continuum and the experimental technique will be discussed first in Chapter 2 and 3, respectively. Then detailed discussions on more specific physics issues and outcomes will be given together with the expected pionic spectroscopy observations in Chapter 4. Some specific physics discussions and examples are already included in the previous E08-012 proposal. To reduce the length of this document, the

E08-012 proposal will be included as the appendix and the pre-existent specific discussions will be referenced.

2. Continuum phase of hypernuclei – A rich source of a variety of hypernucei

The hypernuclear continuum refers to the production of a quasi-free Λ in the continuum energy phase with respect to the residual nuclear core in a two body frame work. Using Λ electro-production as an example, the production of a hypernucleus or a free Λ is illustrated by diagrams in Fig.1.

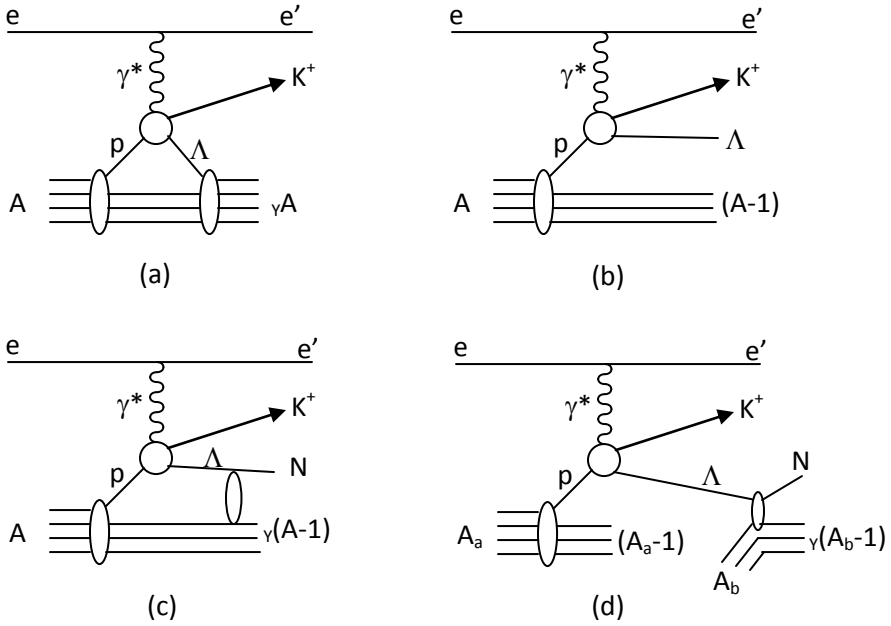

Figure 1. (a) Electroproduction of a bound hypernucleus; (b) A real quasi-free process in which the residual nucleus can be treated as a spectator; (c) A "virtual" process in which a Λ is considered to be "recaptured" to form a lighter hypernucleus while the excitation energy is released by ejecting nucleon(s); and (d) A real Λ re-scattering process off an unrelated target nucleus which forms a hyperfragment (a light hypernucleus) while releasing nucleon(s) or nuclear fragment(s) similar to (c).

The process as shown in Fig. 1(a) is the well known one which has been used by the JLAB Hall A and C experiments to measure the mass spectroscopy of bound hypernuclei electro-produced by the primary $A(e,e'K^+)_YA$ reaction. By absorbing the virtual photon on one proton from the target nucleus, the K^+ and Λ are associatedly produced. A bound hypernucleus is formed by coupling the Λ back to the residual core with various level and spin/parity configurations. Some well defined unbound states with sufficiently narrow decay widths may also be formed appearing above but close to the Λ particle emission threshold in the continuum region. This is similar to production by the (π, K) reaction in which the elementary electro-production is replaced by the strong strangeness associated production reaction or by the (K, π) reaction which replaces it with the strong strangeness exchange reaction. These different production reactions provide selectivity with respect to the spin configurations of the produced

hypernuclei because of differences in momentum and angular momentum transfers to the Λ. All current experimental investigations on spectroscopy of hypernuclei use these types of processes, depending on the facility.

The other three processes all contribute to quasi-free production. In mass spectroscopy they cannot be distinguished but form a summed distribution of masses or excitation energies starting from the Λ particle emission threshold with respect to the ground state core nucleus. This energy spectrum is more forwardly peaked and less pronounced when the reaction has small momentum transfer to the Λ, but broadened, strongly produced, and extended up close to about 400MeV in excitation energy above threshold when reactions with large momentum transfer are used, such as (e,e'K^+) at JLAB, (π, K) at BNL and KEK, or (K_{stop}, π) at FINUDA. However, they are rather different in terms of the final state produced since two of them can actually create a variety of lighter hypernuclei or hyperfragments. For the case as shown in Fig.1(b), the process represents free Λ production from nuclei. This production contributes no physics to hypernuclei and can be described well by Plane Wave Impulse Approximation (PWIA) calculations in which the Λ is treated basically as a free particle taking most of the momentum transfer from the primary reaction while the residual core is simply a spectator. This free Λ decays via the well known weak (ΔS=1) mesonic modes: $\Lambda \rightarrow \pi^- + p$ (64%) or $\pi^0 + n$ (36%). Other than the final state, the case shown as (d) in Fig.1 is just a part of the case (b) in the overall contribution to the quasi-free mass distribution; thus, they cannot be distinguished and separated in terms of PWIA calculations.

In contrast in the sense of the final state, in the processes shown in Fig. 1(c) and (d) the Λ interacts either with the residual nucleus in a "virtual" process or with an independent target nucleus in a real re-scattering process. A significant portion of these reactions can result in production of hyperfragments or lighter hypernuclei by emitting nucleon(s) or a light nucleus (d, t, ^{3}He, α, or others) or combinations. Since a Λ lives long enough (decaying only weakly) while the reaction process is rather fast, the final state light hypernuclei may be reached in multiple steps through a cascade process, i.e., a sequence of break ups. About 60 MeV above the Λ emission threshold, almost all channels for possible light (below target mass A) hypernuclei are open, i.e., the energy is above all the break up thresholds. Therefore, the continuum is a rich source of a variety of hypernuclei, or hyperfragments which have been known for a long time, including those held important but which have not been seen and thus remain undiscovered by other means [1]. For example, it has been known that a Λ increases the binding of nuclear cores which may be unbound and unstable; the neutron drip line may thus be increased. Study of highly neutron rich hypernuclei and a search for heavy hyper-Hydrogen were suggested even at early stage of hypernuclear physics [2] and their importance has been continuously emphasized [3, 4]. They may hold the answers to questions about the role of Λ-Σ mixing [5, 6] and the existence of long-lived isomeric states. The hyperfragment process from the continuum may become an effective source to access these important hypernuclear isotopes.

Only limited Λp scattering data exist, primarily the total cross sections that do not adequately constrain potential models [7]. Thus, precise predictions of the cross sections for hyperfragment production or for formation of lighter hypernuclei by Λ scattering off nuclear targets cannot be made reliably at the present time. However, study of lighter hypernuclei produced by the breakup of heavier hypernuclei (above nuclear break up thresholds) has already

used. As one of the examples, $^{5}_{\Lambda}$He (used recently to study extensively the non-mesonic weak decay) is commonly produced from the breakup of $^{6}_{\Lambda}$Li which is first produced by primary reaction, since no ^{5}Li or ^{5}He targets are available as direct production targets. More significantly, the ground states of many light p-shell hyperrnuclei, which could not be directly produced by primary reactions, were measured in emulsion by recognition of certain decay modes. On the other hand, light hypernuclei, such as $^{3}_{\Lambda}$H, $^{4}_{\Lambda}$H, and $^{5}_{\Lambda}$He, were found as hyperfragments from a wide range of nuclear targets (Li, Be, C, N, O, Ca, Ag, and Br) [22]. However, none of the past and current experiments can really utilize the rich continuum. Nevertheless, from the limited experimental information it is believed that roughly 10% of all quasi-free products from primary reactions convert into hyperfragments or lighter hypernuclei following the processes in (c) and (d) as shown in Fig.1, in which the process (c) is considered dominating. An extensive discussion on hyperfragments as well as references can be found in the previous E08-012 proposal, in Section 4.2 "Indirect production mechanism", attached in Appendix II.

3. Mesonic decay, π^- spectroscopy, and experimental technique at JLAB

3.1 Mesonic decay of hypernuclei

In free space, the Λ decays only via the well known weak mesonic decay modes as mentioned previously. The energy release is low, about 37.8 MeV. The ground state of hypernuclei can only decay via weak decay modes: non-mesonic ΛN→NN mode or the mesonic mode as in free Λ decay. However, since the nucleon momentum from mesonic decay is below the Fermi momentum, the nucleon from Λ mesonic weak decay will have to remain inside the nuclear system, i.e., reinserted back into the nuclear core. In general, for hypernuclear systems that have most of the inner nucleon shells closed, the mesonic decay channels are severely suppressed or Pauli blocked. Medium modification of the core due to the Λ may reduce such blocking effects so that the mesonic decay channels can remain significant up to a certain mass limit. It is proven both by theory and experiment that the mesonic decay rate for all p-shell hypernuclei ranges from 10-40% (see Fig.2 [8]). This makes the final states of nuclei from two body mesonic decay highly spin/parity selective depending on the spin/parity of the hypernuclear ground state [9, 10]. On the other hand, the emitted π's are monochromatic corresponding to the final states of the nuclei; for example, $^{3}_{\Lambda}$H (hypertriton) → ^{3}He + π^- with P_π=114.29 MeV/c.

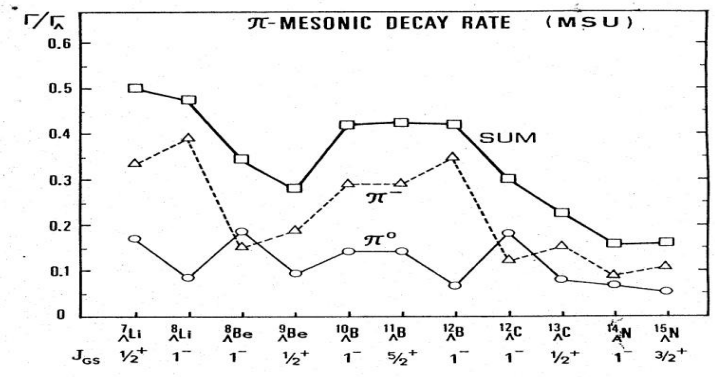

Figure 2. Ratio of the Λ mesonic decay rate in the nuclear medium to the free decay rate for the p shell hypernuclei [8].

Fig.3 shows an example of the predicted two body decay π^- momentum spectroscopy of the ground state of $^7_\Lambda$Li. Significant spectroscopic change will occur if the ground state $^7_\Lambda$Li spin is altered from $1/2^+$ to $3/2^+$. Until now, the spin/parity of many light hypernuclei is still unknown or unconfirmed. Predicted Λ binding energies or spin orders are often contradictory or vary widely vary with theory. More discussion on π^- decay spectroscopy in determining the spin order for puzzling low lying states of light hypernuclei can also be found in Section 2.4 "Impurity nuclear physics II" in the previous E08-012 proposal attached as Appendix II.

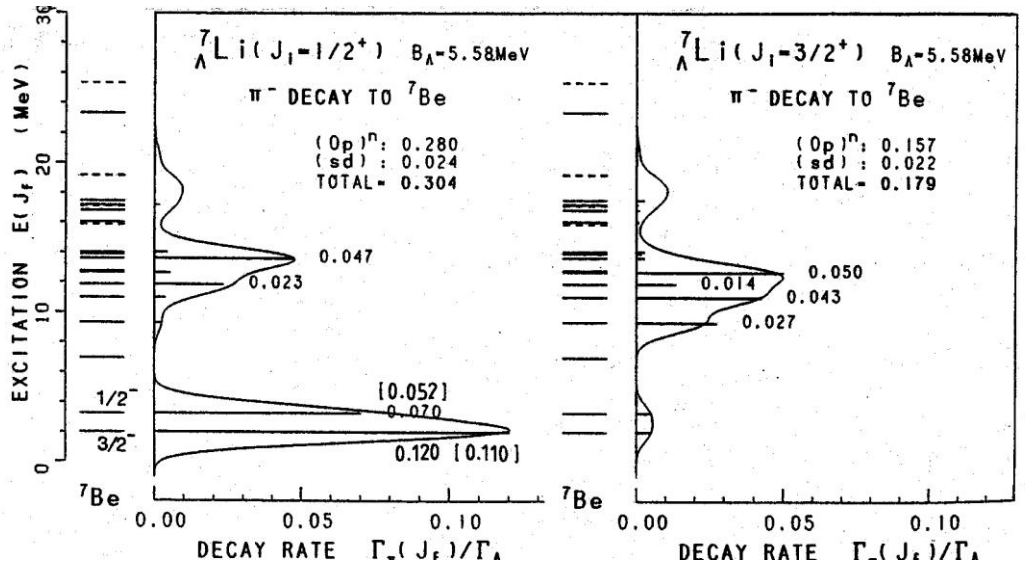

Figure 3. Relative π^- decay yields if the hypernuclear ground state has spin 1/2 (left) or 3/2 (right) [9].

Hypernuclei at higher excitation energy but below the nuclear breakup threshold decay dominantly via electromagnetic γ transitions to lower states and eventually cascade down to the ground state or to a low lying excited state that has significant stability against electromagnetic decay. Weak decay is then the only decay channel. Despite the success in recent high precision γ spectroscopy in the HYPERBALL experiments at KEK and BNL, there exist puzzles of missing γ transitions for certain expected low lying states of light hypernuclei and unexplained spectroscopy occurs [11, 12]. The debate over whether long-lived hypernuclear isomeric states exist is still ongoing. An isomeric state is considered to have a core structure that may add additional orthogonality thus reduces γ transition rate significantly. The possible $3/2^+$ and $5/2^+$ low lying excited states of $^7_\Lambda$He were interpreted as isomeric states, which although separated by about 1.7 MeV from the $1/2^+$ ground state could be stable enough against γ transitions to explain the wide spread of events in the binding energy [13]. More detailed discussions can be found in section 2.3 "Impurity nuclear physics I" in Appendix II. The current problems are clearly exacerbated by the incompleteness of our current understanding of YN and Y-nucleus interactions and lack of high precision data. The unique characteristics of mesonic decay of hypernuclei is obviously an effective tool to explore new mechanisms that we have not yet fully understood.

3.2 Decay π^- spectroscopy from hypernuclear continuum

As presented above, the monochromatic two body decay π^- is an effective tool with which to access the rich continuum as a source for new findings and new discoveries. However, it needs an experimental technique that can filter the background, has sufficient energy resolution to resolve the complex spectroscopy, and can reach the reasonable statistics needed to draw instructive conclusions. The experimental technique at JLAB will be presented in the next section. Here we focus on the hyperfragments that can be observed via two body decay π^-.

Three groups of charts are attached in Appendix I. They are made based on the production targets: ^{7}Li, ^{9}Be, and ^{12}C, for primarily produced ground states of $^{7}_{\Lambda}$He, $^{9}_{\Lambda}$Li, and $^{12}_{\Lambda}$B, respectively, from electro- or photo-production reactions. They list only the ground states of lighter hypernuclei that can be obtained by two body decay from the continuum of the primary hypernuclei by breakup or fragmentation. The first row is the two body decay of the primary hypernuclei without breakup. Number of breakup nucleons (in terms of n, p, α, and nuclei) is listed as well as the needed excitation energy (Q value) with respect to the ground state of the primary hypernucleus. A negative Q value means an energy shortage, i.e., the breakup channel can be open only from the continuum. The in-medium π^- two body decay mode and released energy Q are then listed. Some channels have both two body and three body breakup channels due to the nearby three body breakup threshold. Only those whose widths remain significantly narrow, i.e., not significantly broadened by the instability for three body decay, remain to be possibly observed in the spectroscopy but with reduced yield. The monochromatic momentum of the two body decay π^- is listed for every channel. Many of the hypernuclei are yet to be discovered or observed for the first time; thus, the π^- momenta of these hypernuclei are given based on assumed Λ binding energies suggested by theory. The listed widths of ground states depend on the stability of the two body decay nuclei as mentioned previously. 165keV/c FWHM momentum width (or a corresponding 130 keV FWHM energy width) is assumed for the π^- from all stable two body decays. Energy broadening is included for the channel that decays to unstable nucleus but with narrow width (< 1 MeV FWHM). An illustration of possible spectroscopy including excitation of decayed nuclei will be presented and discussed in the next Chapter, incorporated with physics outcomes and experimental approaches.

The richness of the continuum is clear but it is also obvious that there will be a great technical challenge in utilizing it. A variety of hypernuclei, highly interesting neutron rich hypernuclei, neutron drip line hypernuclei, and mirror pairs of hypernuclei which provide direct measurements of binding energy differences which can be used to study charge symmetry breaking as a function of isospin, can be observed. One can also notice that heavier targets provide more hypernuclear species but repeat all the lighter ones that lighter targets can produce. Reaction mass spectroscopy cannot resolve them. In principle, γ transitions from hyperfragments produced by the continuum exist in all γ spectroscopy experiments. Unfortunately, they are completely overwhelmed by the enormous nuclear γ transition background. Experiments must rely on gating on the events from the primary production, such as (K,$\pi\gamma$), and only in the bound region to reduce the challenge of huge accidental backgrounds [14].

To utilize the mesonic decay π^- as a tool, it is clear that momentum resolution better than 200keV/c FWHM is needed to resolve the complicated spectroscopy with potential mixing or

overlaping between hypernuclear species. High primary continuum production yield is needed to ensure reasonable statistics. Background must be sufficiently clean. A phased light to heavy approach is necessary to resolve the complication. Emulsion has the advantage on that because of the event recognition but suffers the problems of poor statistics and low energy resolution (~2MeV FWHM) (see binding energy spectra from emulsion presented in Fig. 10 in Chapter 3 in our E08-012 proposal attached in Appendix II). In addition, unique two body decay channel cannot be utilized by emulsion. Many highly interesting hypernuclei could not be found, because of the restriction that required good recognition of more than two charged particles in the final state. The complicated event recognition and selection often yielded conflicting results when selection conditions changed.

Recently, the FINUDA collaboration analyzed the existing $A(K^-_{stop}, \pi^-)_Y A$ data for two body π^- decay and its spectroscopy. The results showed fragmentation production from primary hypernuclei and π^- spectroscopy featured by the nature of the ground state of the decayed hypernuclei [15], thus providing an extremely encouraging demonstration of the technique and uniqueness of the future JLAB experimental program. Because of the very limited resolution (~7 MeV/c FWHM), the events must be selected in a way to isolate a single type of hypernucleus and suppress the contribution from quasi-free in order to reduce complexity.

Fig. 4(b) shows the π^- momentum spectroscopy from the ground state $^7_\Lambda$Li two body decay (i.e., $^7_\Lambda\text{Li} \rightarrow {}^7\text{Be} + \pi^-$). The events were selected from the primary production with excitation energy below ~4 MeV (Fig. 4(a)) to keep only the $^7_\Lambda$Li two body mesonic decay channel open. The π^- momentum distribution shows the excitation spectroscopy of ^{7}Be from two body decay. The dominant peak contains the $3/2^-$ ground state and $1/2^-$ first excited state (E_x = 0.429 MeV) of ^{7}Be (see Fig. 3). Although the resolution does not allow a precise measurement of the binding energy of $^7_\Lambda$Li, the spectroscopy provides evidence of the $^7_\Lambda$Li ground state spin/parity ($1/2^+$) [9]. In general, the events gate suppressed all other hypernuclear species in the spectrum.

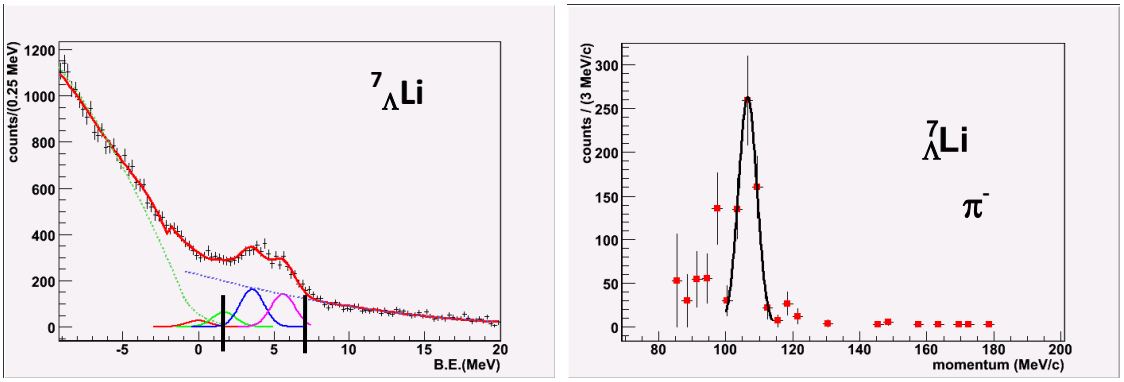

(a) (b)

Figure 4. (a) $^7_\Lambda$Li hypernuclei produced by the (K^-_{stop}, π^-) reaction. (b) $^7_\Lambda$Li hypernuclei obtained from two body decay: $^7_\Lambda\text{Li} \rightarrow {}^7\text{Be} + \pi^-$. Events were selected from the bound region of $^7_\Lambda$Li [15].

In a different case, Fig. 5(b) shows the π^- momentum spectrum from $^{11}_\Lambda$B two decay mesonic decay, i.e., $^{11}_\Lambda\text{B} \rightarrow {}^{11}\text{C} + \pi^-$, after a breakup of $^{12}_\Lambda\text{C}^* \rightarrow {}^{11}_\Lambda\text{B} + \text{p}$. The fragmentation

requires an additional 9.2 MeV excitation energy above the $^{12}_{\Lambda}$C ground state. The gate was specifically set to choose events having excited energy ranging from 8.7 to 13.6 MeV, i.e., around the p-shell excited states of $^{12}_{\Lambda}$C (Fig. 5(a)). Fig. 5(c) and (d) compare the π^- kinetic energy after subtraction of the quasi-free background to the theory prediction in terms of ^{11}C excitation energy [16]. With the $^{11}_{\Lambda}$B ground state spin/parity defined as $5/2^+$, in comparison to the $3/2^-$ ground state the $7/2^-$ excited state (Ex = 6.339 MeV) of ^{11}C was predicted to have almost equal (or slightly more) strength. The FINUDA result demonstrates the concept of hyper-fragments and decay π^- spectroscopy. The FINUDA resolution is clearly insufficient for further detailed analysis.

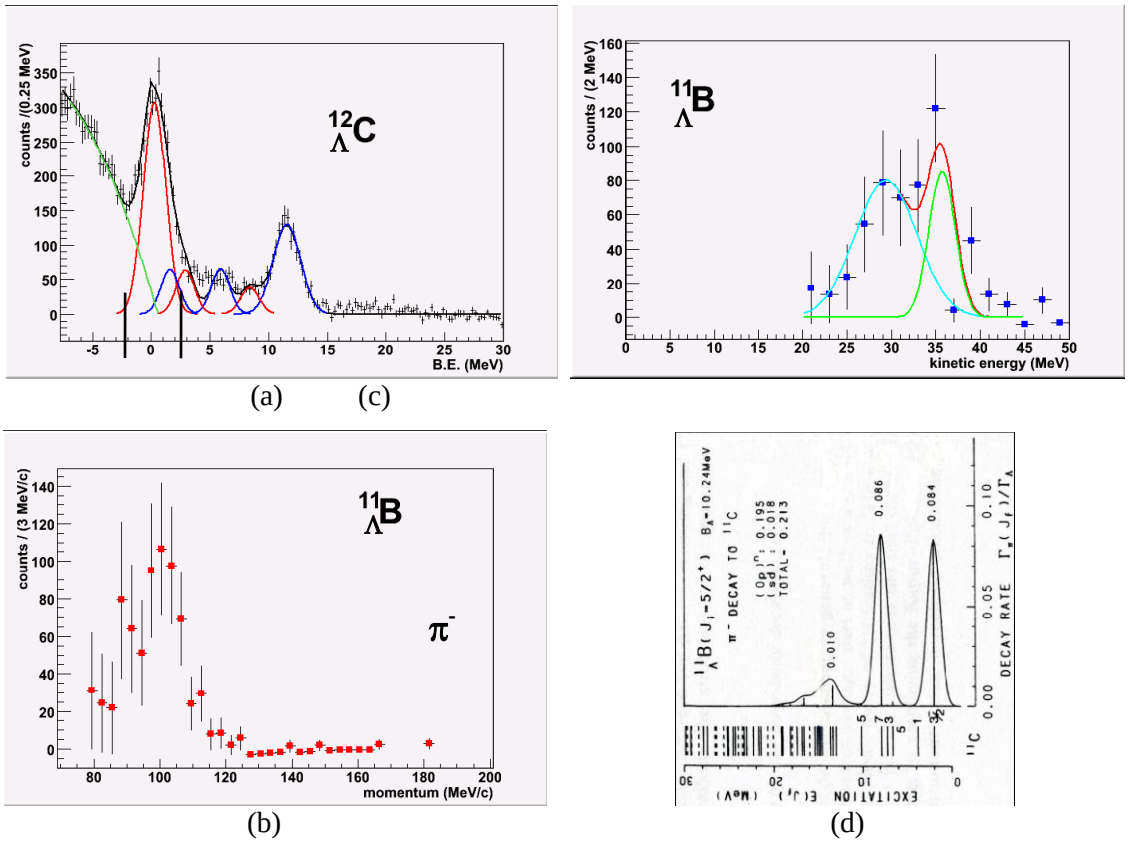

Figure 5 [15]. (a) $^{12}_{\Lambda}$C hypernuclei produced by the (K^-_{stop}, π^-) reaction; (b) π^- momentum spectrum for $^{11}_{\Lambda}$B obtained from breakup: $^{12}_{\Lambda}C \rightarrow {}^{11}_{\Lambda}B + p$ with events selected from the p-shell excitations of $^{12}_{\Lambda}$C; (c) π^- kinetic energy spectrum after quasi-free background subtraction; (d) theoretically predicted spectrum in terms of ^{11}C excitation energy.

The goal of the proposed JLAB experiment is to utilize the excellent characteristics of the CEBAF beam, the features of electro-production, and the well established experimental technique and equipment at JLAB to create a new experimental program that should be able to access the rich physics that can be offered by the continuum with potential for new discoveries/findings and new precision results which will be extremely valuable.

3.3 The experimental technique for the proposed JLAB experiment

The proposed JLAB experiment can (1) have a momentum resolution better than 200 keV/c FWHM for π^- (sufficient to separate states ~130 keV apart); (2) observe two body hypernuclear mesonic decay π^- clearly separated from background quasi-free Λ decay π^-; and (3) have a high enough primary production yield to secure sufficient statistics with small systematic error (<±20keV). These are the key conditions for study of hyper-fragments from the continuum to obtain high precision results that provide stringent limits on generation of correct theory.

3.3.1 Experimental configuration

There are three experimental configuration options: (1) Splitter and HKS coupled with HES in Hall A; (2) Septum and HRS coupled with Enge in Hall A; and (3) Splitter and HKS coupled with Enge in Hall C. All equipment exists. The basic experimental technique is the same for all three options. Comparison of these options will be detailed later and here we use the Option (1) to illustrate the general technique and physics features of the proposed experiment. This configuration is quite similar to the HKS (JLAB E01-011) experiment for hypernuclear mass spectroscopy, see the illustration in Fig. 6. The major differences are (1) removing the electron arm and not tagging on the scattered electron and (2) mounting the new high resolution electron spectrometer (HES), which was built for the HKS/HES (JLAB E05-115) experiment, at 110 degrees with respect to the beam direction and with face normal to the thin target foil to detect the decay pions.

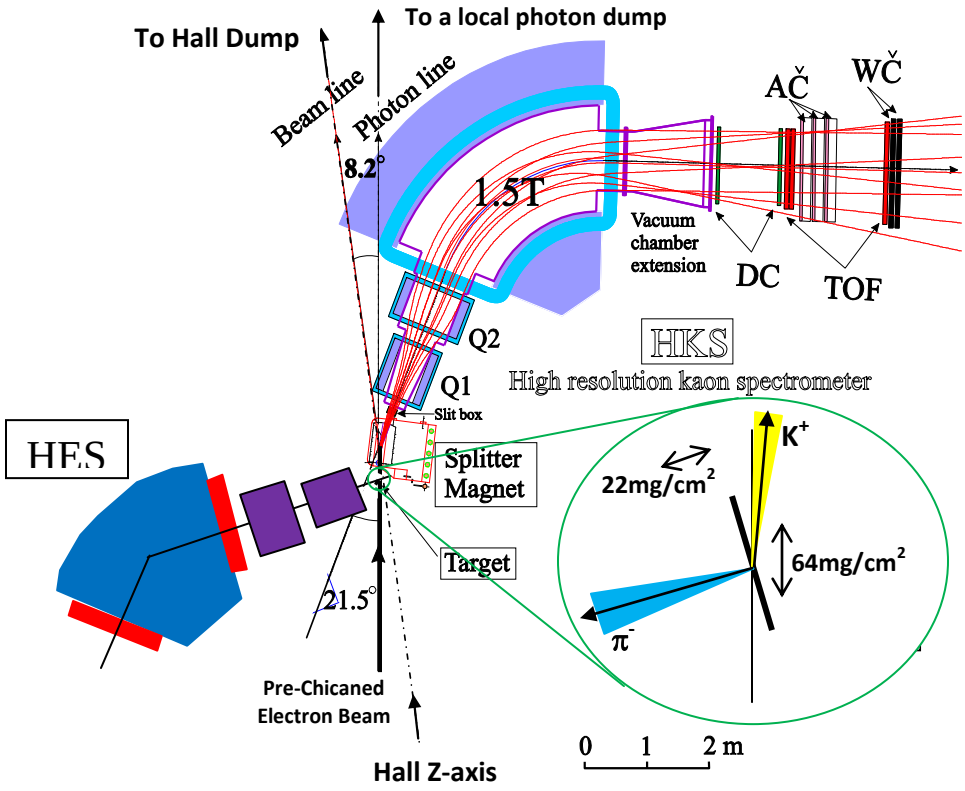

Figure 6. Schematic top view of the experimental configuration for the JLAB hypernuclear decay pion spectroscopy experiment (Hall A).

The experimental target must be thin. The thickness depends on the type of target to be used and the amount of target straggling energy loss allowed. Thus it varies. For example, in case of a ^{12}C target, the thickness is only 22mg/cm^2 (0.1mm). It is tilted to 20 degrees with respect to the beam so that the production thickness is about 64mg/cm^2. The standard luminosity used for the HKS experiment in case of such a ^{12}C target is 30μA×100mg/cm^2. With the same luminosity, this experiment will use a 47μA beam current to have the same hadron rates in the HKS - the kaon arm. The tilted target plane ensures the minimum target thickness in the direction of decay pions. The average energy shift (kinetic energy loss from target straggling) is about 40keV (63keV/c in momentum) for 116 MeV/c π^-, for instance. This uncertainty mainly contributes to the resolution for separation of individual states but small to the precision in determination of Λ binding energy after the mean shift is known (see detailed discussion in the E08-012 proposal section 5.3 in Appendix II).

The configuration for the kaon arm is almost the same, i.e., Splitter + HKS combination to detect kaons at forward direction. The central scattering angle is 6 degrees and the solid angle acceptance is reduced to 12 msr from 15 msr because of the target relocation upstream by about 25 cm. This relocation is to move the target out of the magnetic field of the Splitter and ensure high momentum resolution of the HES. This reduction can be recovered by increasing the beam current to 60μA (in the case of the ^{12}C target). Since this experiment does not have a high accidental trigger rate, the maximum beam current is not limited as in the HKS experiment. In this case, the HKS will have the same hadron rates or yield as that measured by the HKS experiments. The same standard detector system will be used to identify kaons and to reconstruct the kaon momentum, scattering angle, and production time (with the CEBAF pulse width 1.67ps and pulse separation of 2ns). The HKS momentum resolution is known to be 2×10^{-4} FWHM and the angular resolution is about 2.5mr FWHM. The detected K^+ gates the strangeness production. The typical time resolution for reconstructed production time is about 130ps (r.m.s.). The performance of this kaon spectrometer system has been well tested by the previous experiment (E01-011).

The scattered electrons will not be tagged in this experiment in order to gain a higher physics yield rate (see later discussion on the yield rate).

The HES spectrometer will be used to detect the decay pions from two body mesonic decay. The central momentum is 116 MeV/c with ±20% acceptance so that the momentum range will be from 92.8 MeV/c to 139.2 MeV/c. This covers the monochromatic two body decay pions from all the Λ-hypernuclei that can be produced from the continuum through the fragmentation process. The momentum resolution of the HES with its originally designed momentum range is also 2 ± 10^{-4} FWHM, same as that of the HKS. The average lifetime of all light hypernuclei is about 240 ps. The momentum transfer in the beam direction to the primary hypernuclei and the angular change due to fragmentation will distribute the decay point in an extended space region instead of a point spot on target. Within the range of momentum transfer in the primary reaction and the kinetic energy released from fragmentation, this extended spot remains small (<0.3mm in the transverse direction of the HES central z-axis). With a reduced momentum range and a spread of decay position, the resolution is reduced to 6 ± 10^{-4}. For central momentum of 116 MeV/c, this means a 70keV/c FWHM resolution. Thus, the overall combined resolution is dominated by the target straggling loss and about 165keV/c FWHM, sufficient to separate states by ≥140 keV/c. The systematic error in terms of binding energy will be

dominated by the calibration method on the HES central momentum. The goal of the binding energy precision of this experiment is ±20keV. The solid angle acceptance is 20msr. Considering a uniform 4π distribution of the decay pions, the acceptance is 0.16%. Finally, the precision on the measured decay time is about 100ps (r.m.s.). Lifetime of hypernuclei can be measured. The coincidence time gate between K^+ and π^- is 2ns.

The same pre-chicaned beam (~2.2 GeV) will be used so that the beam will go directly to the hall dump after being bent by the Splitter magnet. A low power local dump will be used in the hall as a photon dump. Table 1 is a summary of the general experimental parameters.

Table 1 General experimental parameters

Beam energy	~2.2 GeV
Luminosity (beam current × target thickness)	60 μA × 64 mg/cm^2
Target thickness toward HES	22 mg/cm^2
Target tilt angle	20^o
Average energy shift due to target straggling loss	~40 keV
Momentum resolution due to target straggling	61 keV/c (r.m.s.)
Experimental targets	Phase-I: ^{7}Li; -II: ^{9}Be; and -III: ^{12}C
HKS central angle (horizontal)	6^o
HKS momentum and acceptance	P_o = 1.2 GeV/c and ±12.5%
HKS solid angle acceptance	12 msr
HKS (K^+) momentum resolution	2×10^{-4} FWHM
HKS scattering angle resolution	2.5 mr FWHM
HKS production time resolution	130 ps (r.m.s.)
HES central angle (horizontal)	110^o
HES momentum and acceptance	P_o = 116 MeV/c and ±20%
HES solid angle acceptance	20 msr
Detection efficiency	80%
π^- survival rate	~32%
Decay pion acceptance	0.16%
HES (π^-) mom. resolution w/ extended "beam spot"	6×10^{-4} FWHM
HES scattering angle resolution	6 mr FWHM
HES decay time resolution	100 ps (r.m.s.)
Overall decay pion momentum resolution	165 keV/c FWHM
Absolute energy scale precision	~ ±20 keV

3.3.2 Backgrounds

The background in the decay π^- spectroscopy comes from three distinguished sources: (1) accidental K^+ and π^- coincidences (accidentals); (2) in-medium produced free Λ decay; and (3) π^- from three body decays. They will be evaluated based on known experimental data or the best available knowledge.

3.3.2.1 Accidentals

The K^+ singles rate in the HKS was measured during the HKS (E01-011) experiment. With the designed luminosity for this experiment, the K^+ singles rate (from all strangeness production channels dominated by the Λ, $\sum^o$, and $\sum^-$) will be ~200 Hz in HKS. At 110 degrees, the maximum π^- singles rate (dominated by the nuclear pions) can be ~10^3 Hz in HES. The coincidence time window in offline analysis is 2 ns (2×10^{-9} sec). This gives the estimated accidental rate as:

Acc. Rate = $200 \times 10^3 \times 2 \times 10^{-9} = 4.2 \times 10^{-4}$ Hz, or 1.52 counts/hour.

This accidental background will be uniformly distributed over the 46.4 MeV/c HES momentum acceptance. If a 40 keV/c bin size is assumed, there will be 1160 bins. The accidental rate will then be 0.0012 counts/bin/hour, thus this background is negligible.

3.3.2.2 In-medium free Λ decay

The in-medium produced free Λ decays via mesonic modes only. The π^- decay is a potential source of background. Since the Λ does not have charge, it decays mainly in-flight. As discussed previously in Chapter 2 and referred to in the case illustrated in Fig. 1(b), this free Λ takes all the momentum transfer and leaves the core nucleus as a spectator. Electro-production of quasi-free Λ's was studied by the early Hall C K^+ production experiment (Ben Zeidman et al.). The current Hall C SEMC simulation code includes this free Λ in-medium production. With this code and the given K^+ momentum and scattering angle ranges, simulation on the decay π^- momentum and angular distributions was done. Due to momentum transfer direction being limited at the forward direction, the decay π^- momentum and angle are strongly correlated in the Lab coordinate system.

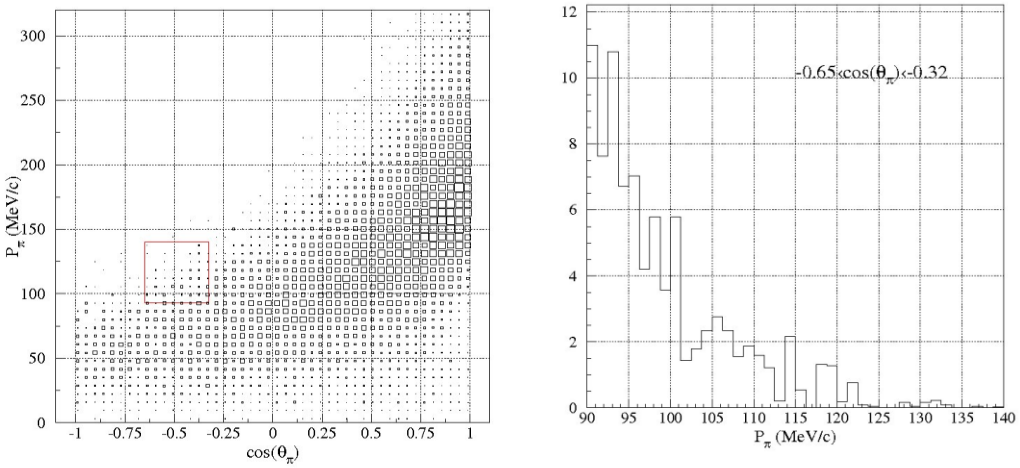

Figure 7. Left: Correlation between momentum and lab angle for decay pions from in-medium produced free Λ's. Right: Momentum distribution of the survived pions. The survival rate is one out of 50,000 quasi-free Λ's with K^+ detection required and assumption of 100% π^- decay.

Fig. 7(left) shows the correlation between momentum and angle with respect to the electron beam direction. The red box shows the momentum range corresponding to the two body decay of hypernuclei and maximum possible angular coverage range. The HES can easily be placed

outside of this distribution because of the momentum and angular selections for the K^+ from the HKS. Fig. 7(right) shows the momentum distribution for the surviving pions from the total quasi-free Λ's that were generated. The ratio is extremely small: 2×10^{-5}. Since the π^- channel is only 64%, the overall survival rate is thus only 1.3×10^{-5}. Therefore, this background is completely swept away by Lorentz boost when K^+ coincidence is required.

3.3.2.3 π^- from three body decay

The π^-'s can also come from three body decays of hypernuclei, such as those primary ones listed in the tables in Apendix I. The momentum of three body decay π^-'s ranges from zero to the maximum P_{max}, with a typical three body phase space distribution. The P_{max} depends mainly on the masses of hypernuclei and the decayed nuclei. In case of the $^7_\Lambda$He continuum, the lowest P_{max} (~102 MeV/c) is from the $^5_\Lambda\text{He} \rightarrow {}^4\text{He} + p + \pi^-$ decay, and the highest P_{max} (~139 MeV/c) is from the possible $^5_\Lambda\text{H} \rightarrow {}^4\text{He} + n + \pi^-$ decay. The continued momentum distributions from various hypernuclear three body decays super position together to potentially form a continued background in the momentum range where monochromatic momentum of two body decay π^-'s are interested. Fig. 8 shows the three body π^- momentum distribution from the $^4_\Lambda\text{He} \rightarrow {}^3\text{He} + p + \pi^-$ decay. Due to high resolution and narrow width of the hypernuclear states, the momentum bin size will be as small as 40 keV/c. For 10,000 three body events, the statistically averaged maximum height of the distribution is only 8 counts.

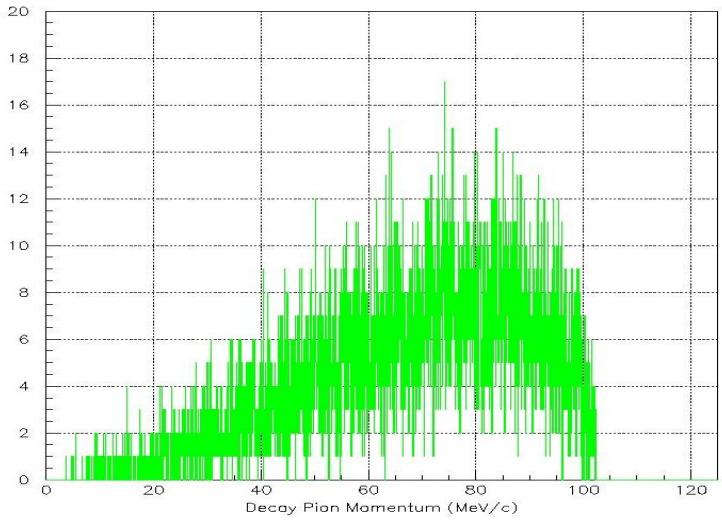

Figure 8. The three body decay π^- momentum distribution from the $^4_\Lambda\text{He} \rightarrow {}^3\text{He} + p + \pi^-$ decay. Total of 10,000 events were generated and the bin size is 40 keV/c. The P_{max} is 103.15 MeV/c and peak is around 80 MeV/c.

The total combined three body distribution will come from the primary channels plus the channels originated in two body decays in which the nuclei are excited over one nucleon emission threshold. Each individual three body distribution will have the same shape as shown in Fig. 8 for $^4_\Lambda\text{He} \rightarrow {}^3\text{He} + p + \pi^-$, except the scale stretches corresponding to the specific P_{max} (ranged from 102 to 139 MeV/c). The combined spectrum from all three body decays will be

superposition of all the decay channels and the total is considered to be comparable to the overall combined yields of all two body π^-'s, thus about 2,500 – 5,500 overall counts from the proposed three targets presented later may be expected. This background is cut off at the lower end of the HES momentum acceptance and has in general a shape that smoothly raises from 0 counts around 139 MeV/c at the higher end to a statistically averaged height of about 4-7 counts at the lower end of the acceptance, if a 40 keV/c bin size is assumed. Although this background is not negligible, it is quite small (due to high resolution which allows fine bin size), especially on the higher momentum option of the spectroscopy.

In conclusion for the background, the two body decay pion spectroscopy from the proposed JLAB experiment is clean from any type of backgrounds. Such cleanliness results from (1) the highly defined beam or momentum transfer direction; (2) high momentum resolution; and (3) a tiny time coincidence window. Therefore, clean spectroscopy and well formed sharp states from two body decay are expected.

3.3.3 Yield rate

From the JLAB Hall C HKS (E01-011) experiment using the (e,e'K^+) reaction, the yield rates for the bound $^{7}_{\Lambda}$He, $^{9}_{\Lambda}$Li, and $^{12}_{\Lambda}$B hypernuclei (from targets ^{7}Li, ^{9}Be, and ^{12}C) as well as for the quasi-free productions were measured. The comparison of the yield rates of the quasi-free production with the scattered electrons tagged to the measured K^+ singles rates (without the e' tagging), the tagged rates with the electron arm used by the HKS experiment is about 0.21% of the untagged primary production rates. The contribution from the production of bound hypernuclei is known to be less than 1%, thus, the measured K^+ singles rate is considered to be from the quasi-free production only. On the other hand, the calculated ratio of the integrated virtual photon flux within the same angular and momentum acceptances over the total flux is 0.23% which is in a reasonable agreement with the measured ratio. Therefore, a gain factor of about 476 is expected when the scattered electron tagging is not used in this experiment.

3.3.3.1 The $^{7}_{\Lambda}$He system with ^{7}Li target

The measured yield of the ground state $^{7}_{\Lambda}$He was 4.5 counts/hour. Since the target straggling in the ^{7}Li is much smaller than ^{12}C due to a much longer radiation length, the target thickness can be increased to correspond to the same level of target straggling energy loss, as we did in the HKS experiment. The luminosity of 30 μA × 128 mg/cm^2 (beam direction) will be used and it is the same as that used in the HKS experiment. Thus, the production rate of the initial K^+ tagged $^{7}_{\Lambda}$He ground state will be 4.5 × 476 = 2142 counts/hour.

Assuming $\Gamma_{\pi^-}/\Gamma_{\Lambda}$ = 0.3, the HES acceptance to be 0.16%, 80% detection efficiency, 32% average π^- survival rate, and running time to be 1000 hours, we will have a total of:

$$2142 \times 0.3 \times 0.0016 \times 0.8 \times 0.32 \times 1000 \approx \underline{263 \text{ counts}},$$

for the $1/2^+$ ground state of $^{7}_{\Lambda}$He in the π^- decay momentum spectrum. This is the two body decay of the primarily produced hypernuclear ground state. Since the momentum resolution is σ = 70 keV/c, the statistical error for the binding energy determination can still be smaller than ±5 keV. The directly produced $^{7}_{\Lambda}$He is an important reference for the rest of the hyperfragments in

the entire spectroscopy investigation. Thus, the assumed beam time is to ensure the statistics for a meaningful result for this specific hypernucleus.

For the quasi-free Λ production, the K^+ singles rate is known to be 115 Hz from the HKS experiment with the proposed luminosity. Assuming 10% of all quasi-free events results to various hyperfragments, which we assume here the same average π^- decay branching ratio (0.3), the same acceptance (0.16%), the same detection efficiency (80%), and the same survival rate (32%), we should have:

$$115 \times 0.1 \times 0.3 \times 0.0016 \times 0.8 \times 0.32 \times 1000 \times 3600 \approx 5{,}087 \text{ counts},$$

for the overall accepted hyperfragment two body π^- decay events. Furthermore, the nuclei emitted from the two body decay can be selected excited states; thus, the spectroscopy can be used to determine the spin/parity order of the ground states of hypernuclei. If we assume only 30% of the decay π^- events belong to the ground state of the emitted nuclei (with 20% to the excited states and 50% to one nucleon emission thus becoming three body decay in final state), the total number of events resulting in nuclear ground states that correspond to the hyperfragment ground states will be about 1,526 counts.

The yields of various hyperfragments vary and there are no solid experimental results available other than general expectations. Therefore, for estimation and illustration purposes, we temporarily assume equal yield for all types. In case of the $^{7}_{\Lambda}$He system, there are five fragments expected as listed in the table in Appendix I. We then anticipate an average yield of 1,526/5 ≈ 305 events per hyperfragment ground state.

3.3.3.2 The $^{9}_{\Lambda}$Li system with ^{9}Be target

The luminosity used in the 2005 HKS experiment in testing the $^{9}_{\Lambda}$Li yield was 190mg/cm^2 × 20 μA with 60 hours of beam time. To get the same yield rate with reduced target thickness, this experiment will have to use 120mg/cm^2 (beam direction) × 32 μA, which is similar with that used in the HKS experiment. The total number of observed events in the bound region was 250 counts; thus, the rate is 4.2 counts/hour. The yield of bound states in electro-production for $^{9}_{\Lambda}$Li is dominated (by a factor of ~4) by the first excited $5/2^+$ (spin-flip) state instead of the $3/2^+$ ground state. In addition, the two additional ($1/2^+$ and $3/2^+$) excited states are expected to have similar cross sections in comparison to the ground state [17]. In terms of mesonic weak decay, this comes mainly from the ground state while these excited states are stable against breaking up into hyperfragments so that they decay primarily via γ transitions to the ground state. Therefore, here all the yield from the bound region can be included in the estimate. With the same yield increase factor, without tagging on scattered electrons, the effective K^+ tagged $^{9}_{\Lambda}$Li yield will be 1999 counts/hour. Since this target can take extra beam power, the beam current can be increased to 64 μA to double the yield rate to 4,998 counts/hour.

$\Gamma_\pi/\Gamma_\Lambda$ = 0.2 can be assumed with the same the HES acceptance, detection efficiency, survival rate, and running time, thus we will have total of:

$$3{,}998 \times 0.2 \times 0.0016 \times 0.8 \times 0.32 \times 1000 \approx \underline{327 \text{ counts}}$$

for the ground state of $^{9}_{\Lambda}$Li. The statistical error in binding energy will be at the level of ±4 keV.

The measured K^+ single rate is 140 Hz and it will be increased to 280 Hz when the beam current increases to 64 μA. Using the same estimate as that done for the $^{7}_{\Lambda}$He continuum, the overall hyperfragment yield with two body π^- detected is expected to be:

$$280 \times 0.1 \times 0.2 \times 0.0016 \times 0.8 \times 0.32 \times 1000 \times 3600 \approx 8{,}258 \text{ counts.}$$

Using the same 30% ratio for the ground states of hyperfragments, the overall yield for ground states of hyperfragments will be about 2,477 counts.

From the $^{9}_{\Lambda}$Li continuum, the hyperfragments seen from the $^{7}_{\Lambda}$He continuum will be seen again. In addition, there will be five additional possible light hypernuclei from the fragmentation process. Thus, there will be total of 11 light hypernuclei (hyperfragments excluding the primary $^{9}_{\Lambda}$Li) potentially observable. Their yields vary depending on production and two body π^- decay branching ratios. For an estimate, assuming equal yield rate, the average yield per hyperfragment will be $\underline{2{,}477/11 \approx 225}$ counts.

3.3.3.3 The $^{12}_{\Lambda}$B system with ^{12}C target

As listed in Table 1, the luminosity can be 64mg/cm^2 × 60 μA for the $^{12}_{\Lambda}$B system with a ^{12}C target. This is to reach the same yield rate as the HKS experiment. The yield by electro-production from the bound region dominantly comes from the ground state doublet (1^- and 2^-) states which are separated only by about 150 keV and the p-shell excited (3^+ and 2^+) states. These p-shell states are below the one nucleon emission threshold (i.e. $^{12}_{\Lambda}\text{B} \rightarrow {}^{11}_{\Lambda}\text{B} + \text{n}$) thus stable against fragmentation and all the excited states are considered to decay primarily to the ground state via γ transitions. The overall combined (s- and p-shell states) production yield is observed to be about 12 counts/hour (with scattered electrons tagged by Enge spectrometer). Thus, the production yield for the K^+ tagged bound $^{12}_{\Lambda}$B without electron tagging will be 12 × 476 = 5,712 counts/hour.

$\Gamma_{\pi^-}/\Gamma_{\Lambda} = 0.3$ can be assumed for $^{12}_{\Lambda}$B. With the same HES parameters and running time, we can expect to have total of:

$$5{,}712 \times 0.3 \times 0.0016 \times 0.8 \times 0.32 \times 1000 \approx \underline{702 \text{ counts}}$$

for the ground state of $^{12}_{\Lambda}$B. The statistical error in the binding energy will be also at the level of ±3 keV.

The K^+ singles rate will be 200 Hz with the proposed luminosity. Using the same average branching ratio for all hyperfragmentgs as in the estimate for both $^{7}_{\Lambda}$He and $^{9}_{\Lambda}$Li continua, the overall hyperfragment yield with two body π^- detected is expected to be:

$$200 \times 0.1 \times 0.3 \times 0.0016 \times 0.8 \times 0.32 \times 1000 \times 3600 \approx 8{,}847 \text{ counts.}$$

Using the same 30% ratio for the ground states of hyperfragments, the overall yield for ground states of hyperfragments will be about 2,654 counts.

From the $^{12}_{\Lambda}$B continuum, the hyperfragments seen from both the $^{7}_{\Lambda}$He and $^{9}_{\Lambda}$Li continuums will be seen again. In addition, there will be eleven additional possible hyperfragments. Thus there will be total of 22 light hypernuclei excluding the primary $^{12}_{\Lambda}$B potentially observable. For an estimate, assuming equal yield rate, the average yield per hyperfragment will be 2,654/22 ≈ 120 counts.

In terms of statistics, 120 counts is sufficient for a precision binding energy (~±6.4 keV) on average, because of the high resolution.

3.3.4 Features and approaches for decay π^- spectroscopy

As presented previously, below the fragmentation threshold the Λ quasi-free systems are either in the form of highly excited unbound states or of in-flight Λ's that decay mesonically. As do the bound excited states, the unbound states decay to the ground state via γ transitions in single or multiple step cascades. About 60 MeV above Λ quasi-free threshold, all two body mesonic decay channels that emit stable or sub-stable nuclei are open. From electro-production the relative energy of the Λ with respect to the core nucleus in the continuum is extended up close to 400 MeV.

It is obvious that the continuum from heavier targets may produce a larger variety of hyperfragments; thus more physics can be explored, such as direct measurements of the binding energy differences from multiple simultaneously produced hypernuclear mirror pairs for the investigation on CSB as a function of isospin. Many interesting but not yet well studied hypernuclei appear in the same decay π^- spectrum. Thus, direct spectroscopic comparisons in terms of Z and A differences can provide valuable information that could not otherwise be obtained reliably.

On the other hand, the heavier continuum produces a more complicated spectroscopy in which some of the hypernuclear spectra may overlap, raising technical difficulties in separating them. One important feature is that the heavier target continuum produces repeated spectroscopy from the lighter target continuum with additions. The primary hypernucleus from a lighter target becomes a hyperfragment from the heavier continuum, either gaining strength or losing domination. Therefore, the spectroscopy from a lighter continuum can be a reference for the heavier one. In other words, the program must start from the best selected light target and proceed to heavier targets after a full understanding of the lighter ones. For that reason, the JLAB experiment proposes three phases: I – ^{7}Li; II – ^{9}Be; and III – ^{12}C targets (in the 12GeV period), plus a shorter parasitic feasibility test run in advance of Phase-I (in the 6GeV period). The test run will provide the adjustments needed to optimize the experimental technique/equipment and obtain important yield rates to confirm the required beam time for the actual experiment. Fig. 9 is a spectroscopy illustration based on the tables shown in Appendix I and the above yield rate discussions. Spectroscopy from $^{7}_{\Lambda}$He (Fig. 9(a)) is the primary one. For $^{9}_{\Lambda}$Li (Fig. 9(b)) and $^{12}_{\Lambda}$B (Fig. 9(C)) only the additions are shown. All states from each target are illustrated with the same yield rate except changes due to known reductions or enhancements. The only background, coming from three body decay π^-'s, is presented to illustrate the level and its general shape which may vary in reality. In the next chapter, a detailed discussion of the physics outcome will be given following the sequence of the proposed three phases.

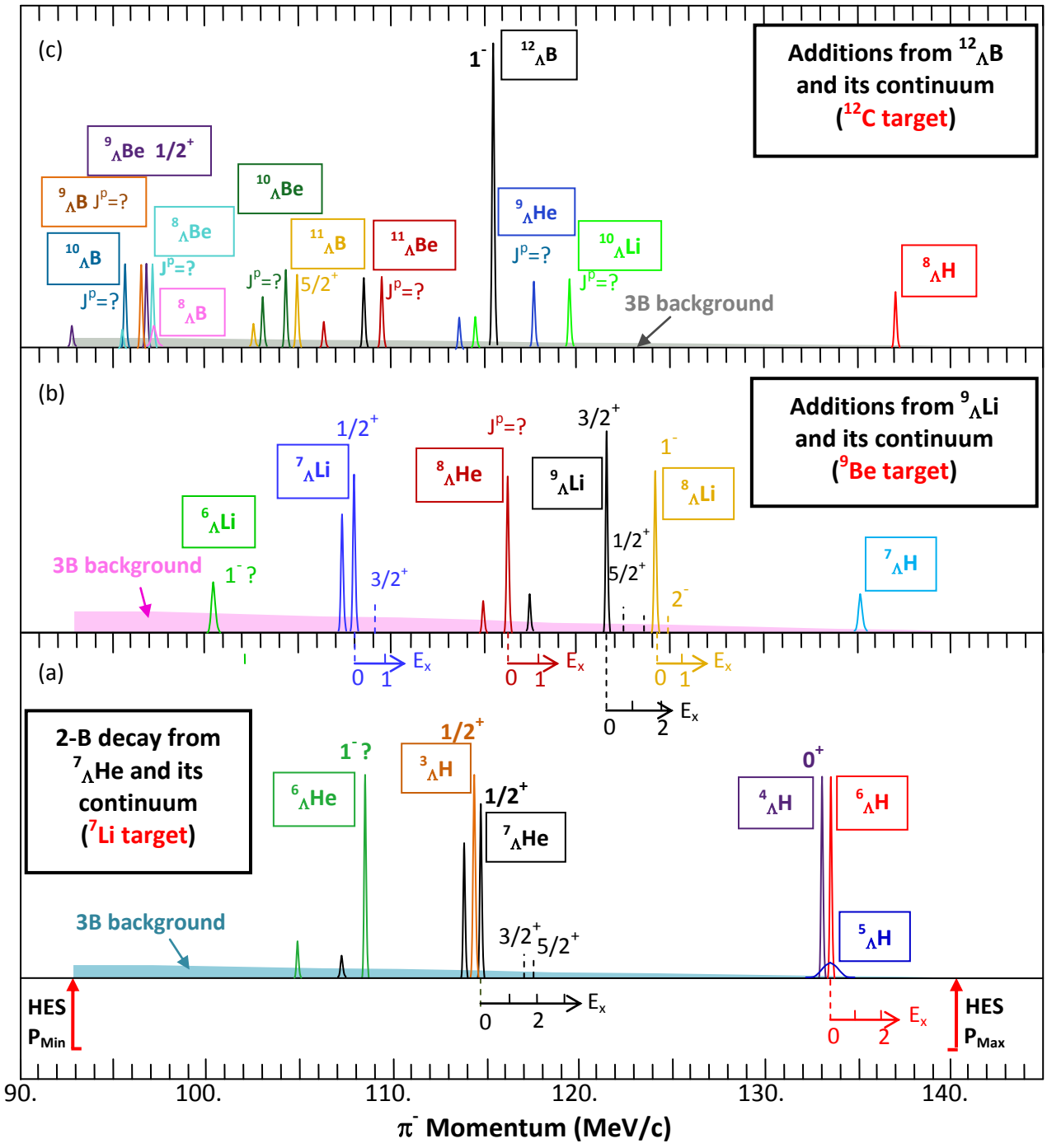

Figure 9. Illustration of the decay π^- spectroscopy from three different targets: (a) ^{7}Li; (b) ^{9}Be; and (c) ^{12}C. For each target, an estimated average yield is used for all possible hyperfragments. States observed from a lighter target will be observed again in the heavier target. Only the additional states are shown for heavier targets. For example, the sum of all three spectroscopy will be the complete one for ^{12}C target, except the yield variation with respect to the primary hypernucleus $^{12}_{\Lambda}$B which is reduced by 40% to better illustrate the hyperfragments.

4. Spectroscopy of light hypernuclei – what can this experiment achieve and why are they new and so important?

So far, the ground state Λ binding energies, the B_Λ values, of many light hypernuclei are still unknown, especially those highly neutron rich ones or those at drip lines. To make illustration on the possible new findings and their importance, assumed values are taken from a theoretical estimate [29].

4.1 Phase I: ^{7}Li target

The π^- momentum spectroscopy from two body hypernuclear decay of the bound $^7_\Lambda$He and its continuum is the simplest and cleanest spectroscopy. Still, it can have number of clearly defined and significant physics goals accomplished. There are total of six possible hypernuclei to be observed, four previously measured ($^3_\Lambda$H, $^4_\Lambda$H, $^6_\Lambda$He, and $^7_\Lambda$He) with known Λ binding energies for the ground states and two possible hyper-hydrogen or neutron drip line hypernuclei ($^5_\Lambda$H and/or $^6_\Lambda$H) to be searched for. The basic physics justifications can be outlined as the followings.

4.1.1 $^3_\Lambda$H and $^4_\Lambda$H

A = 3-5 systems provide the essential testing ground for YN interaction models. A good YN model must be able to reproduce, or predict correctly, the ground state B_Λ and spin/parity for all A = 3-5 hypernuclei. On the other hand, precise experimental results are able to provide crucial and stringent constraints in determining the correct YN model, one that has the proper ingredients to model the YN interaction.

$^3_\Lambda$H is known to be the lightest hypernucleus and its ground state B_Λ (i.e. the Λ separation energy) is very small and difficult to measure. From the early He Bubble Chamber (HeBC) studies [18], the value was given to be 0.25 ± 0.31MeV if events were selected only from two-body π^- decay ($^3_\Lambda\mathrm{H} \rightarrow {}^3\mathrm{He}+\pi^-$), while it became 0.07 ± 0.27MeV if all π^- decays (i.e. the addition of the three body $^3_\Lambda\mathrm{H} \rightarrow {}^2\mathrm{H}+\mathrm{p}+\pi^-$ channel) were included. The $R_3 = \Gamma_{\pi^-}/\Gamma$ was quoted as 0.36 ± 0.07. The B_Λ value with statistical mean over two- and three-body decays using this measured R_3 was then given as 0.11+0.06/-0.03MeV. The result is certainly questionable [19]. The most commonly used value of $B_\Lambda = 0.13 \pm 0.05(\mathrm{stat.}) \pm 0.04(\mathrm{sys.})$ MeV was from a later emulsion study [20] which could not analyze well the two body decay; thus, mainly comes from three body decay. Actually, as discussed previously the three body decay is from an excited two body state; i.e., first $^3_\Lambda\mathrm{H} \rightarrow {}^3\mathrm{He}^*+\pi^-$, then $^3\mathrm{He}^* \rightarrow {}^2\mathrm{H}+\mathrm{p}$ or d+p. In our proposed JLAB experiment, this channel contributes three body pion background with almost equal yield to that of two body decay. Exclusive three body events can certainly reconstruct the mass of $^3_\Lambda$H but with higher systematic uncertainty, while unfortunately emulsions cannot analyze effectively the two body decay. Whether B_Λ is 0.13MeV or 0.25MeV (although a seemingly small difference) holds an important key to one mystery of the YN interaction (see further discussion below).

$^4_\Lambda$H is another important few body (or s-shell) hypernucleus among the A = 3-5 systems. $^4_\Lambda$H and $^4_\Lambda$He form the mirror pair of hypernuclei and are believed to have similar structure, 0^+ for the ground state and 1^+ for the first excited state. The currently accepted B_Λ values for their ground states come from an emulsion study [21, 22]: $2.04 \pm 0.04(\mathrm{stat.}) \pm 0.04(\mathrm{sys.})$ MeV and

2.39±0.03(stat.)±0.04(sys.) MeV, respectively. Combining them with the ground state B_Λ values of $^3_\Lambda$H and $^5_\Lambda$He, they form a testing ground for the correctness of YN interaction models. In addition, their difference is commonly used to demonstrate charge symmetry breaking (CSB) in the YN interaction, since the contribution from the difference of Coulomb effect for these two systems is estimated to be small and negligible. However, their γ (M1) transitions from the 1^+ first excited state to the 0^+ ground state were measured as 1.04±0.04MeV and 1.15±0.04MeV [23]. The B_Λ difference of the ground states is 350keV, while it is only 240keV for the first excited states. The CSB energies are inconsistent. Furthermore, none of the most commonly considered theoretical YN models can consistently reproduce the B_Λ values for all A = 3-5 systems nor agree with the measured CSB energies from both ground states and first excited states (see Table. 1 [24].) The experimental ground state B_Λ values quoted in the table were from the best estimate given in Ref. 22 of Ref. 21. The B_Λ values for $^4_\Lambda$H* and $^4_\Lambda$He* (first excitation) were obtained as ground state values minus the observed E_γ's.

Table 1: Λ separation energies, given in units of MeV, of A = 3-5 Λ hypernuclei for different models of YN interaction.

YN	$B_\Lambda(^3_\Lambda H)$	$B_\Lambda(^4_\Lambda H)$	$B_\Lambda(^4_\Lambda H^*)$	$B_\Lambda(^4_\Lambda He)$	$B_\Lambda(^4_\Lambda He^*)$	$B_\Lambda(^5_\Lambda He)$
SC97d(S)	0.01	1.67	1.2	1.62	1.17	3.17
SC97e(S)	0.10	2.06	0.92	2.02	0.90	2.75
SC97f(S)	0.18	2.16	0.63	2.11	0.62	2.10
SC89(S)	0.37	2.55	Unbound	2.47	Unbound	0.35
Experiment	0.13 ±0.05	2.04 ±0.04	1.00 ±0.04	2.39 ±0.03	1.24 ±0.04	3.12±0.02

Given that $^4_\Lambda$He (also $^5_\Lambda$He) decays only by a three body mode (see tables in Appendix I), the main question with the experimental results is the significant inconsistency for the B_Λ values of the $^4_\Lambda$H ground state measured by emulsion for events associated with two body or three body decays, a similar problem as seen for $^3_\Lambda$H.

The JLAB experiment can measure B_Λ values of the ground states of both $^3_\Lambda$H and $^4_\Lambda$H with high precision from the monochromatic two body decay π^-'s. Although the $^3_\Lambda$H peak is only about 320keV/c away from the ground state of $^7_\Lambda$He, the separation is more than 4σ with respect to the momentum resolution (σ = 70keV/c). The primary contribution and achievement for the Phase-I JLAB experiment to the study of few body hypernuclear systems will come from the simultaneous precision measurement of the B_Λ values of the ground state $^3_\Lambda$H and $^4_\Lambda$H, to provide a testing ground with better precision and less ambiguity for the YN interaction model.

4.1.2 $^6_\Lambda$He and $^7_\Lambda$He

$^6_\Lambda$He and $^7_\Lambda$He are among the lightest p-shell hypernuclei for which extensive studies [25] based on shell or cluster models can be performed to understand the dynamical change of the core nuclei due to the insertion of strangeness degree of freedom, a Λ particle, extending the study of the YN interaction beyond few body systems. Despite the theoretical interest, very little is known about these species experimentally.

For $^{6}_{\Lambda}$He (which is the mirror hypernucleus to $^{6}_{\Lambda}$Li), its core ^{5}He is unbound by 0.89MeV with respect to the α+n breakup threshold while the ground state $^{6}_{\Lambda}$He lies 0.16MeV below the $^{5}_{\Lambda}$He+n threshold. $^{6}_{\Lambda}$He and $^{6}_{\Lambda}$Li (see also discussion for Phase II) are expected to have very similar properties and both are believed to have a 1^- ground state and a 2^- first excited state. Theoretical considerations lead to one to expect the 2^- excited state is separated from the 1^- ground state about 0.32MeV (0.42MeV) for $^{6}_{\Lambda}$He ($^{6}_{\Lambda}$Li); thus, the excited state is unbound and could not be studied by observing the γ transition. So far only the ground state B_Λ value (Λ separation energy or binding energy) of 4.18 ± 0.1MeV was determined experimentally by emulsion techniques, the very same scenario as for $^{6}_{\Lambda}$Li. Until now, the A=6 hypernuclear systems remain poorly known.

The JLAB experiment has the capability to measure the B_Λ value of the ground state $^{6}_{\Lambda}$He with high precision. In addition, the spin/partity of $^{6}_{\Lambda}$He may be determined. In two body decay, $^{6}_{\Lambda}$He g.s. $\rightarrow$ ^{6}Li+π^-, the spectroscopy will feature the excitation spectrum of ^{6}Li with known 1^+ g.s., 3^+ 1st and 0^+ 2nd excited states. The selectivity among these states will determine the initial spin/parity of the decay $^{6}_{\Lambda}$He g.s (as shown in Fig. 3).

$^{7}_{\Lambda}$He is rather interesting, because of its unique structure with the Λ coupled to a neutron halo core nucleus ^{6}He (α+n+n). Through the investigation of this hypernucleus one hopes to gain knowledge on the "glue-like" role of the Λ or the modification of the core structure because of the presence of Λ. This neutron rich hypernucleus may provide important information to understand the contribution of ΛN-ΣN coupling (i.e. a ΛNN three-body interaction) which is thought to contribute to the current inconsistency problems seen in the A=3-5 systems [26]. The coherent ΛN-ΣN coupling from all neutrons is anticipated to be quite strong in a neutron star. The basic structure of $^{7}_{\Lambda}$He corresponds to a $1/2^+$ ground state (Λ coupled to bound 0^+ ^{6}He ground state core) while the $3/2^+$ and $5/2^+$ excited states are the non-spin flip and spin flip partners generated by Λ coupled to the unbound 2^+ excited state ^{6}He neutron halo core. They are predicted to be bound.

The emulsion result for $^{7}_{\Lambda}$He is quite puzzling as mentioned early in the introduction. The very limited number of events recognized uniquely from their weak decay seemed to spread over a wider excitation energy range than expected. This prompted rather hot debate since the 1970's as to the existence of isomeric hypernuclear states, from which the M1 γ transitions are so hindered that such isomeric excited states decay via weak decay [13]. The system remained little understood until electroproduction at JLAB was carried out by the HKS program. The current test run result of a mass spectroscopy shows a clear observation of the ground state (assuming it is a $1/2^+$ state) but no observation of the $3/2^+$ and $5/2^+$ excited states could be made due to low statistics. The next phase HKS (E05-115, 2009) plans a high statistical mass spectroscopy study of $^{7}_{\Lambda}$He.

From this proposed experiment, the ground state B_Λ will be precisely measured. Secondly, from the stable low lying ^{7}Li structure ($3/2^-$ g.s. and $1/2^-$ 1st excited state with E_x = 0.4776MeV with respect to the $7/2^-$ excited state having E_x = 4.652MeV) the spin/parity of $^{7}_{\Lambda}$He can be determined. Finally, existence of the excited $^{7}_{\Lambda}$He* states can be investigated. If isomerism occurs and an isomeric state does exist in the $^{7}_{\Lambda}$He spectrum, the weak π^- decay may have the best chance to prove it.

4.1.3 $^{6}_{\Lambda}$H and/or $^{5}_{\Lambda}$H – the neutron drip line hypernuclei (heavy hyper-hydrogen)

Hypernuclei provide an interesting possibility of extending the nucleon (especially the neutron) drip line beyond that for ordinary nuclei. Identifying such drip line hypernuclei can provide important information in understanding the YN interaction in the nuclear medium. In general, it was believed that at least one or two more neutrons can be attached to the system beyond ordinary neutron drip line if a Λ is included [27]. There is no experimental data available since producing them directly from a primary reaction is rather difficult. This interesting possibility is considered also in heavy ion collisions. There is no sufficient theoretical work at present to predict the drip line limit. It is the unique opportunity for JLAB in such a study. The focus for the proposed JLAB experiment is on heavy hyper-hydrogen [4], although neutron drip line hypernuclei with Z > 1 may also be observed.

$^{6}_{\Lambda}$H is predicted as a possible result from fragmentation in the $^{7}_{\Lambda}$He continuum. It is the most neutron rich hypernucleus in the A=6 family. In the absence of a Coulomb force the Λ is expected to bind the system tighter; thus, B_Λ may be in the range of 4.1 to 6.1 MeV [29]. In the table in Appendix I as well as in the illustrated spectroscopy, it was assumed to be 5.1 MeV. If it exists, the ground state will appear close to $^{4}_{\Lambda}$H (see Fig. 9). If it is bound 0.2-0.4 MeV deeper, these two states may merge together. On the other hand, if B_Λ value is outside the range from 5.3 MeV to 5.5 MeV, the state moves away from the $^{4}_{\Lambda}$H peak. Thus there is a 0.2 MeV blind spot. Its B_Λ can be measured precisely. It can be an important and an extremely valuable discovery and achievement.

$^{5}_{\Lambda}$H is another member in the heavy hyper-hydrogen family. However, since the two body decay of $^{5}_{\Lambda}$H results a ^{5}He (α+n) nucleus which is known to be unbound by 0.89MeV with respect to the breakup threshold. It may decay in both two body and three body modes. Less yield and peak broadening (as the width of the ^{5}He g.s. known to be ~0.65MeV FWHM) is expected (see Table in Appendix I and Fig. 9). If it can be observed, we expect a peak width of about 0.9 MeV FWHM. Here a B_Λ value of 4.1 MeV is assumed.

4.1.4 Lifetime measurements

Utilizing the excellent beam time zero width (~1.7ps) and time reconstruction capability commonly seen for all spectrometers at JLAB, the lifetime of all the identifiable hypernuclear states can be measured. The most important lifetimes are those of the isomeric states. If they exist, lifetimes of individual states (g.s. and isomeric excited states) permit study of medium modification due to the presence of a Λ and of change of baryonic property in nuclear medium through investigations of the branching ratios of B(M1) and B(E2). The technique is described in detail in the E08-012 proposal, in Section 2.3, attached in Appendix II.

Overall, ^{7}Li is an ideal starting target due to the cleanness of the spectra and simplicity of its structure but a significant amount of physics will be its outcome. As one can see the same spectroscopy, except for the change in yield rates, will always appear again when a heaver target is used in future phases, with additional heaver hypernuclear species. Fully understanding the spectroscopy will not only provide unprecedented information about few body hypernuclei but also make a clear reference when the spectroscopy becomes more complicated as heavier systems are added using a heavier target (see the following).

4.2 Phase II: ^{9}Be target

From the Phase II target ^{9}Be, which produces $^{9}_{\Lambda}$Li and its continuum, the physics outcome is greatly extended into p-shell hypernuclei yielding new valuable information.

4.2.1 $^{6}_{\Lambda}$Li and CSB

$^{6}_{\Lambda}$Li is the lightest addition and will add important information for the A=6 family. Similar to $^{6}_{\Lambda}$He discussed earlier but with the contrast that $^{6}_{\Lambda}$Li is 0.59MeV above the $^{5}_{\Lambda}$He+p breakup threshold. This makes impossible γ spectroscopy studies but is an excellent source for $^{5}_{\Lambda}$He production [28]. This hypernucleus is poorly known except the B_{Λ} value (Λ separation or binding energy) of 4.5 MeV given by emulsion studies. Since the breakup of $^{6}_{\Lambda}$Li can be viewed either as $^{6}_{\Lambda}\text{Li} \rightarrow {}^{5}_{\Lambda}\text{He} + p \rightarrow (\alpha + p + \pi^{-}) + p$ or as $^{6}_{\Lambda}\text{Li} \rightarrow {}^{6}\text{Be} + \pi^{-} \rightarrow (\alpha + p + p) + \pi^{-}$ with exactly the same final state, the width of ^{6}Be can be used to estimate the observation of $^{6}_{\Lambda}$Li via two body decay. Although ^{6}Be is unstable (1.37MeV above the threshold for two proton emission), the width of the ^{6}Be g.s. is sufficiently narrow, only 0.092MeV (FWHM), which is smaller than the JLAB experimental resolution. Thus, the width of the $^{6}_{\Lambda}$Li g.s. is anticipated to be ~220 keV/c FWHM. Although it stands on top of the three body decay background, it is in the clean region of the spectrum away from other observable hypernuclei. Thus its g.s. B_{Λ} can be precisely measured.

The most significant point is that the ground state B_{Λ} values of the mirror pair $^{6}_{\Lambda}$He and $^{6}_{\Lambda}$Li will be simultaneously measured, so that the CSB energy of the A=6 system can be determined, although it was predicted very small for this pair. The results provide a stringent limit on the effective models of p-shell hypernuclei, providing another independent investigation of CSB for the pair with non-negligible Coulomb force.

4.2.2 $^{7}_{\Lambda}$Li and $^{7}_{\Lambda}$H

In addition to $^{7}_{\Lambda}$He as an observable in Phase I, two additional hypernuclei in the A=7 family may show up in the decay π^{-} spectroscopy with ^{9}Be target. From the emulsion data, the B_{Λ} value of the $^{7}_{\Lambda}$Li g.s. is given as $5.58 \pm 0.03(\text{stat.}) \pm 0.04(\text{sys.})$ and the spin/parity is already confirmed as $1/2^{+}$. In addition, a high precision γ spectroscopy study by HYPERBALL assigned the 0.69 MeV γ transition to be the M1 transition from its $3/2^{+}$ first excited state. It is unclear if any isomeric excited state exists in this system. The JLAB experiment will make an independent precision measurement of the g.s. B_{Λ}. Combining with all the results from the observed A=6 and 7 systems, the measurements provide the important data base to fully test the theoretical model predictions for hypernuclei just beyond few body systems.

$^{7}_{\Lambda}$H is an important test for the drip line limit of heavy hyper-hydrogen. Due to instability of ^{7}He, via to 1 neutron emission, it may decay in both two and three body modes. In the two body mode, the intrinsic width of the ground state ^{7}He is only 150 keV FWHM, so that the peak may still be sufficiently narrow for observation, depending on the two body decay branching ratio. The B_{Λ} value is considered to be in the range of 5.1-7.1 MeV [29]; and it is assumed to be 6.1 MeV in the spectroscopy illustration and in the table attached in Appendix I.

4.2.3 $^{8}_{\Lambda}$He and $^{8}_{\Lambda}$Li

$^{8}_{\Lambda}$He and $^{8}_{\Lambda}$Li are the first two p-shell hypernuclei in the A=8 family appearing in the spectroscopy when a ^{9}Be target is used. $^{8}_{\Lambda}$Li is better known with its g.s. B_Λ determined by the emulsion data to be $6.8 \pm 0.03(\text{stat.}) \pm 0.04(\text{sys.})$ MeV [22], and the g.s. spin/parity is quoted as 1^- by observation of γ transitions from the 2^- first excited state that is separated by 0.442 MeV. However, this γ transition was not observed unambiguously. The JLAB experiment will provide a precise g.s. B_Λ measurement to confirm the emulsion result as well as to investigate the possible existence of an isomeric excited state.

The g.s. state B_Λ value of $^{8}_{\Lambda}$He was poorly determined as 7.16 ± 0.7MeV from only 6 uniquely identified events [22]. The spin/parity is unknown as are its excited states. The JLAB experiment can measure the B_Λ value precisely. Utilizing the uniquely known stable low lying structure of the two body decay nucleus ^{8}Li (2^+ g.s., 1^+ 1^{st} and 3^+ 2^{nd} excited states), the spin/parity of $^{8}_{\Lambda}$He can be solidly determined. In addition, $^{8}_{\Lambda}$He is a highly neutron rich hypernucleus which clearly demonstrates that the added Λ stabilizes the unbound nuclear core ^{7}He.

4.2.4 $^{9}_{\Lambda}$Li

$^{9}_{\Lambda}$Li is the hypernucleus primarily produced from a ^{9}Be target. This neutron rich system is interesting for investigating the importance of Λ-Σ coupling [30]. The g.s. B_Λ was given by emulsion analysis as 8.50 ± 0.12MeV from only 8 identifiable events. The spin/parity assignment is not experimentally confirmed. Theoretically, the g.s. was assumed to be a $3/2^+$ state and there are three low lying excited states. The first excited state is assumed to be a $5/2^+$ state. The separation is about 0.7MeV. However, the expected second excited state is assumed to be a $1/2^+$ state which comes from a different core state. So far, no primary production experiment has resolved the structure of this system. The JLAB experiment can measure its g.s. B_Λ with high precision as well as determine its spin/parity from the two body decay spectroscopy of ^{9}Be. In addition, if all the spins are assigned correctly, the $1/2^+$ excited state may not be able to decay via γ transition, and thus may be another good candidate for evidence of an isomeric state.

Overall, by using a ^{9}Be target in Phase II, additional hypernuclear species with a rich physics contents can be studied. These additions are still relatively clean with respect to those already appearing in the spectroscopy from the ^{7}Li target.

4.3 Phase III: ^{12}C target

The number of new additional hypernuclei increases significantly when using a ^{12}C target in the Phase III experiment. New physics opportunities as well as spectroscopy complications are enhanced. High resolution and clear understanding of the spectroscopy from the initial phases are key factors required to extract new findings from the ^{12}C target spectroscopy.

4.3.1 $^{8}_{\Lambda}$H, $^{8}_{\Lambda}$Be, and $^{8}_{\Lambda}$B

$^{8}_{\Lambda}$H, $^{8}_{\Lambda}$Be, and $^{8}_{\Lambda}$B are the three hyperfragments in the A=8 family coming from the $^{12}_{\Lambda}$B continuum in addition to $^{8}_{\Lambda}$He and $^{8}_{\Lambda}$Li already expected from the $^{9}_{\Lambda}$Li continuum.

Since ^{7}H was recently found to be unbound only by 0.84 MeV; this suggests that the system can be stable when a Λ is added [4]. The existence of $^{8}_{\Lambda}$H will push the neutron drip line to the extreme, providing the best evidence along with other heavy hyper-hydrogen in testing the role of Λ-Σ mixing. The B_Λ value may range from 6.1 to 8.1 MeV [29] and here we assume 7.1 MeV. The isotopes $^{4}_{\Lambda}$H, $^{6}_{\Lambda}$H, and $^{8}_{\Lambda}$H are expected to have similar but very simple low lying structure – ground state doublet. Therefore, they are also important systems in which to search for evidence of the existence of long lived isomeric states.

The $^{8}_{\Lambda}$Be and $^{8}_{\Lambda}$B ground states appear at the region most complicated by the three new additions: $^{9}_{\Lambda}$Be, $^{9}_{\Lambda}$B, and $^{10}_{\Lambda}$B. However, this cluster of states is sufficiently isolated from the rest at the lowest momentum. Secondly, none of them has a ground state doublet for the two body decay nucleus. Thus all have relatively simple spectroscopy featuring dominantly the ground state. While the width of the $^{8}_{\Lambda}$Be g.s. is expected to be narrow (sharp), the $^{8}_{\Lambda}$B g.s. is broader (365keV/c FWHM) with ~120 keV offset. This feature helps to resolve the potentially dissolved spectroscopy. $^{8}_{\Lambda}$B has not been observed; thus, it provides additional information for A=8 systems. Since $^{8}_{\Lambda}$Li (as measured in Phase II) and $^{8}_{\Lambda}$Be (new), another important mirror pair, will appear in the same spectrum, their ground states will be measured simultaneously so that the binding energy difference can be precisely measured to investigate the CSB energy again for A=8 to gain knowledge on isospin dependency. Any correct YN model must be able to predict CSB energy correctly for all three pairs: $^{4}_{\Lambda}$H - $^{4}_{\Lambda}$He (not measured by this experiment; $^{6}_{\Lambda}$He - $^{6}_{\Lambda}$Li; and $^{8}_{\Lambda}$Li - $^{8}_{\Lambda}$Be. Therefore, this experiment can provide solid information in determining correct YN models.

4.3.2 $^{9}_{\Lambda}$He, $^{9}_{\Lambda}$Be, and $^{9}_{\Lambda}$B

An additional three hypernuclei in the A=9 family can be produced. Among them, $^{9}_{\Lambda}$He is the most neutron rich hypernucleus in this family but has not yet been found. This is due to the difficulty in utilizing the existing production mechanisms and in problems in emulsion event recognition. If it can be found in this experiment with a precisely measured B_Λ and unambiguously determined spin/parity, it will be a good candidate in this family to study the importance of "coherent Λ-Σ coupling".

$^{9}_{\Lambda}$Be was measured by emulsion techniques, and its ground state B_Λ value is $6.71 \pm 0.04(\text{stat.}) \pm 0.04(\text{sys.})$ with its spin/parity determined as $1/2^{+}$. This experiment will confirm its B_Λ value as well as use it as an important reference. $^{9}_{\Lambda}$B is the most proton rich hypernucleus that so far has been observed in this A=9 system. Its ground state B_Λ value, $8.29 \pm 0.18(\text{stat.}) \pm 0.04(\text{sys.})$, was not precise nor its spin parity determined. These two systems are tightly packed together and very close to the two members from the A=8 family with all the separations around 2σ. Thus, this part of the spectroscopy may come closest to a dissolved spectroscopy. High resolution and a well understood reference from $^{9}_{\Lambda}$Be is crucial to resolve it.

4.3.3 $^{10}_{\Lambda}$Li, $^{10}_{\Lambda}$Be, and $^{10}_{\Lambda}$B

$^{10}_{\Lambda}$Li is the most neutron rich hypernucleus in the A=10 family that can be found by this experiment using two body decay. It has not been found yet although it is expected to exist [31].

Its spectroscopy appears in the relatively clear region; thus, its g.s. B_Λ should be determined with high precision.

Ground states of both $^{10}_{\Lambda}$Be and $^{10}_{\Lambda}$B are poorly determined as, $9.11 \pm 0.22(\text{stat.}) \pm 0.04(\text{sys.})$ and $8.89 \pm 0.12(\text{stat.}) \pm 0.04(\text{sys.})$ nor are their spin/parity determined. On the other hand, both of them are expected to exhibit similar ground state doublets with a separation smaller than 100keV. However, the M1 transitions between the g.s. doublet states are missing in γ transition experiments, such as the recent high precision γ spectroscopy experiment on $^{10}_{\Lambda}$B by HYPERBALL. Therefore, these are the two important new additions to be studied for the A=10 family and for new evidences of isomerism.

Again, simultaneous measurement of $^{10}_{\Lambda}$Be and $^{10}_{\Lambda}$B provide precise and direct information on CSB energy, extending the test base for the correctness of YN models to A=10.

4.3.4 $^{11}_{\Lambda}$Be and $^{11}_{\Lambda}$B

$^{11}_{\Lambda}$Be, $^{11}_{\Lambda}$B, and $^{11}_{\Lambda}$C are the only members possible with particle stable states in the A=11 family. Restricted to two body decay, only $^{11}_{\Lambda}$Be and $^{11}_{\Lambda}$B can be observed by this JLAB experiment. So far, only $^{11}_{\Lambda}$B is known with a ground state B_Λ value of $10.24 \pm 0.05(\text{stat.}) \pm 0.04(\text{sys.})$ measured by emulsion technique and the ground state spin/parity is known to be $5/2^+$. This hypernucleus was theoretically calculated (Millener's shell-model calculation) and predicted to have many bound excited states [32]. The system is suitable for a test of the ΛN interaction parameters and the theoretical framework and was thus studied by high precision γ spectroscopy (KEK, E518 Experiment). Six transitions were observed but only two of them were able to be assigned for the M1 transition between the g.s. doublet states: $7/2^+ \rightarrow 5/2^+$ and the E2 transition between the first $1/2^+$ core excited state and $5/2^+$ g.s. state. However, the experimentally observed separation energies did not agree with the theoretical calculation (M1: 0.264 vs 0.418MeV and E2: 1.48 vs 1.02MeV) nor are explained by the theory that describes the observations on other light hypernuclei so well (see discussions also in E08-012 proposal, section 2.3.3 in Appendix II). It remains an important puzzle that will be investigated by the HYPERBALL-J program at J-PARC [33]. This experiment can confirm the g.s. B_Λ with high precision as well as investigate the possibility of the existence of isomeric, long lived states. If they do exist in this system, they signify a significant core (^{10}B) structure change due to the presence of Λ. This may be the source of the puzzle.

On the other hand, $^{11}_{\Lambda}$Be has not yet been observed but is expected to have similar structure as $^{11}_{\Lambda}$C, which is also not observed. It has much simpler structure than $^{11}_{\Lambda}$B. Thus precise determination of its g.s. B_Λ and spin/parity will provide important information for the A=11 family.

4.3.5 $^{12}_{\Lambda}$B

This is the hypernucleus from the primary production. It is one of the only two particle stable hypernuclei (as well as a charge symmetry pair) in the A=12 family, besides $^{12}_{\Lambda}$C with great structure similarity. The g.s. doublet for both has a small separation, ~150keV. Although the g.s. spin/parity is commonly believed to be 1^-, a solid confirmation is valuable since A=12 hypernuclei are the characteristic ones commonly used as references.

4.4 Physics outcome summary – uniqueness and importance of the JLAB experiment

With the advantages offered by the intense CEBAF beam, the well defined momentum transfer direction, and the known experimental technique/equipment, the hypernuclear continuum can be uniquely utilized to observe a wide range of light hypernuclei from A=3 to 12 with various (Z,A) combinations. The high resolution achievable allows one unprecedented investigation of:

(1) Precise ground state binding energies;
(2) Precise and direct CSB measurements on multiple mirror pairs;
(3) Determination of the ground state spin/parity for most of the observed hypernuclei;
(4) Potential discovery of evidences for long lived isomeric states;
(5) Finding the drip line limit such as for the heavy hyper-hydrogen; and
(6) Investigation of medium modification of core structure due to addition of Λ and medium effect to the baryon property such as change of the Λ's magnetic moment.

These results will provide important and solid information for positively determining the correct YN interaction models and the effects on the dynamical changes of the nuclear medium such as isomerism and charge symmetry. It may result in significant findings that our understanding of the fundamental mechanism and dynamics of the YN interaction and medium effects must build on.

5. Comparison of experimental configuration options and proposal requirement

5.1 Option (2)

The Option (2) is simply adding the existing Enge spectrometer in the backward angle to the Hall A hypernuclear experiment as the illustration seen in Fig. 10.

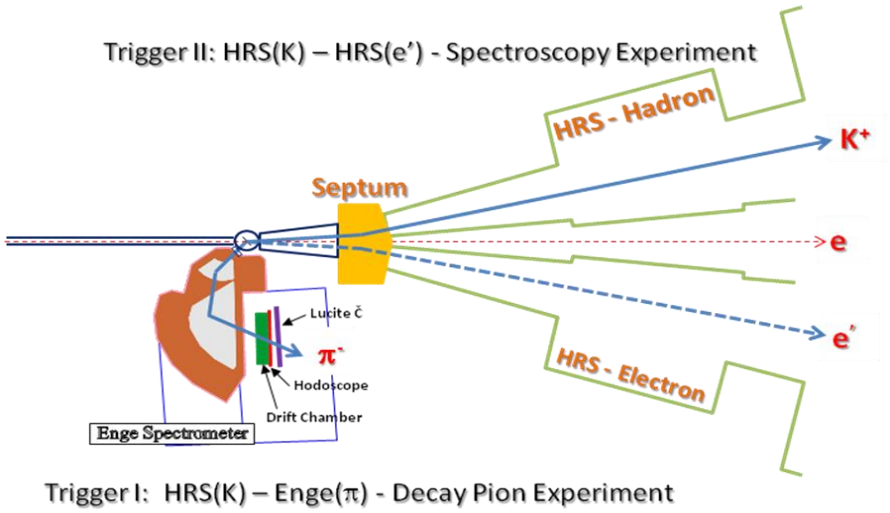

Figure 10. Schematic view of the Option (2) experimental configuration with the Hall A Septum, HRS, and Enge spectrometer.

Most of the basic experimental features discussed in Chapter 3 are valid. Small differences are the following.

Advantages:

(1) Septum+HRS system for kaon detection exist;
(2) Enge system used for Hall C HNSS (E89-009/2000) and HKS (E01-011/2005) exist and it is easy to transfer and install it to Hall A without significant cost;
(3) Enge path length is short (only ~4.2 Meters) thus it is suitable for short lived particles (noting that $\beta_\pi =$ 0.54 – 0.71 in this experiment);
(4) Enge is designed for low momentum and it can maintain high resolution ($3x10^{-4}$) for the entire momentum acceptance which is only a few % larger than the required range;
(5) Enge uses single power supply and its installation is relatively minor;
(6) With 4.0 – 4.4 GeV beam energy momentum transfer to the gated Λ's in quasi free region is higher so that the background is even more forward thus the background is further cleaner; and
(7) There is no need for pre-chicaned beam thus the beam operation is simple. Combining that this proposed experiment does not have stringent beam precision requirement, operation for this experiment is relatively easy in comparison to the mass spectroscopy experiments in both Hall A and C.

Disadvantages:

(1) Due to long path length and small soild angle acceptance of the Septum+HRS system, the kaon single rate is ~4 times smaller. This is a significant reduction to the physics yield rate.

This lone disadvantage can be partially overcome by mounting the Enge to the minimum distance to the target with a small target chamber which contains only a solid target ladder. The solid angle acceptance can be as large as that given by HES. The shorter path length gains more than a factor of 2 survival rate for the decay π's. Thus with the proposed beam time (1000 hours) the physics yield will be about 50% of that presented in Chapter 3.

5.2 Option (3)

For this option, the configuration including the pre-chicaned beam requirement is identical to Option (1). The only difference is to replace HES by Enge. As the advantages presented in 5.1, the physics yield rate will be further increased by a factor of 2 which either reduces the beam time requirement or gains twice better statistics. However, since Enge is to be mounted extremely close to the target, the pre-chicaned beam line components (pre-target beam diagnoses and correctors) may interfere with Enge. Thus, it is harder to design, install, and carry out the experiment than using HES which has clearer space in front of the first quadruple.

5.3 Considerations on these options

The Option (1) is clearly the best one. However, Hall C does not have space for such layout due to SHMS for the future 12 GeV operation. It needs HKS and HES to be relocated to Hall A. This relocation costs. It worths it only if future HKS-HES mass spectroscopy program moves from Hall C to Hall A so that this system becomes a part of Hall A common equipment.

The Option (3) has the same problem as Option (1) associated with the unclear question on the future location of the HKS and HES spectrometers. Given the technical difficulty discussed in 5.2, this option should be considered only when the physics yield rate is the sole concern. For example, if HKS and HES remain in Hall C and space is sufficient when mirror flipping them, then the space limitation besides SHMS may make this to be the only option.

Although the yield rate is smaller (~50% as that estimated for Option (1)), Option (2) is the easiest and simplest one in terms of design, installation, operations, and beam requirements. For the beam, only the stability for the beam on target is required and it can be easily achieved by fast feedback beam position lock. Thus the experiment is even suitable to run at the beginning of the 12 GeV beam period when beam energy stability and other qualities are still questionable.

5.4 Requirement of this proposal

This proposal request to carry out the Phase I experiment in Hall A after completion of the 12 GeV upgrade with the Option (2) experimental configuration. The required beam energy will be 4.4 GeV. The beam energy precision and stability do not affect the outcome of this experiment except for the beam on target position and orientation stabilities. The required beam current will range from 50μA and target will be ^{7}Li target. The Hall C E05-115 experiment has proven that this target can take such beam current point beam spot. The proposed experiment request 1000 beam hours to achieve the minimum required statistics.

To ensure the proposed systematic precision and the momentum resolution, the small target chamber will be designed as part of the Enge system. A series of point α sources with well known energies will be mounted on the target ladder. This will allow a precise map on the absolute momentum and paths with precisely measured magnetic field. This work can be done outside of experimental hall ahead of the experiment.

The later phases (II - ^{9}Be target and III - ^{12}C) will be proposed separately when the spectroscopy and yield rates of the earlier phase becomes clear and well understood.

A feasibility test run is important and necessary ahead of the Phase I experiment. The PR08-012 which presented at PAC33 was based on Option (3) in Hall C accept the orientation of the Enge spectrometer. It was conditionally approved but recommended 5 days test beam. It is not feasible to carry out this test in Hall C for short time but long and major installation. With this new proposal and Option (2) in Hall A, feasibility test becomes straight forward. Since this option uses the identical Septum + HRS system, we request approval of transferring the 5 days test from Hall C to Hall A and grant an approval to carry out the test run together with the hypernuclear experiment E07-012. The 5 days test will be dedicated with the ^{7}Li target to examine the features and yield rate of the decay π spectroscopy. The decay π's will be studied parasitically when E07-012 takes data from its water target. This study will allow us to examine the level of complication from O and π's from free Λ's produced from H. These will provide us knowledge on background.

The only difference between the test run and Phase I experiment is the target chambers. For the Phase I experiment, a small and dedicated chamber will be used so that Enge is closer to the target to significantly increase the solid angle acceptance and the physics yield. During the 12 GeV shut down, Enge will be mapped precisely.

6. Summary

At JLAB a unique experimental program, based on study of the precisely measured monochromatic π^-'s from hypernuclear two body mesonic weak decay to identify variety of hyperfragments from the primarily produced hypernuclear continuum, can open a new era in the hypernuclear physics research. High precision, high primary production yield, and well constrained momentum transfer direction to remove quasi-free Λ decay background are the keys that only the experiment at CEBAF can have. The program can obtain important and crucial information to determine the correct theoretical models that describes the fundamental YN interaction and hypernuclear (mass γ, and weak-π) spectroscopy. The experiment can provide precisely measured ground state B_Λ values for a wide range of light hypernuclei with various (Z, A). The CSB energy, its isospin dependence, and its importance in construction of YN interaction models can be investigated by the directly measured Λ binding energy differences from multiple mirror pair hypernuclei. The current inconsistency between theory and high precision γ transition results and possible isomerism can be investigated and verified. It is unique to probe the neutron drip line limit of hypernuclei through searching for the heaviest hyper-hydrogen (as well as those with different Z). The program offers a lot of intriguing tasks that could not be done in the past and should have great impact on improving our current understandings.

Since PAC33 which conditionally approved E08-012 with recommendation of a feasibility test, the new FINUDA result with limited resolution on two body decay π^- spectroscopy demonstrated the principle of this proposed experiment. With about 50 times better resolution, the JLAB experiment will be able to open this new era. The advantages become clearer. The backgrounds and possible hyperfragment channels are better understood and evaluated. Therefore, it is proper to propose the Phase I experiment of this new hypernuclear physics program for the JLAB 12 GeV period. To ensure the successful and unambiguous physics output, the program must take phased approach and each phase can be evaluated and approved accordingly by PAC separately. We hereby request approval for the Phase I as well as for the request parasitic test run in Hall A with the Hall A hypernuclear experiment.

References

1. S.Ajimura *et al*.: *Nucl. Phys.* A **547** 47c (1992) and *Phys. Lett.* B **282** 293 (1992); B.D. Jones *et al*., *Phys. Rev.*,Vol. **127**, No. 1 236 (1962).
2. R.H. Dalitz, R. Levi Setti, *Nuuovo Cimento* **30**, 489 (1963).
3. L. Majling, *Nucl. Phys.* A **585**, 211c (1995).
4. L. Majling, "What can we learn from hypernucleus $^{6}_{\Lambda}$H?", *IX International Conference on Hypernuclear and Strange Particle Physics*, October 10-14, 2006, Mainz, Germany
5. K.S. Myint, Y.Akaishi, *Progr. Theor. Phys. Suppl.* **146**, 599 (2002).
6. S. Shinmura *et al*., *J. Phys.* G **28**, L1 (2002).
7. J.J. deSwart *et al*., *Springer Tracts in Modern Physics* **60**, 138 (1971).
8. T. Motoba, K. Itonoga and H. Bando, *Nucl. Phys.* A**489** (1988) 683.
9. T. Motoba and K. Itonaga, "Pi-Mesonic Weak Decay Rates of Light-to-Heavy Hypernuclei", *Progress of Theoretical Physics Supplement*, No. **117**, (1994) p.477

10. T. Motoba, "Mesonic weak decay of strange nuclear systems", *Proceedings of the IV International Symposium on Weak and Electromagnetic Interactions in Nuclei*, 12-16 June 1995, Osaka, Japan. Edited by H. Ejiri, T. Kishimoto and T. Sato, World Scientific, 1995, p.504.
11. H. Tamura, *et al.*, *Nucl. Phys.* A**754** (2005) 58c.
12. R. E. Chrien, *et al*., *Phys. Rev* C**41** (1990) 1062.
13. J. Pniewski and M. Danysz, "A note on the $^{7}_{\Lambda}He$ hypergragments", *Phys. Lett.* V. **1**, n. 4 (1962) 142; R.H. Dalitz, A. Gal, *Nucl Phys.* B**1** ('67) 1; and M. Juric et al., *Nucl. Phys.* B**52** ('71) 1.
14. H. Tamura, *Eur. Phys. J.* A **13**, 181 (2002).
15. E. Botta et al., *presentation at Sendai08*, December 18-25, 2008.
16. H. Bando et al., *Perspectives in Meson Science, Eds. T. Yamazaki, K. Nakai, and K. Nagamine*, p.571.
17. M. Sotona and S. Frullani, "Electroproduction of Stangeness and Spectroscopy of Light Hypernuclei", *Progr. Theor. Phys Suppl*. **117**, 151 (1994).
18. G. Keyes, M. Derrick, T. Fields et al., "Properties of the hypertriton", *Phys. Rev.* D**1**, 66 (1970).
19. R.H. Dalitz, "50 years of hypernuclear physics, II. The later years", *Nucl. Phys.* A**754** (2005) 14c.
20. D. H. Davis, "50 years of hypernuclear physics, I. The early experiments", *Nucl. Phys.* A**754** (2005) 3c
21. M. Juric, G. Bohm, J. Klabuhn et al., "A new determination of the binding-energy values of the light hypernuclei ($A \leq 15$)", *Nucl. Phys*. B **52** (1973) 1.
22. D.H. Davis, in *Proc. of the LAMPF Workshop on (π, K) Physics, AIP Conf. Proc. 224, ed. by B.F. Gibson, W.R. Gibbs, and M.B. Johnson* (AIP, New York, 1991), p. 38.
23. Bamberger et al., *Nucl. Phys*. B**60**, 1 (1973) and Bejidian et al., *Phys. Lett.* B**62**, 467 (1976) and B**83**, 252 (1979).
24. H. Nemura, Y. Akaishi, and Y. Suzuki, "Ab initio Approach to s-Shell Hypernuclei $^{3}_{\Lambda}$H, $^{4}_{\Lambda}$H, $^{4}_{\Lambda}$He, and $^{5}_{\Lambda}$He with a ΛN - ΣN Interaction", *Phys. Rev. Lett*. **89** (2002) 142504-1.
25. E. Hiyama, et al., "Three-body model study of *A* = 6-7 hypernuclei: Halo and skin structures", *Phys. Rev*. C**53**, 2075 (1996).
26. Y. Akaishi et al., "Coherent Λ-Σ Coupling in s-Shell Hypernuclei", *Phys. Rev. Lett.* **84** 3539 (2000).
27. C. Samanta et al., "Lambda hyperonic effect on the normal drip lines", *J. Phys. G: Nucl. Part. Phys*. **35** (2008) 065101.
28. Szymanski et al, *Phys. Rev. Lett.* **43** (1991) 849; Ajimura et al., *Phys. Rev. Lett.* **84** (2000) 4052; and Kang et al., *Phys. Rev. Lett.* **96** (2006) 062301.
29. L. Majling, *private communications*.
30. Sotona and S. Frullani, "Electroproduction of Strangeness and Spectroscopy of Light Hypernuclei", *Progress of Theoretical Physics Supplement* No. **117** (1994) 151.
31. P.K. Saha *et al*., *Phys. Rev. Lett*. **94** 052502 (2005).
32. D. J. Millener, *Nucl. Phys*. A**754** (2005) 48c.
33. H. Tamura et al., "Gamma ray spectroscopy of light hypernuclei", *J-PARC 50-GeV PS proposal E13* (2006), http://j-parc.jp/NuclPart/pac_0606/pdf/p13-Tamura.pdf.

Appendix I

Light Hypernuclei Produced from the Quasi-free Continuum by Breakup or Fragmentation and Mesonic Decay

1. Mesonic decays of ground state hyperfragments from $^{7}_{\Lambda}$He when using ^{7}Li target

(The intrinsic width is based on the expected resolution of the JLAB experiment)

2-body decays

Breakup Mode	Q value (MeV)	π^- Decay	P_π (MeV/c)	Width (keV/c) FWHM
$^{7}_{\Lambda}$He	-	^{7}Li + π^-	114.61	165
p + $^{6}_{\Lambda}$H	-23.503 (B_Λ=5.1)	^{6}He + π^-	133.47	165
n + $^{6}_{\Lambda}$He	-3.409	^{6}Li + π^-	108.39	165
d + $^{5}_{\Lambda}$H	-23.011 (B_Λ=4.1)	^{5}He + π^-	133.42	~900*
^{3}H + $^{4}_{\Lambda}$H	-16.995	^{4}He + π^-	132.95	165
^{4}H + $^{3}_{\Lambda}$H	-26.981	^{3}He + π^-	114.29	165

3-body decays

Breakup Mode	Q value (MeV)	π^- Decay	P_π max (MeV/c) – cut off
d + $^{5}_{\Lambda}$H	-23.011 (B_Λ=4.1)	^{4}He + n + π^-	139.27*
2n + $^{5}_{\Lambda}$He	-3.567	^{4}He + p + π^-	102.42
3n + $^{4}_{\Lambda}$He	-24.868	^{3}He + p + π^-	103.15

Notes:

* $^{5}_{\Lambda}$H can have both 2- and 3- body mesonic decays due to the instability of ^{5}He to 1 n emission. The width of the possible g.s. peak in 2-body decay spectrum is broadened by the width of g.s. ^{5}He (648 keV FWHM).

2. Mesonic decays of ground state hyperfragments from $^{9}_{\Lambda}$Li when using ^{9}Be target

(The intrinsic width is based on the expected resolution of the JLAB experiment)

2-body decays

Breakup Mode	Q value (MeV)	π^- Decay	P_π (MeV/c)	Width (keV/c) FWHM
$^{9}_{\Lambda}$Li	-	^{9}Be + π^-	121.18	165
p + $^{8}_{\Lambda}$He	-13.817	^{8}Li + π^-	116.40	165
n + $^{8}_{\Lambda}$Li	-3.756	^{8}Be + π^-	124.12	165
2p + $^{7}_{\Lambda}$H	-40.328 (B_Λ=6.1)	^{7}He + π^-	135.17	~270*
d + $^{7}_{\Lambda}$He	-12.568	^{7}Li + π^-	114.61	165§
2n + $^{7}_{\Lambda}$Li	-12.218	^{7}Be + π^-	108.02	165
^{3}He + $^{6}_{\Lambda}$H	-29.608 (B_Λ=5.1)	^{6}He + π^-	133.47	165§
^{3}H + $^{6}_{\Lambda}$He	-9.745	^{6}Li + π^-	108.39	165§
3n + $^{6}_{\Lambda}$Li	-18.957	^{6}Be + π^-	100.58	~220**
α + $^{5}_{\Lambda}$H	-11.749 (B_Λ=4.1)	^{5}He + π^-	133.42	~900*§
n + α + $^{4}_{\Lambda}$H	-12.005	^{4}He + π^-	132.95	165§
^{6}He + $^{3}_{\Lambda}$H	-18.183	^{3}He + π^-	114.29	165§

3-body decays

Breakup Mode	Q value (MeV)	π^- Decay	P_π max (MeV/c) – cut off
2p + $^{7}_{\Lambda}$H	-40.328 (B_Λ=6.1)	^{6}He + n + π^-	137.42*
α + $^{5}_{\Lambda}$H	-11.749 (B_Λ=4.1)	^{4}He + n + π^-	139.27*
^{4}H + $^{5}_{\Lambda}$He	-12.729	^{4}He + p + π^-	102.42§
n + ^{4}H + $^{4}_{\Lambda}$He	-34.030	^{3}He + p + π^-	103.15§

Notes:

§ These hypernuclei can be seen when using ^{7}Li target, except change of fragmentation modes and required Q values.

* Same as $^{5}_{\Lambda}$H (see tables for ^{7}Li target), $^{7}_{\Lambda}$H (if exists) can have also both 2- and 3- body mesonic decays due to the instability of ^{7}He to 1 n emission. The width of the possible g.s. peak in 2-body decay spectrum is broadened by the width of g.s. ^{7}He (150 keV FWHM).

** $^{6}_{\Lambda}$Li peak in the 2-B spectrum will be broadened due to the instability of ^{6}Be to 2p emission. The width of g.s. ^{6}Be is 92 keV FWHM.

3. Mesonic decays of ground state hyperfragments from $^{12}_{\Lambda}$B when using ^{12}C target

(The intrinsic width is based on the expected resolution of the JLAB experiment)

2-body decays

Breakup Mode	Q value (MeV)	π^- Decay	P_π (MeV/c)	Width (keV/c) FWHM
$^{12}_{\Lambda}$B	-	^{12}C + π^-	115.49	165
p + $^{11}_{\Lambda}$Be	-12.280 (B_Λ=10.5)	^{11}B + π^-	109.66	165
n + $^{11}_{\Lambda}$B	-12.765	^{11}C + π^-	105.99	165
2p + $^{10}_{\Lambda}$Li	-32.908 (B_Λ=12.3)	^{10}Be + π^-	119.78	165
d + $^{10}_{\Lambda}$Be	-18.264	^{10}B + π^-	104.31	165
2n + $^{10}_{\Lambda}$B	-22.544	^{10}C + π^-	95.84	165
3p + $^{9}_{\Lambda}$He	-48.534 (B_Λ=7.8)	^{9}Li + π^-	117.83	165
^{3}He + $^{9}_{\Lambda}$Li	-30.237	^{9}Be + π^-	121.18	165[§]
^{3}H + $^{9}_{\Lambda}$Be	-16.072	^{9}B + π^-	96.88	165[*]
3n + $^{9}_{\Lambda}$B	-41.713	^{9}C + π^-	96.71	165
4p + $^{8}_{\Lambda}$H	-68.937 (B_Λ=7.1)	^{8}He + π^-	137.15	165
^{4}Li + $^{8}_{\Lambda}$He	-46.961	^{8}Li + π^-	116.40	165[§]
α + $^{8}_{\Lambda}$Li	-14.444	^{8}Be + π^-	124.12	165[§]
^{4}H + $^{8}_{\Lambda}$Be	-37.659	^{8}B + π^-	97.09	165
4n + $^{8}_{\Lambda}$B	-56.317 (B_Λ=6.7)	^{8}C + π^-	97.21	365[**]
p + ^{4}Li + $^{7}_{\Lambda}$H	-73.473 (B_Λ=6.1)	^{7}He + π^-	135.17	~270[*§]
^{5}Li + $^{7}_{\Lambda}$He	-26.436	^{7}Li + π^-	114.61	165[§]
^{5}He + $^{7}_{\Lambda}$Li	-25.782	^{7}Be + π^-	108.02	165[§]
^{6}Be + $^{6}_{\Lambda}$H	-48.317 (B_Λ=5.1)	^{6}He + π^-	133.47	165[§]
^{6}Li + $^{6}_{\Lambda}$He	-24.186	^{6}Li + π^-	108.39	165[§]
^{6}He + $^{6}_{\Lambda}$Li	-27.663	^{6}Be + π^-	100.58	~220[**§]
^{7}Be + $^{5}_{\Lambda}$H	-44.499 (B_Λ=4.1)	^{5}He + π^-	133.42	~900[*§]
2α + $^{4}_{\Lambda}$H	-22.693	^{4}He + π^-	132.95	165[§]
^{9}Be + $^{3}_{\Lambda}$H	-27.244	^{3}He + π^-	114.29	165[§]

3-body decays

Breakup Mode	Q value (MeV)	π^- Decay	P_π max (MeV/c) – cut off
$^3H + {}^9_\Lambda Be$	-16.072	$^8Be + p + \pi^-$	97.21*
$2p + {}^7_\Lambda H$	-40.328 (B_Λ=6.1)	$^6He + n + \pi^-$	137.42*
$\alpha + {}^5_\Lambda H$	-11.749 (B_Λ=4.1)	$^4He + n + \pi^-$	139.27*
$^4H + {}^5_\Lambda He$	-12.729	$^4He + p + \pi^-$	102.42§
$n + {}^4H + {}^4_\Lambda He$	-34.030	$^3He + p + \pi^-$	103.15§

Notes:

§ These hypernuclei can be seen when using ^{9}Be target, except change of fragmentation modes and required Q values.

* Same as $^5_\Lambda$H and $^7_\Lambda$H (see tables for ^{7}Li and ^{9}Be targets), $^9_\Lambda$Be g.s. can have also both 2- and 3- body mesonic decays due to the instability of ^{9}B to 1 p emission. However, the width of the g.s. ^{9}B is only 0.54 keV FWHM, thus this 3B decay does not affect 2-body decay peak width.

** Same as $^6_\Lambda$Li, the $^8_\Lambda$B peak in the 2-B spectrum will be broadened due to the instability of ^{8}C to 2p emission. The width of g.s. ^{8}C is 230 keV FWHM.

Appendix II: Previous E08-012 Proposal to PAC33

Note: The estimated decay π momentum spectroscopy in this proposal was not correctly done. Two body and three body decay channels for various hypernuclei were not properly evaluated and separated. Therefore, both of potential physics outcome and discovery, production yield rate, as well as sources of background were not fully identified properly. However, many physics discussions are good references for the new proposal.

Study of Light Hypernuclei by Pionic Decay at JLab

N. Grigoryan, S. Knyazyan, A. Margaryan (*spokesperson*), G. Marikyan,
L. Parlakyan, S. Zhamkochyan, H. Vardanyan
Yerevan Physics Institute, 375036 Yerevan, Armenia

M. Christy, C. Keppel, M. Kohl, Liguang Tang (*spokesperson*),
L. Yuan (*spokesperson*), L. Zhu
Department of Physics, Hampton University, VA 23668, U.S.A.

O. Hashimoto, S.N. Nakamura (*spokesperson*)
Department of Physics, Tohoku University, Sendai, 98-77, Japan

P. Markowitz, J. Reinhold (*spokesperson*)
Department of Physics, Florida International University, Miami, FL , U.S.A.

Ed.V. Hungerford
Department of Physics, University of Houston, Houston, TX 77204, U.S.A.

P. Bosted, A. Bruell, R. Ent, H. Fenker, D. Gaskell, T. Horn, M. Jones, S. Majewski,
G. Smith, W. Vulcan, S.A. Wood, C. Yan
Thomas Jefferson National Accelerator Facility, Newport News, VA 23606, USA

B. Hu, J. Shen, W. Wang, X. Zhang, Y. Zhang
Nuclear Physics Institute, Lanzhou University, China

J. Feng, Y. Fu, J. Zhou, S. Zhou
Department of Physics, China Institute of Atomic Energy, China

Y. Jiang, H. Lu, X. Yan, Y. Ye
Department of Modern Physics, University of Science & Technology of China, China.

D. Androic, M. Furic, T. Petkovic, T. Seva
Departments of Physics & Applied Physics, University of Zagreb, Croatia

A. Ahmidouch, S. Danagoulian, A. Gasparian
Department of Physics, North Carolina A&T State University, Greensboro, NC 27411, U.S.A.

G. Niculescu, I. Niculescu
Department of Physics, James Madison University, Harrisonburg, VA 22807, U.S.A.

E. F. Gibson
Department of Physics, California State University, Sacramento, CA 95819, U.S.A.

E. Cisbani, F. Cusanno, S. Frullani, F. Garibaldi, M.L. Magliozzi
Istituto Nazionale di Fisica Nucleare, Sezione di Roma, Gr. Coll. Sanita', Viale Regina Elena 299, Rome, Italy

M. Iodice
Istituto Nazionale di Fisica Nucleare, Sezione di Roma Tre, I-00146 Roma, Italy

G.M. Urciuoli
Istituto Nazionale di Fisica Nucleare, Sezione di Roma1, Piazza A. Moro, Rome, Italy

R. De Leo, L. Lagamba, S. Marrone
Istituto Nazionale di Fisica Nucleare, Sezione di Bari and University of Bari, I-70126 Bari, Italy

H.J.Schulze
Istituto Nazionale di Fisica Nucleare, Sezione di Catania, I-95123 Catania, Italy

Others to be confirmed

December 10, 2007

Abstract

We propose to investigate Λ hypernuclei in the A≤12 mass region by using decay pion spectroscopy. Binding energies and lifetimes of all separable hypernuclei or hyperfragments will be simultanuously measured with high precision. The project aims to determine precisely the binding energies of light hypernuclei, investigate production of exotic hypernuclei, and study impurity nuclear physics and the medium effect of baryons from lifetimes of identifiable low lying excited states determined by π^- mesonic decay.

These investigations will fully utilize the unique parameters (high intensity, small emittance, and fine beam bunch time structure) of the CW electron beam at Jefferson Laboratory, and are enabled by the use of the high-resolution kaon spectrometer (HKS) in combination with a high-resolution magnetic spectrometer for hypernuclear decayed pions (*HπS* -Enge) in Hall C (or in Hall A). The experimental system is almost identical to the HKS (E01-011) experiment completed in 2005.

Ground state binding energy measurement for light hypernuclei must have a resolution better than σ=100 keV in order to separate possible doublets. For the proposed experiment, their absolute values will be determined with a precision better than 10 keV while the energy resolution will be σ≈55 keV.

The lifetimes of all separatable hypernuclear states (including low lying excited states) can be measured by π^--mesonic decay. The timing resolution in determining the decay time is about 100 ps or better, thus suitable to measure lifetime in the range of 50-400 ps.

We propose to start by using existing spectrometers (HKS and Enge) and their detector packages, and two production targets ^{7}Li and ^{12}C. Upon successful establishment of the program, future experiments may select the targets focused for specific hypernuclear and nuclear physics.

1. Introduction

The binding energies of the Λ particle coupled to the nuclear core at ground state give one of the basic pieces of information on the Λ-nucleus interaction. Most of the observed hypernuclear decays take place from the ground states (or some of the long lived low lying states), because the electromagnetic interactions or Auger neutron emission process are generally faster than the weak decay of the Λ particle. The binding energy of Λ of a hypernucleus at ground state is defined by:

$$B_\Lambda(g.s.) = M_{core} + M_\Lambda - M_{HY}.$$

The mass M_{core} is merely the mass of the nucleus that is left in the ground state after the Λ particle is removed. The M_Λ and M_{HY} are the masses of Λ and ground state hypernucleus, respectively. The binding energies, B_Λ, have been measured in emulsion for a wide range of light ($3 \le A \le 15$) hypernuclei [1]. These have been made exclusively from the unique weak π^--mesonic decay of Λ. The precise values of the binding energies of Λ in the few-baryon systems provide filters through which one can look at particular aspects of the *YN* interaction, and one of the primary goals in hypernuclear physics is to extract information about *YN* interactions through precise calculations of few-body systems such as $^{3}_{\Lambda}H$, $^{4}_{\Lambda}H$, and $^{4}_{\Lambda}He$. The existing situation can be summarized by the help of words from R. Dalitz [2]:

"$^{3}_{\Lambda}H$ was well known very early and has been studied a great deal. Its B_Λ value is quite small and difficult to measure. It was the first hypernucleus to be considered a "Λ halo". The value of 0.13±0.05 MeV by Don Davis [1] quoted above was from emulsion studies. From HeBC studies, Keyes et al. [3] have given 0.25±0.31 MeV for all events ($^{3}He\pi^-$) but got -0.07±0.27 when they added in all other π^- modes, which is not reassuring. For $R_3 = n(^{3}He\pi^-)/n(^{3}H\pi^-\rightarrow$all π^- modes) they gave $R_3 = 0.36\pm0.07$, and consider this to correspond to $0.11^{+0.06}_{-0.03}$ MeV for its B_Λ value, I feel that we are far from seeing the end of this road. A good deal of theoretical work on this 3-body system would still be well justified."

In addition, a rich amount of physics associated with the new degree of freedom brought by Λ particle into the nuclear medium can be offered by the weakly decayed pions from various parent hypernuclear species as we will discuss in detail in the next chapter. High precision energy calibration to reduce systematic errors was difficult for emulsion and He bubble chamber (*HeBC*) besides very low statistics. In modern counter type of experiments using mesonic beams (such as pions and kaons), thick targets which were used to compensate the low beam intensity caused problems in poor resolution and precision of the order of a few MeV. High statistics and thin targets can be achieved by the FINUDA experiment using an e^+e^- collider to produce Φ mesons at rest, but the detector system cannot provide a resolution better than 2 MeV for the decay pions with momentum of about 100 MeV/c.

Recent accomplishment of high precision γ-spectroscopy experiments with resolution in the order of a few keV have demonstrated the power of studying the transitions from the electromagnetic decay of selectively excited hypernuclear states by the (K, π) or (π, K) reactions. However, γ-spectroscopy cannot provide information about the B_Λ of the ground states besides the limitation of selectivity on specific excited states.

Therefore, pionic decay spectroscopy with high energy resolution and precision in terms of binding energy determination and good statistics is highly attractive and needed. We propose a new experiment for precise measurement of the decay pions on their momenta and decay time for a light ($A \leq 12$) mass range of hypernuclei (ordinary or exotic, produced either directly or indirectly through the process of fragmentations) at CEBAF. Binding energies B_Λ and lifetimes on various hypernuclear species (ground states and separable low lying states) can be simultaneously obtained. JLAB is the unique and only facility to establish such a program because of the following reasons:

(1) High precision beam provides point reaction position on target;
(2) High intensity, 100% duty factor, and excellent kaon spectrometer (HKS) with large solid angle acceptance at small forward scattering angle besides its high momentum resolution (2×10^{-4}) and short path length, allow to use thin target to minimize the target loss uncertainty because of high production yield of hypernuclei;
(3) Because of high yield a high resolution low momentum spectrometer with reasonably large solid angle acceptance can be used to study the decay pions with high energy resolution of ~55 keV rms, sufficient to isolate states separated by ~120 keV or larger;
(4) Excellent calibration tool using elementary production of Λ particle can ensure a binding energy precision at the level of 10 keV; and
(5) Precise beam time structure and excellent production and decay time reconstruction capability from the high resolution spectrometers make possible to measure lifetimes in the range of 50-400 ps for all isolatable hypernuclear states with good precision.

Wide range of physics (to be discussed in the next chapter) can be studied from single experiment, such as precise B_Λ for ground states and low lying states of ordinary hypernuclei, investigation of exotic

hypernuclei toward neutron and proton drip-lines, study of impurity nuclear physics (probing nuclear structure by insertion of a Λ, glue-like role of Λ particle in the nuclear medium, and the medium effect of baryons).

We propose to carry out an experiment for these investigations by using the existing HKS+Splitter system and a HπS magnetic spectrometer (existing Enge spectrometer) in Hall C (or Hall A) with thin ^{12}C and ^{7}Li targets.

2. Physics Subjects

The physics subjects that can be pursued by precision hypernuclear spectroscopy are enlightening in particular in the current projects [4, 5] (see also [6-12]). The physics subjects which can be specifically studied but not limited by precise decay pion spectroscopy can be summarized as:

1) YN interactions,
2) Study of exotic hypernuclei, and
3) Impurity nuclear physics

2.1 YN interaction

From precise binding energy B_Λ of hypernuclear ground states and detailed low lying structure, we can establish the ΛN spin-dependent (spin-spin, spin-orbit, and tensor forces) interaction strengths, investigate ΣN-ΛN coupling force, and study charge symmetry breaking. Experimental information on these characteristics of the ΛN interaction plays an essential role to discriminate and improve baryon-baryon interaction models, not only those based on the meson-exchange picture but also those including quark-gluon degree of freedom, toward unified understanding of the baryon-baryon interactions. In addition, understanding of the *YN* and *YY* interactions is necessary to describe high density nuclear matter containing hyperons.

The binding energies of the ground state of light hypernuclei are the most valuable experimental information for checking different models of *YN* interaction. Table 1 taken from reference [12] lists the results of the Λ separation energies obtained as a result of ab initio calculations using *YN* interactions with an explicit Σ admixture. Experimental results from emulsion are listed as comparison and additional systematic error in the order of about 40 keV is not included. It is demonstrated that for future theoretical developments more precise experimental measurements for binding energies are needed. The precision of the proposed experiment can put further stringent limit on the theoretical models.

Table 1: Λ separation energies, given in units of MeV, of A = 3-5 Λ hypernuclei for different models of YN interaction.

YN	$B_\Lambda(^3_\Lambda H)$	$B_\Lambda(^4_\Lambda H)$	$B_\Lambda(^4_\Lambda H^*)$	$B_\Lambda(^4_\Lambda He)$	$B_\Lambda(^4_\Lambda He^*)$	$B_\Lambda(^5_\Lambda He)$
SC97d(S)	0.01	1.67	1.2	1.62	1.17	3.17
SC97e(S)	0.10	2.06	0.92	2.02	0.90	2.75
SC97f(S)	0.18	2.16	0.63	2.11	0.62	2.10
SC89(S)	0.37	2.55	Unbound	2.47	Unbound	0.35
Experiment	0.13 ± 0.05	2.04 ± 0.04	1.00 ± 0.04	2.39 ± 0.03	1.24 ± 0.04	3.12± 0.02

One good example is the binding energies of ${}^{4}_{\Lambda}H$ and ${}^{4}_{\Lambda}He$ hypernuclei, which show the charge symmetry breaking in *YN* interactions. In case of ${}^{4}_{\Lambda}H$, the high energy of the pion from the ${}^{4}_{\Lambda}H \rightarrow {}^{4}He + \pi^-$ two body decay should put it in a clean part of the spectrum (see Table 11 and Fig. 23 in Chapter 5, Section 5.4) and this two body decay has significantly more statistics over the decay modes. However, due to the large uncertain in the range-energy relationship in emulsion, the two body decay mode could not be used. In fact, the B_Λ values of ${}^{4}_{\Lambda}H$ and ${}^{4}_{\Lambda}He$ came from other decay modes in which the pion energy is similar to reduce systematic error. Since, so far, the values of B_Λ for light hypernuclei were almost determined only by emulsion, an accurate check on the emulsion values of B_Λ is important. Similar problems related to the emulsion values will be discussed further in the later parts of proposal.

In addition, with high precision and resolution the π^- decay can be used as effective tool to obtain spectroscopic information on hypernuclear structure, due to the selective character and sensitive shell-structure dependence [13, 14].

2.2 Study of exotic hypernuclei

There is currently in the nuclear physics community a strong interest in the study of nuclei very far from the valley of stability. It would allow one to comprehend the behavior of nuclear matter under extreme conditions. Hypernuclei can be even better candidates than ordinary nuclei to study nuclear matter with extreme N/Z ratios because more extended mass distributions are expected than in ordinary nuclei thanks to the glue-like role of the Λ due to the short range interaction nature by missing *OPE* force, and its effect on neutron halo [15] (such as the case of ${}^{7}_{\Lambda}He$). In Table 2 (see in later Chapter), especially, we see many particle stable hypernuclei with unstable nuclear cores: ${}^{6}_{\Lambda}He$, ${}^{7}_{\Lambda}Be$, ${}^{8}_{\Lambda}He$, ${}^{9}_{\Lambda}Be$. Other exotic hypernuclei with neutron excess may exit: e.g. ${}^{6}_{\Lambda}H$, ${}^{7}_{\Lambda}H$, ${}^{8}_{\Lambda}H$, ${}^{10}_{\Lambda}He$, ${}^{11}_{\Lambda}Li$ (see also [16, 17]). These hypernuclei and other exotic hypernuclei with neutron and proton excess are expected to be photo-produced indirectly through the process of fragmentation – hyperfragments - from heavier targets and their two-body pionic decays can be detected by *HπS*. Therefore, the proposed experiment is capable to search for and to precisely determine the binding energy of such exotic hypernuclei.

2.3 Impurity nuclear physics I

Since hyperons are free from the Pauli effect and feel nuclear forces different from those nucleons do in a nucleus, a hyperon introduced in a nucleus may give rise to various changes of the nuclear structure, such as changes of the size and the shape, change of the cluster structure, emergence of new symmetries, change of collective motions, etc. A beautiful example of how we may modify a nucleus by adding to it a distinguishable baryon in a well defined state is given by the experiment on γ-spectroscopy of ${}^{7}_{\Lambda}Li$. ${}^{7}_{\Lambda}Li$ is produced by means of the reaction $\pi^+ + {}^{7}Li \rightarrow {}^{7}_{\Lambda}Li + K^+$ at 1.05 GeV/c using the SKS spectrometer at KEK. ${}^{7}_{\Lambda}Li$ may be formed in the ground or low lying excited states. When a Λ in a 1s orbit is added to a loosely bound nucleus such as ${}^{6}Li$, the nucleus is expected to shrink into a more compact system due to the attractive force between Λ and nucleons ("glue-like" role of the Λ) which results from the property of the Λ of being free from the Pauli blocking in a nucleus. This effect can be verified from the E2 transition probability B(E2), which contains information of the nuclear size. The E2 ($5/2^+ \rightarrow 1/2^+$) transition of ${}^{7}_{\Lambda}Li$ is essentially the E2 ($3^+ \rightarrow 1^+$) transition of the core nucleus ${}^{6}Li$, but the existence of a Λ in the 1s orbit is expected to shrink the ${}^{6}Li$ core. Experimentally, B(E2) is derived from the lifetime of the $5/2^+$ state. The expected lifetime (~10^{-11} sec) is of the same order of the stopping time

of the recoil ${}^{7}_{\Lambda}Li$ in lithium in the case of the (π^+, K^+) reaction at 1.05 GeV/c and was derived to be $5.8^{+0.9}_{-0.7} \pm 0.7$ ps with the Doppler shift attenuation method (DSAM). B(E2) was then derived to be $3.6 \pm 0.5^{+0.5}_{-0.4}$ e^2fm^4. This result, compared with the B(E2) = 10.9 ± 0.9 e^2fm^4 of the core nucleus ${}^{6}Li$ ($3^+ \rightarrow 1^+$), indicates a shrinkage of the ${}^{7}_{\Lambda}Li$ size from ${}^{6}Li$ by about 20% [18, 19].

The Doppler shift attenuation method (DSAM) can be applied to measure lifetimes in the range of 10^{-12} – 10^{-11}sec, as in the B(E2) measurement of ${}^{7}_{\Lambda}Li$. For the M1 transition with energy about or less than 0.1 MeV and the E2 transition with energy around 1 MeV the expected lifetimes will be too long (~ 10^{-10}sec) for DSAM and the γ transition competes with weak decay. Thus a new "γ-weak coincidence method" has been proposed [20] for the future J-PARC experiment.

This method is to determine the transition probability from the total decay rate (λ_B) of the upper state B (see in Fig. 1) and branching ratio (m) of the γ decay. The lifetime of B is directly measured from the time difference of hypernuclear production and emission of weak-decay particles (p and π^-). If γ transitions to populate B state from upper states (such as C) are much faster than the total decay rate of B(λ_B), as is usually the case for a small ground doublet spacing, the time spectrum of weak decay particles measured in coincidence with the $B \rightarrow A\gamma$ ray is expressed as:

$$P^{B\rightarrow A}(t) = \frac{\lambda_A \lambda_B}{\lambda_A - \lambda_B} m N_B (e^{-\lambda_A t} - e^{-\lambda_B t}),$$

where λ_A denotes the decay rate of A and N_B denotes the initial population of the state B (including $C \rightarrow B$). From this growth-decay function, λ_A and λ_B can be determined.

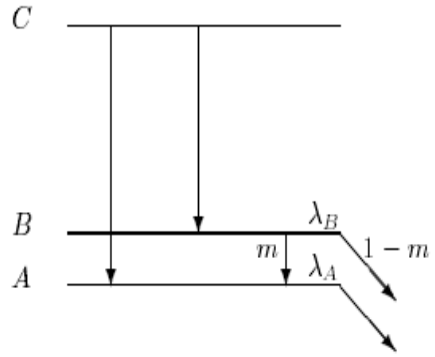

Figure 1: Method of B(E2) and B(M1) measurement from coincidence events of γ-ray and weak-decay particles.

When the $B \rightarrow A$ transition is much slower than the weak decay, λ_B is determined from the time spectrum of weak decay particles in coincidence with $C \rightarrow B\,\gamma$ rays, which is expressed as:

$$P^{C\rightarrow B}(t) = \lambda_B N_B^{C\rightarrow B}[(1 - m\frac{\lambda_B}{\lambda_B - \lambda_A})e^{-\lambda_B t} + m\frac{\lambda_A}{\lambda_B - \lambda_A}e^{-\lambda_A t}].$$

Here, $N_B^{C\to B}$ is the population of B via the fast C$\to$B transition. In general by measuring both $P^{B\to A}(t)$ and $P^{C\to B}(t)$, and fitting them to the equations above, λ_B can be determined precisely in a wide range. The branching ratio m of the B$\to$A transition is measured from the γ-ray yield of B$\to$A transition in coincidence with the C$\to$B transition.

In our case the high momentum resolution and high time resolution of *HπS* allow us to separate the A and B states (see e.g. in Fig. 2) and to measure the weak decay time spectra $P^{B\to weak}(t)$ and $P^{A\to weak}(t)$ separately from the pionic decays. The time spectrum of weak-decay pions from the B state can be expressed as:

$$P^{B\to weak}(t) = (1-m)\lambda_B(\lambda_B^{\pi^-}/\lambda_B)N_B e^{-\lambda_B t},$$

while the time spectrum of weak-decay pions from A state consists with two parts:

$$P^{A\to weak}(t) = (P^{B\to A}(t) + \lambda_A N_A e^{-\lambda_A t})(\lambda_A^{\pi^-}/\lambda_A),$$

Where $\lambda_A N_A e^{-\lambda_A t}$ corresponds to the weak decay of initial N_A population of the state A, including C$\to$A transitions, $\lambda_A^{\pi^-}$ and $\lambda_B^{\pi^-}$ are the π^- decay rates from A and B states, respectively. The other part, $P^{B\to A}(t)$, is the weak decay time spectrum of the state A populated due to the B$\to$Aγ electromagnetic transition and it is exactly the same as in the case of "γ-weak coincidence method" presented above. In general the weak decay rates of A and B states can be the different, i.e.

$$\lambda_A = \lambda_W^A, \quad \lambda_B = \lambda_W^B + \lambda_\gamma^{B\to A} \text{ and } m = \frac{\lambda_\gamma^{B\to A}}{\lambda_\gamma^{B\to A} + \lambda_W^B}.$$

By measuring both of $P^{B\to weak}(t)$ and $P^{A\to weak}(t)$ and fitting them together to the equations above, λ_W^A, λ_W^B and m can be determined. Indeed, from $P^{B\to weak}(t)$ distribution the decay constant λ_B can be determined precisely. By using this and growth-decay function $P^{A\to weak}(t)$, the λ_A, and m can be determined. We call it the "tagged-weak pi-method". In this method the time measuring precision is a key issue. With the precision of our experiment, it can be used for investigating the E2 or M1 transitions with lifetimes in the range of about 50-400 ps. Since the "γ-weak coincidence method" is a high-statistical triple coincidence experiment, it need a long beam time of a few weeks per target with the full beam intensity at future experiments at J-PARC. Also it is impossible to apply for study of hyperfragments in which γ transitions like C$\to$B is absent. Therefore, our experiment will provide complementary results to the "γ-weak coincidence" experiment at J-PARC and may have significant advantages on some hypernuclei.

2.3.1 Medium effect of baryons – B(M1) measurement

Using hyperons free from the Pauli effect, we can investigate possible modification of baryons in nuclear matter through magnetic moments of hyperons in a nucleus. Magnetic moments of baryons can be well described by the picture of constituent quark models in which each constituent quark has a magnetic moment of a Dirac particle having a constituent quark mass. If the mass (or the size) of a baryon is changed in a nucleus by possible partial restoration of chiral symmetry, the magnetic moment of the baryon may be changed in a nucleus. A Λ particle in a hypernucleus is the best probe to see

whether such an effect really exists or not. Here we propose to derive a g-factor of Λ in the nucleus from a probability (B(M1) value) of a spin-flip M1 transition between hypernuclear spin-doublet states. In the weak coupling limit between a Λ and a core nucleus, the B(M1) is expressed as [21]:

$$B(M1) \propto \left|\left\langle \phi_{lo} \left| \mu^z \right| \phi_{up} \right\rangle\right|^2 = \left|\left\langle \phi_{lo} \left| g_N J_N^z + g_\Lambda J_\Lambda^z \right| \phi_{up} \right\rangle\right|^2 \propto (g_N - g_\Lambda)^2,$$

where g_N and g_Λ denote effective g-factors of the core nucleus and the Λ, and J_N^z and J_Λ^z denote their spin operators, respectively. Here the space components of the wave functions of the lower and upper states of the doublet (ϕ_{lo}, ϕ_{up}) are assumed to be identical.

Transition probabilities such as B(M1) are derived from lifetimes of low lying excited states, using the "Doppler shift attenuation method" or "γ-weak coincidence method" [7, 8, 20]. We propose to use "tagged-weak pi-method" in our experiment.

2.3.2 Example of $^7_\Lambda He$

We will focus on the example of $^7_\Lambda He$ to demonstrate the ability of the π^- decay spectroscopy and compare it with the γ-ray spectroscopy. We will follow reference [6], where the $^7_\Lambda He$ experiment, planned at J-PARC with the $^7Li(K^-, \pi^0)$ reaction and high resolution π^0 spectrometer, is described.

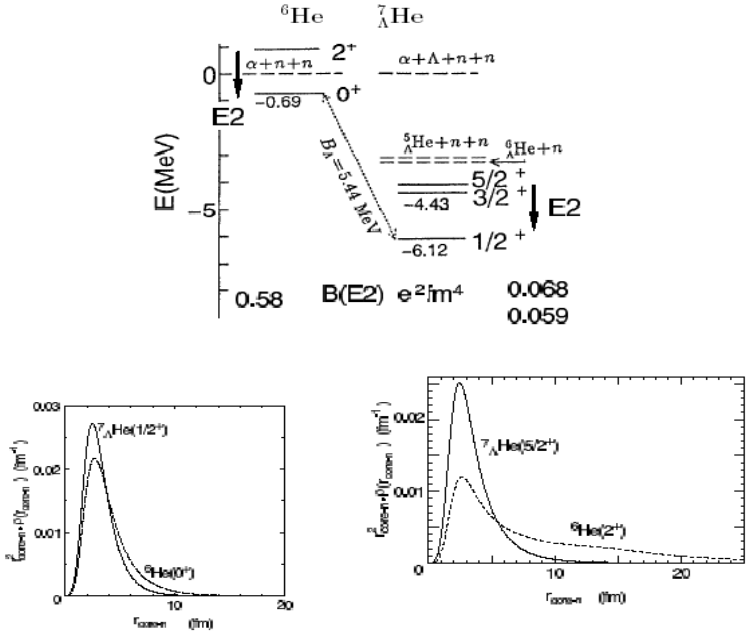

Figure 2. Top: Expected level scheme of $^7_\Lambda He$ and $B(E2)$ calculated by Hiyama et al. with a 3-body $^7_\Lambda He$+n+n cluster model [15]. Bottom: Calculated density distribution of valence neutrons are compared for $^6He(0^+)$ and $^7_\Lambda He(1/2^+)$, and for $^6He(2^+)$ and $^7_\Lambda He(5/2^+)$.

The ^6He is a neutron-rich nucleus having a two-neutron skin. The first excited state of 2^+ is observed as an unbound resonance state (see Fig. 2 taken from [6]), but its structure is not well known; the $B(E2; 2^+ \rightarrow 0^+)$ has not been experimentally obtained. Fig. 2 shows the expected level scheme and

the density distribution of valence neutrons of ^{6}He and $^{7}_{\Lambda}He$ calculated by Hiyama et al., with a cluster model for α+n+n and $^{5}_{\Lambda}He$+n+n [15]. When we add a Λ to ^{6}He, the neutron skin in the ground state is expected to shrink. The $^{6}He(2^+)$ state, which has widely-spread two valence neutrons, becomes bound by a Λ , and the core E2 transitions ($5/2^+$, $3/2^+ \rightarrow 1/2^+$) are observed. The $B(E2)$ of ^{6}He ($E2$; $2^+ \rightarrow 0^+$) is calculated to be 0.58 e^2fm^4, while the corresponding $B(E2)$ of $^{7}_{\Lambda}He$ is calculated to be 0.068 and 0.059 e^2fm^4 for $5/2^+ \rightarrow 1/2^+$ and $3/2^+ \rightarrow 1/2^+$ transitions, respectively [15]. The predicted change of $B(E2)$ is caused by a drastic shrinkage of valence neutron wavefunctions in ^{6}He induced by a Λ , as shown in Fig. 2 (taken from [6]).

In the present case, these $E2$ transitions are competing against weak decay. If we assume the weak decay rate of these states to be $(200\ ps)^{-1}$, then it is expected that the lifetimes of these states are 140 ps and 170 ps, and that the branching ratios for the E2 transitions are 42% and 17%. We will directly measure the lifetimes of these excited states with tagged-weak pi method and consequently the branching ratios of these E2 transitions, from which the $B(E2)$'s can be derived.

In the $^{7}_{\Lambda}He$ experiment at J-PARC, the $^{7}Li(K^-, \pi^0)$ reaction will be used with the high-resolution π^0-spectrometer. There are no hope that the production peaks for the $5/2^+$, $3/2^+$, and $1/2^+$ states will be resolved. Even in order to separately identify production peaks for the ($5/2^+ + 3/2^+$) and $1/2^+$ states which are expected to be 1.7 MeV apart from each other, the π^0 spectrometer should have a resolution better than 2 MeV FWHM. In the J-PARC experiment 1700 events for weak decay particles and 330 events for the $E2$ γ-rays in a beam time of 10 days is expected [6]. Statistical accuracy for $B(E2)$ will be less than 10%, although it may have a systematic error from decomposition of the $3/2^+$ (T=1) peak from the $5/2^+$ (T=1) peak in the $^{7}Li(K^-, \pi^0)^{7}_{\Lambda}He$ reaction spectrum.

We propose to employ the "tagged-weak pi-method" to measure $B(E2)$'s for $5/2^+ \rightarrow 1/2^+$ and $3/2^+ \rightarrow 1/2^+$ transitions of $^{7}_{\Lambda}He$ produced with the $^{7}Li(\gamma, K^+)^{7}_{\Lambda}He$ reaction. Due to high momentum and time resolutions of the Enge spectrometer, the expected monochromatic pions from the $5/2^+$, $3/2^+$, and $1/2^+$ states will be isolated cleanly (see Fig. 3) and the lifetimes of those states will be determined precisely. From the measured lifetimes the $B(E2)$'s of the $5/2^+ \rightarrow 1/2^+$ and $3/2^+ \rightarrow 1/2^+$ transitions can be determined separately. The expected statistical accuracies will be less than 10% in a beam time of 20 days and results will be almost free from systemic error.

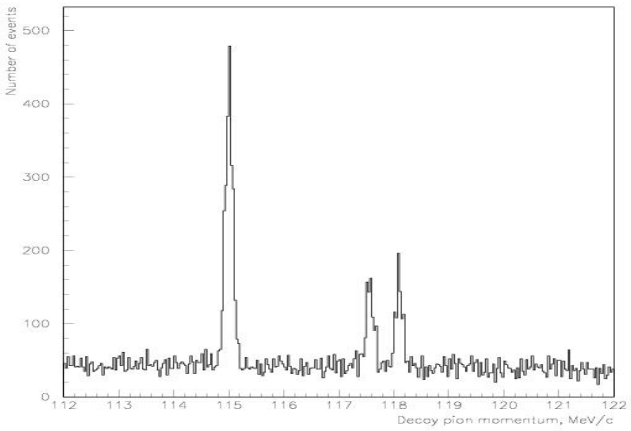

Figure 3: Simulated spectrum of the decayed pions from $^{7}_{\Lambda}He \rightarrow {}^{7}Li + \pi^-$ decay [21] (96.8% - quasi-free, 2% - 115.06, 117.63 and 118.15 MeV/c monochromatic lines each with 0.6% probability). The monochromatic lines corresponds binding energies: 5.44, 3.75, and 3.4 MeV, respectively. Target

thickness is 25 mg/cm^2, precision of the $H\pi S$ is σ = 4.9×10^{-4}, and target energy loss uncertainty is included (see experimental discussions later). Total number of events is 10^5.

The weak decays from the 5/2$^+$, 3/2$^+$, and 1/2$^+$ states can explain the observed large spread of binding energy values of $^{7}_{\Lambda}He$, measured in emulsion, which was interpreted by Pniewski and Danysz [22] as a weak decay from a long-lived isomeric states. If indeed the energy separation of the 5/2$^+$ and 3/2$^+$ states is large enough for this experiment and their lifetimes are long enough, the "tagged-weak pi-method" will be an ideal tool to investigate this and other similar long-lived states of directly produced hypernuclides or indirectly produced hyperfragments.

2.3.3 Example of $^{11}_{\Lambda}B$

We will consider the $^{11}_{\Lambda}B$ as another hypernucleus for which the π^--decay spectroscopy can play crucial role. The $^{11}_{\Lambda}B$ hypernucleus is expected to have many bound states and is suitable for a test of the ΛN interaction parameters and the theoretical framework. This hypernucleus have been studied via γ-ray spectroscopy by (π^+, K^+) reaction (KEK, E518 Experiment) and six transitions was observed (see [8] and references therein), but only two of them was assigned.

Fig. 4 taken from [8] is the expected level scheme of $^{11}_{\Lambda}B$. The 1483 keV γ-ray peak was assigned to $E2(1/2^+ \rightarrow 5/2^+(gs))$ transition calculated by Millener [23]. But this energy could not be explained by the interaction parameters determined from the γ-spectroscopy of other light hypernuclei. Millener's shell-model calculation:

$$E2(1/2^+ \rightarrow 5/2^+(gs)) = -0.243\Delta - 1.234S_{\Lambda} - 1.090S_N - 1.627T + E_{core}(MeV),$$

with E_{core} = 0.718, gives 1020 keV. The 264 keV γ-ray peak was assigned to be the spin-flip $M1$ transition in the ground states doublet (7/2$^+$ → 5/2$^+$). Also, this energy is lower than the expected value of 418 keV. The other γ-ray peaks were not able to be assigned. More $^{11}_{\Lambda}B$ data for level energies are necessary to solve the problem and a detail study of the problem is planned at J-PARC via γ-ray spectroscopy [8].

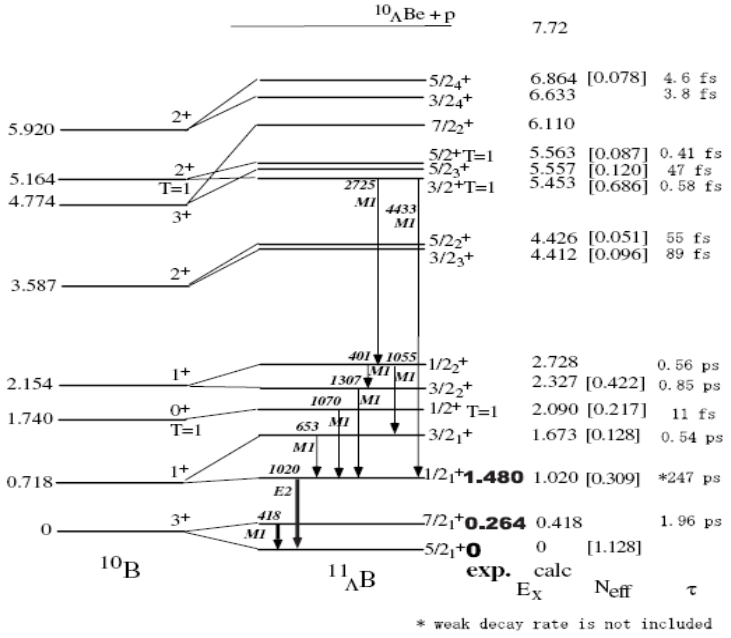

Figure 4: Expected level scheme of $^{11}_{\Lambda}B$ calculated by Millener [23]. Transitions and level energies measured by KEK E518 and E566 experiments are shown in thick arrows (from [8]).

Abundant production of excited $^{11}_{\Lambda}B^{*}$ hyperfragments is expected in the (γ, K^{+}) reaction on ^{12}C target as a result of Auger neutron emission of the photo-produced $^{12}_{\Lambda}B^{*}$ hypernucleus in high energy excited states. All the high energy excited states of $^{11}_{\Lambda}B^{*}$ hypernucleus should eventually be accumulated into $1/2^{+}$ state via γ-ray emissions (see Fig. 4) which according to theoretical prediction must have lifetime 247 ps, without weak decay rate. Therefore, weak decay and in particular the weak π^{-}-decay spectra from $1/2^{+}$ and $5/2^{+}$(*gs*) states must be observed. So this is another example of hyperisomer, besides of $^{7}_{\Lambda}He$ hypernucleus. Here is worthy to mention that the binding energy spectrum of $^{11}_{\Lambda}B$ hypernucleus measured by emulsion does not have large spread as in the case of $^{7}_{\Lambda}He$ hypernucleus, but shows Gaussian like shape (see later Fig. 10 and [28]). This is another puzzle relative to $^{11}_{\Lambda}B$.

Fig. 5 shows the simulated decay π^{-} spectra (assuming 87% q.f. and 1% for each of the $1/2^{+}$ and $5/2^{+}$ states for which the relative strength is not available experimentally nor theoretically), which demonstrate the ability of the proposed experiment. Results which can be obtained in the proposed experiment complementary to more γ-ray data from the future J-PARC E13 experiment [8] can help to solve the problem.

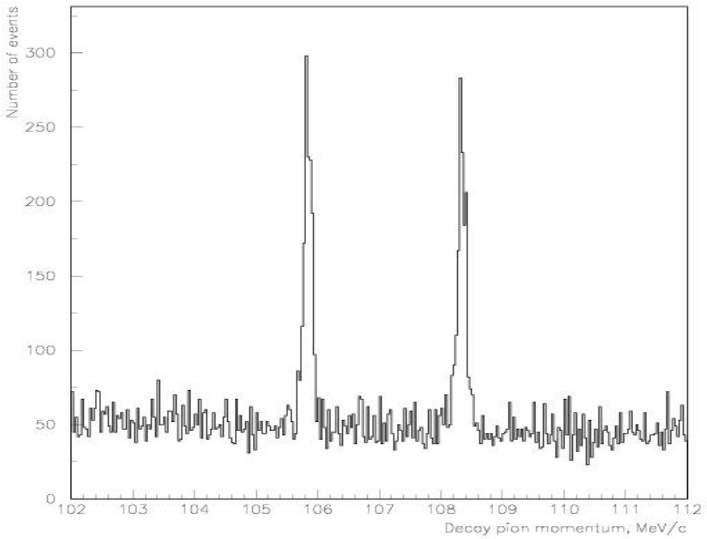

Figure 5: Simulated spectra of the decayed π^{-} from $^{11}_{\Lambda}B \rightarrow {}^{11}C + \pi^{-}$ decay (87% quasi-free, 105.9 and 108.4 MeV/c monochromatic lines each assumed with 1% probability). The monochromatic lines corresponds binding energies of ground $5/2^{+}$ and excited $1/2^{+}$ (1483 keV) states, respectively. Target thickness is 25 mg/cm^2, resolution of the $H\pi S$ is $\sigma = 4.9\times10^{-4}$, and pion energy loss uncertainty is included (see experimental discussions later). Total number of events is 10^5.

From these examples we can conclude that, the beauty of the high precision and high resolution π^{-}-decay spectroscopy is that it not only provides precise binding energy and lifetime of ground states of hypernuclei produced either directly (through photo-production) or indirectly (through fragmentations) as clear references (see later Fig. 19 and 20 in case of ^{12}C target), but also can measure the binding energy and lifetime of the low lying states which may have significant π^{-}-weak decay rate or long

lifetime. In contrast, high precision γ-spectroscopy measures only the level transitions without the knowledge of ground state as reference. Therefore, the "tagged-weak pi-method" has clear advantages for investigation on some hypernuclear species and can provide good complementary information to the γ-spectroscopy program planned at J-PARC. It is the combination of the CEBAF beam and the HKS system makes it possible.

2.4 Impurity nuclear physics II

The Λ in a hypernucleus weak decays by either pion emission (mesonic decay), which is the decay mechanism of a Λ in free space, or by the strangeness changing weak vertex in the reaction $\Lambda + N \rightarrow N + N$, where N is either a proton or neutron (non-mesonic decay). Non-mesonic decay has been extensively studied because the ratio of neutron stimulated to proton stimulated decay was significantly different from theoretical expectations. This problem now seems to be resolved as new nucleon-nucleon coincidence measurements, and improved theoretical calculations are in better agreement. There is still a problem with the measurement of the decay asymmetry of a polarized hypernucleus, so the issue of the mechanisms of non-mesonic decay are not completely settled, and in particular, the applicability of the $\Delta I = 1/2$ rule remains.

On the other hand, mesonic decay, at least of single Λ hypernuclei, has not really been of interest in the last 20 years or so. Early studies of hypernuclei used mesonic decay to obtain binding energies and the spin/parities of light hypernuclear systems. However, the hypernucleus transitions to the ground state before weak decay, and the momentum of the recoiling nucleon in the decay $\Lambda \rightarrow \pi N$ is below the Fermi surface for A≥6. Therefore, mesonic decay becomes significantly inhibited for masses beyond the middle of the 1p shell. In addition, experimental equipment capable of high resolution detection of pions emitted from a tagged hypernuclear reaction was unavailable. However, we point out in this proposal that the well understood weak decay of the Λ can be used as a tool to explore nuclear structure when strangeness is injected into the nuclear medium.

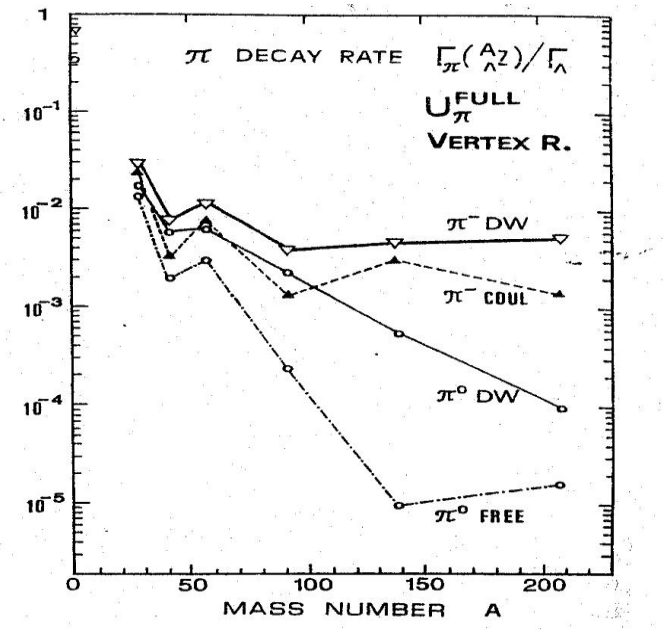

Figure 6: Λ mesonic decay in the nuclear medium to the free decay rate as a function of mass A.

Fig. 6 shows the mesonic decay rate in the nuclear medium to that in free space as various improvements are made in the calculations [13]. There is no available experimental data. Although inclusion of pion distortion, which allows the nucleon to obtain a momentum greater than that of the Fermi surface, enhances both π^0 and π^- decay, Coulomb distortion raises the π^- decay rates to measurable levels. Indeed, the prediction is that the ratio of the in-medium to free rate saturates at about 10^{-2}. However, another calculation, which predicts somewhat similar behavior, results in a rate about a factor of 10 lower for the case of ^{208}Pb [24].

The ratio of the in-medium to free Λ decay rate in the p shell hypernuclei is shown in Fig. 7. The calculation uses the MSU pion-nucleus interaction [25]. Aside from distortion effects as described above, the interesting structure in the decay systematics is due to nuclear shell structure. For example, in $^{12}_{\Lambda}$C, $\Gamma_{\pi 0}$ is higher than Γ_{π^-} even though π^- decay is a factor of 2 larger (isospin). This is because some T=0 states are accessible in π^0 decay at these momentum transfers. Therefore detailed systematics of pion decays offer insights into the hypernuclear and nuclear structure, and the momentum dependence of the single particle wave functions.

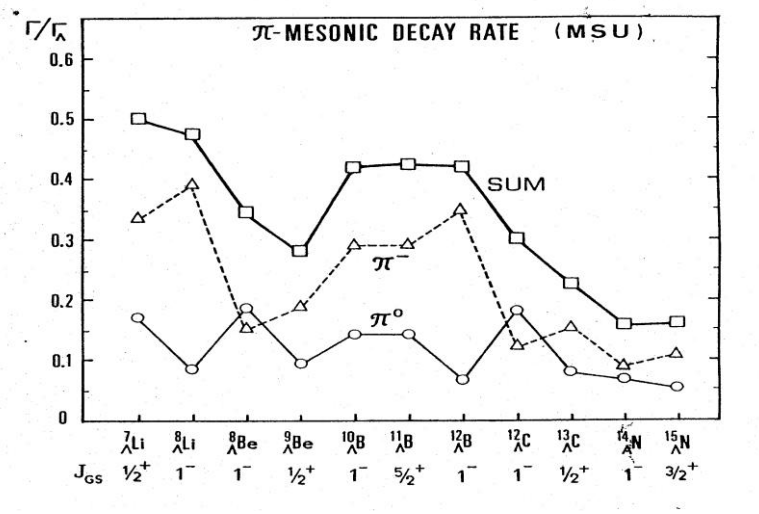

Figure 7: Λ mesonic decay rate in the nuclear medium to the free decay rate for the 1p shell nuclei.

Finally, mesonic decays are dependent on the spins and isospins of the initial and final states, as indicated in the preceding paragraph. Recall that hypernuclei generally transition by gamma emission to the ground state where they weak decay. In some situations, where the ground state is a hyperfine doublet, weak decay from the upper level can successfully compete with an electromagnetic transition. This occurs for higher multi-polarity gamma decays where the transition energy is small. An example of this is possibly the 1^- and 2^- doublet in $^{10}_{\Lambda}$B where the gamma ray between these two levels has not been seen [26, 27]. Either the gamma transition is <100 keV or the level ordering of the spin is reversed. Fig. 8 shows the predicted π^- decay of $^{7}_{\Lambda}$Li to various levels in ^{7}Be. The panel on the left shows decay from the normal order of the doublet spins (1/2 lower that 3/2), and the panel on the right shows the decay if the ground state spins are reversed. In this case other measurements confirm that the spins of the

ground state has the normal order, but it is obvious from the figure that π^- could be used to determine the spin ordering.

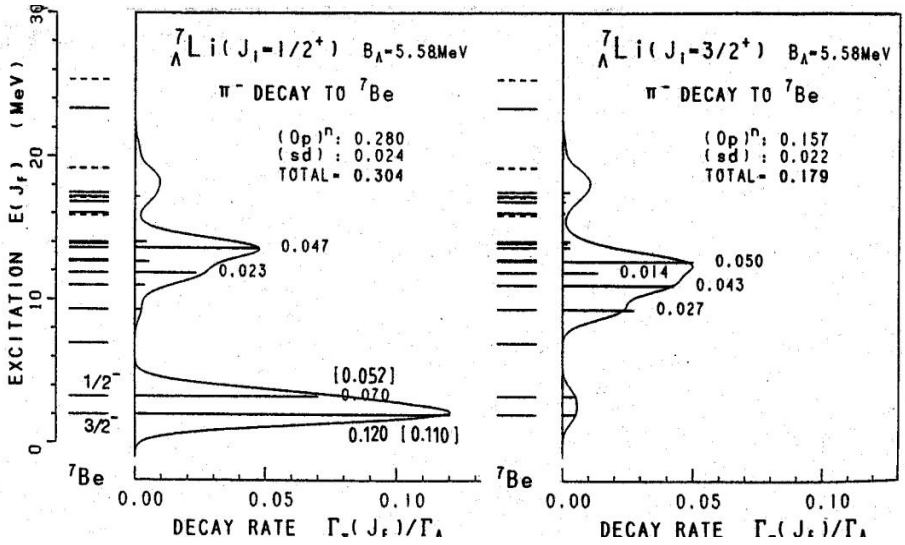

Figure 8: Relative pion decay yields if the hypernuclear ground state has spin 1/2 (left) or 3/2 (right).

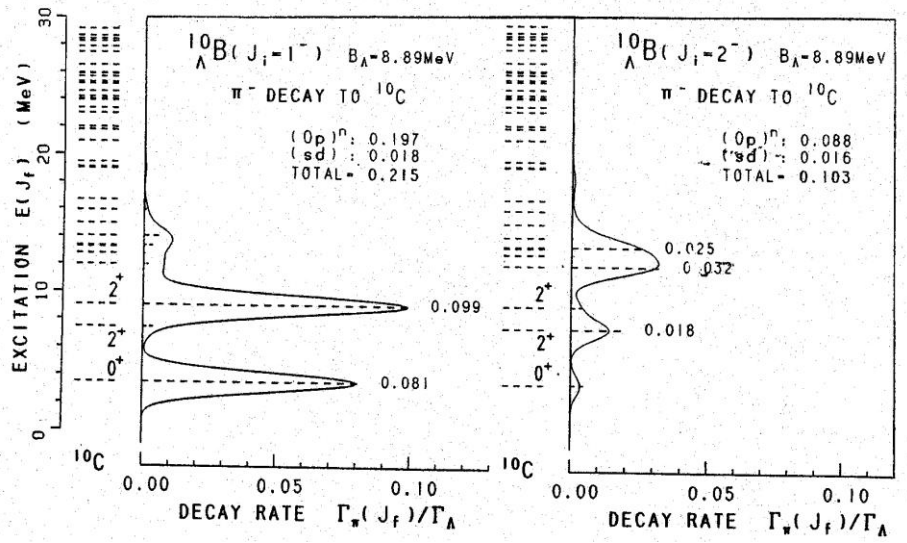

Figure 9: Relative pion decay yields if the hypernuclear ground state has spin 1/2 (left) or 3/2 (right).

For the case of $^{10}_{\Lambda}$B, where the ordering of the doublet spins is not known, the predicted π^- decays for normal order (left) and inverted order (right) show that π^- decay is sensitive to the spin sequence, see Fig. 9. In the most likely case where there is a mixture of weak decays from the doublet levels, a more detailed analysis would be required to extract the decay ratios and determine the

ordering. Note however, that measuring the transition energy of the decays requires the measure of an energy shift of <100 keV, which is possible if sufficient statistics are available, and this along with decay spectrum would allow the order to be determined. While the (e,e'K^+) reaction could not produce $^{10}_{\Lambda}$B, it could produce its isospin partner $^{10}_{\Lambda}$Be, whose level structure would be expected to be similar.

3. Previous Experiments and Current Projects

Λ hyperon separation energies B_Λ have been measured in emulsion for a wide range of light ($3 \le A \le 15$) hypernuclei. The kinematical analysis of the decayed fragments in nuclear emulsion in the past was the best method for determining the binding energy of the Λ particle in the hypernucleus. These have been made exclusively from π^--mesonic decays. Identification was established if one, and only one, energy and momentum balance was obtained after permuting all possible identities of the nuclear decay particles. The emulsion data on B_Λ values, culled from some 36000 π^--mesonic decaying hypernuclei produced by stopping K^- mesons [1, 28], are summarized in Table 2. This compilation included 4042 uniquely identified events.

Table 2: Λ binding energies B_Λ (MeV) of light hypernuclei measured in emulsion. In addition to the quoted statistical errors, there are systematic errors of about 0.04 MeV. Calculated corresponding decay pion momentum and number of observed events are presented as well.

Hypernucleus	B_Λ (MeV)	Decay π^- momentum (MeV/c)	Number of events
$^{3}_{\Lambda}H$	0.13 ± 0.05	114.3	204
$^{4}_{\Lambda}H$	2.04 ± 0.04	132.9	155
$^{4}_{\Lambda}He$	2.39 ± 0.03	97.97	279
$^{5}_{\Lambda}He$	3.12 ± 0.02	99.14	1784
$^{6}_{\Lambda}He$	4.18 ± 0.1	108.4	31
$^{7}_{\Lambda}He$	Not averaged 5.44-expected	115.1 (expected)	16
$^{7}_{\Lambda}Li$	5.58 ± 0.03	107.9	226
$^{7}_{\Lambda}Be$	5.16 ± 0.08	95.8	35
$^{8}_{\Lambda}He$	7.16 ± 0.7	116.3	6
$^{8}_{\Lambda}Li$	6.80 ± 0.03	124.1	787
$^{8}_{\Lambda}Be$	6.84 ± 0.05	97.17	68
$^{9}_{\Lambda}Li$	8.53 ± 0.15	121.1	8
$^{9}_{\Lambda}Be$	6.71 ± 0.04	95.96	222
$^{9}_{\Lambda}B$	8.29 ± 0.18	96.72	4
$^{10}_{\Lambda}Be$	9.11 ± 0.22	104.3	1
$^{10}_{\Lambda}B$	8.89 ± 0.12	100.5	10
$^{11}_{\Lambda}B$	10.24 ± 0.05	105.9	73
$^{12}_{\Lambda}B$	11.37 ± 0.06	115.8	87

The results of the compilation are illustrated also in Fig. 10 giving the B_Λ distributions for all the hypernuclear species, from which it follows that the binding energy resolutions in emulsion lies in the range 0.5-1.0 MeV. As mentioned earlier, from HeBC studies, Keyes et al. [3] have given $B_\Lambda({}^3_\Lambda H) = 0.25 \pm 0.31$ MeV for all events (${}^3He\pi^-$) but got $B_\Lambda({}^3_\Lambda H) = -0.07 \pm 0.27$ MeV when they added in all other π^- modes.

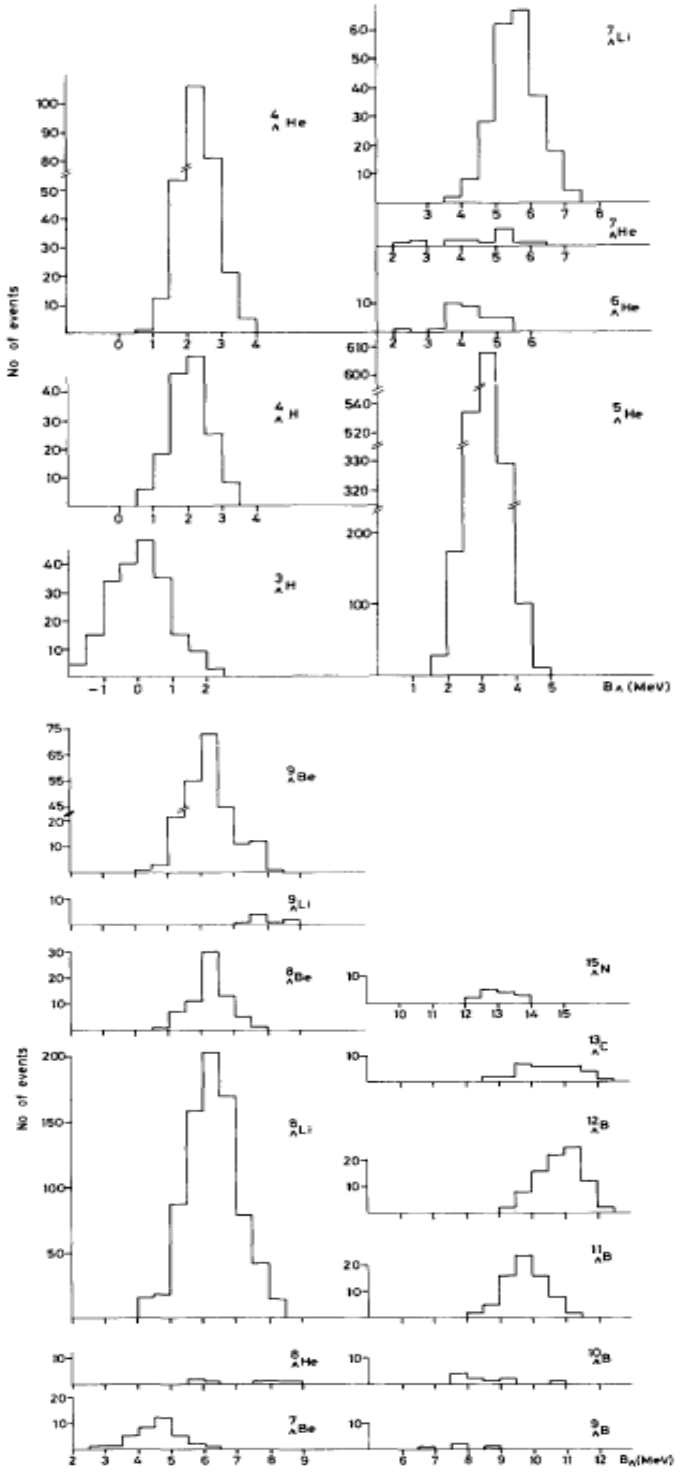

Figure 10: Distributions of the B_Λ values for the hypernuclei of mass number $A \leq 15$. Figure is taken from reference [28].

The Λ binding energies for some light hypernuclei in the upper part of p shell were also measured by mass spectroscopy using the (π^+, K^+) reaction (see e.g. the review paper of Hashimoto and Tamura [7]) and are summarized in Table 3, where the corresponding emulsion data are presented as well for comparison.

Table 3: Λ binding energies B_Λ (MeV) of light hypernuclei measured in emulsion and in (π^+, K^+) reaction spectroscopy. In addition to the quoted statistical errors, there is a systematic error of about 0.36 MeV in the (π^+, K^+) reaction data.

Hypernuclide	B_Λ (MeV) emulsion	B_Λ (MeV) (π+, K^+) reaction spectroscopy
$^{7}_{\Lambda}Li$	5.58 ± 0.03	5.22 ± 0.08
$^{9}_{\Lambda}Be$	6.71 ± 0.04	5.99 ± 0.07
$^{10}_{\Lambda}B$	8.89 ± 0.12	8.1 ± 0.1
$^{12}_{\Lambda}C$	10.76 ± 0.19	10.8 (adjusted)
$^{13}_{\Lambda}C$	11.69 ± 0.12	11.38 ± 0.05

Since the absolute mass scales of (π^+, K^+) reaction spectroscopy could not be calibrated precisely, they were thus adjusted (or normalized) using as a reference the $^{12}_{\Lambda}C$ ground-state peak, whose binding energy is determined by the emulsion experiments to be 10.76 MeV. Disagreement among the other hypernuclei is obvious, especially for $^{7}_{\Lambda}Li$, $^{9}_{\Lambda}Be$, and $^{10}_{\Lambda}B$. Unlike the $^{12}_{\Lambda}B$ which has easily recognizable $3\alpha + \pi^-$ decay mode that resulted with better precision, the binding energy of the $^{12}_{\Lambda}C$ ground state was determined by only 6 events in emulsion experiment and analyzed by Dluzewski et al. [29]. Therefore, the binding energy of the $^{12}_{\Lambda}C$ ground-state cannot be considered well determined. In fact, it is believed that the more accurate value should be quite close to that of the $^{12}_{\Lambda}B$ ground state. In addition, for $^{7}_{\Lambda}Li$, $^{9}_{\Lambda}Be$, and $^{10}_{\Lambda}B$ there is also a problem that the ground state is not fully resolved from the excited states in the (π^+, K^+) reaction spectroscopy. This in part may also contribute to the disagreement.

These results and current theoretical investigations indicate the necessity and importance of new and precise measurement of the B_Λ values of these light hypernuclei. The high precision direct (e,e'K^+) spectroscopy and this proposed high precision decay pion spectroscopy which can measure many ground states of light hypernuclei produced directly or indirectly can make significant contribution.

The hypernuclear decayed discrete π^- spectra can be measured by using a magnetic spectrometer, but in conventional fixed target experiments employing mesonic beams, the need to use thick targets to gain yield rate introduces major limitations on the achievable resolution. The low yield prevents also the usage of spectrometer for decayed pions due to smaller solid anagle acceptance. The momentum resolution of the Tokyo group's magnetic spectrometer e.g. was ~1 MeV [30]. Nevertheless, the Tokyo group was the first to detect the decayed discrete π^- mesons from $^{4}_{\Lambda}H$ hyperfragments as a "*delayed-particle*" in the stopped K^- reactions by a magnetic spectrometer (see Fig. 11 taken from Ref. [31]). This result is a clear demonstration for a new hypernuclear spectroscopy by the π^- decay.

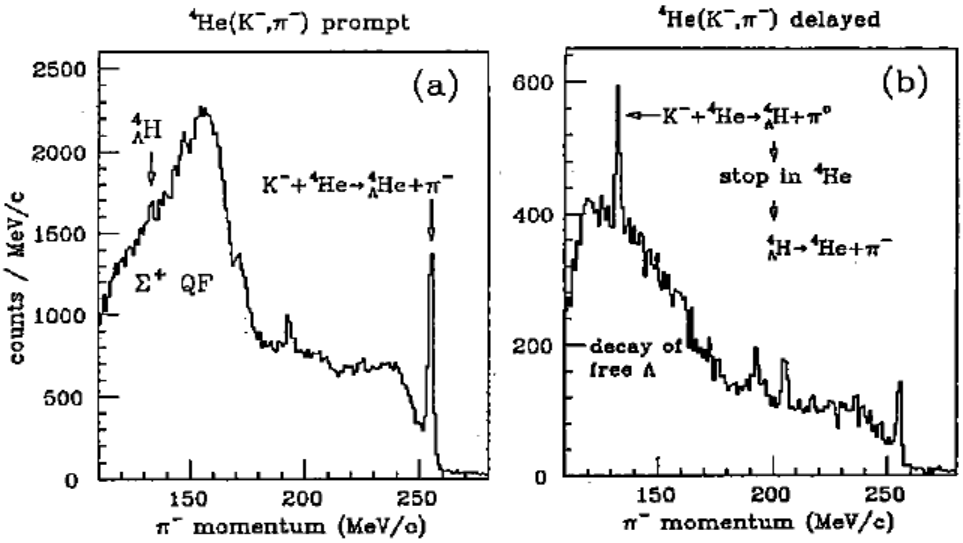

Figure 11: Time gated momentum spectra of π^- from K^- absorption at rest on ^4He target (from Ref. [31]. The $^4_\Lambda H$ peak is enhanced in the spectrum for delayed events: (a) $t_{react.} \leq 0.3$ ns (prompt events); b) $0.3 \leq t_{react.} \leq 1.5$ ns (delayed events).

The ongoing FINUDA experiment studies hypernuclei produced also by the stopped K^- reaction. Due to high low energy K^- production and stop rates, thin targets are allowed to be used. However, the momentum resolution of the FINUDA spectrometer [32] is about 2 MeV in the 100 MeV/c range. The proposed Cylindrical Detector System at J-PARC [6] is also about the same as that from FINUDA [32].

Therefore, the decay π^- study is highly interesting because it offers a rich amount of physics. However, resolution and precision are the keys to be successful.

4. Production of Hypernuclei

Any process which is capable of producing a Λ hyperon, may, when occurring in a nucleus, produce a hypernucleus. Two main mechanisms exist for hypernuclear formation, direct and indirect.

4.1 Direct production mechanism

Various Λ hypernuclear states can be directly populated by means of different reactions. The larger amount of data has been produced so far by means of the strangeness exchange two-body reaction: $K^- n \rightarrow \Lambda \pi^-$ on a neutron of a nucleus with K^- at rest and in flight. Recently, the associated production reactions, $\pi^+ n \rightarrow \Lambda K^+$ and $e p \rightarrow e' \Lambda K^+$, were also proved to be very efficient for producing Λ-hypernuclei at KEK and JLAB, respectively. The photon energy dependence of the elementary cross sections for the six isospin channels of kaon photo-production is shown in Fig. 12, taken from reference [33]. The cross section for the $\gamma p \rightarrow \Lambda K^+$ reaction rises sharply at the threshold energy Eγ = 0.911 GeV and stays almost constant from 1.1 to 1.6 GeV. From Fig. 12, it follows that in case of the photo-nuclear

reaction, we have three sources for K^+ mesons, with approximately equal weights. However, only the reaction $\gamma p \rightarrow \Lambda K^+$ is associated to the direct population of hypernuclear states.

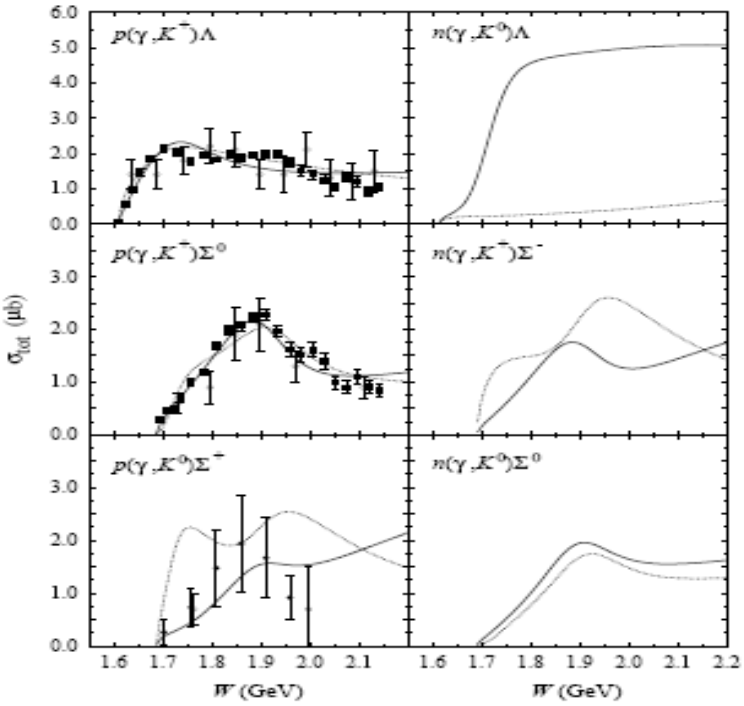

Figure 12: Total cross sections for the six isospin channels of kaon photoproduction on nucleon (from [33]).

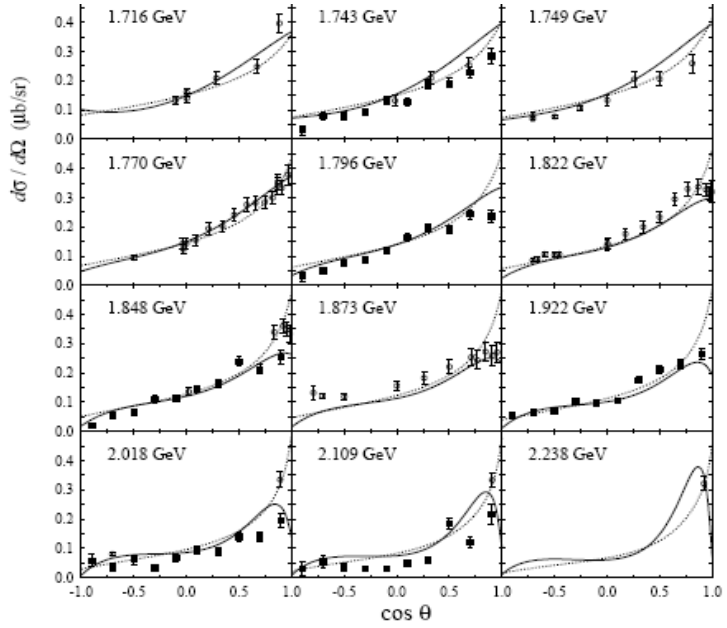

Figure 13: Differential cross section for $p(\gamma, K^+)$ channel. The total c.m. energy W is shown in every panel (for details see [33]).

The differential cross section of the $\gamma p \rightarrow \Lambda K^+$ reaction taken from [33] is shown in Fig. 13. From Fig. 13, it follows that at forward direction $d\sigma/d\Omega\,(0^o,\ \gamma p \rightarrow \Lambda K^+) \approx 0.35\ \mu b/sr$. The quasi-free kaon production cross section on the nucleus can be assumed to scale as $Z^{0.8}$[34] and for the differential cross section of the $^{12}C(\gamma,\ K^+)$ reaction we have about $d\sigma/d\Omega\,(0^o,\ \gamma\,^{12}C \rightarrow K^+ + X) \approx 4.2 \times 0.35 = 1.47\ \mu b/sr$.

The cross sections of the hypernuclear states for the targets ^7Li and ^{12}C have been calculated by Motoba and Sotona for the forward produced K^+ mesons [5, 35] (as well as measured with good agreement by the JLAB experiments in Hall C – HNSS and HKS). They are listed in Table 4. The angular distribution of kaons in the $^{12}C(e,\ e'K^+)^{12}{}_{\Lambda}B$ reaction is displayed in Fig. 14. As shown in Fig. 14, the angular distribution of kaons is forward peaked. From this distribution one can estimate that the total cross section is about $\sigma_t(^{12}C(e,e'K^+)^{12}{}_{\Lambda}B) = \int(d\sigma/d\Omega)d\Omega \approx 31\ nb$.

Table 4: Cross section $d\sigma/d\Omega(\theta = 0^\circ, \gamma + {}^AZ \rightarrow {}^A_\Lambda(Z-1) + K^+$ calculated by DWIA (from [5]).

Target	Hypernucleus	Hypernuclear configuration	Cross section (nb/sr)
^7Li	$^7_\Lambda He$	$s_{1/2}$ (1/2+)	21
		$s_{1/2}$ (3/2+, 5/2+)	9
^{12}C	$^{12}_\Lambda B$	$s_{1/2}$	112
		$p_{3/2}$	79
		$p_{1/2}$	45

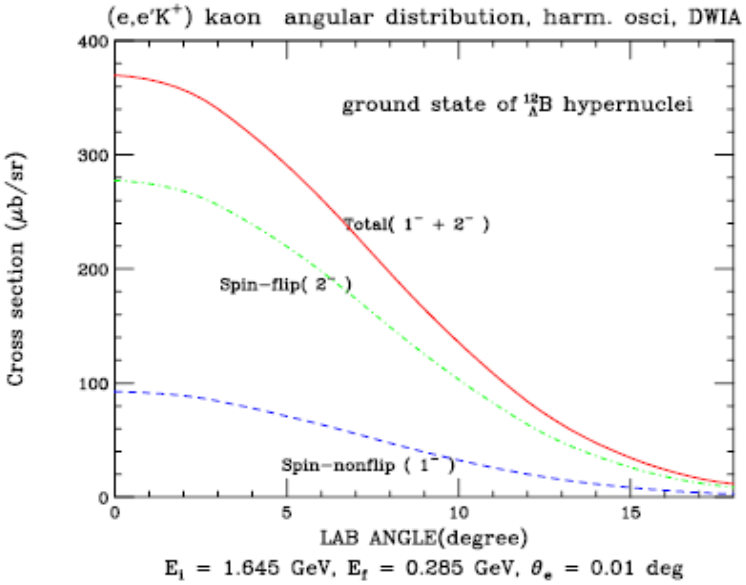

Figure 14: Angular distribution of kaon in the $^{12}C(e,e'K^+)^{12}_\Lambda B$ reaction (taken from Ref. [5]).

However, for kaons produced in the forward direction the probability of bound $^{12}_{\Lambda}B^{*}$ population or the Λ sticking probability, which is equal to the ratio of the corresponding differential cross sections, is quite high and for zero angle amounts: 0.36/1.47 = 0.24. We assume that in the angular range from 0° to 15° the quasi-free produced kaons are distributed uniformly. In such a condition, the average cross section of the $^{12}C(e,e'K^{+})^{12}_{\Lambda}B^{*}$ reaction is: $d\sigma / d\Omega(\gamma + {}^{12}C \rightarrow {}^{12}_{\Lambda}B^{*} + K^{+}) \cong$ *170 nb/sr* (agreed reasonably well with the results from Hall C experiments) and the average probability of $^{12}_{\Lambda}B^{*}$ population, triggered by kaons detected in the 0° to 15° angular range, is equal to the ratio 0.17/1.47 ≅ 0.11. Consequently, in the same conditions the average cross section of the $^{7}Li(e,e'K^{+})^{7}_{\Lambda}He^{*}$ reaction is: $d\sigma / d\Omega(\gamma + {}^{7}Li \rightarrow {}^{7}_{\Lambda}He^{*} + K^{+}) \cong$ *76.5 nb/sr*. These cross sections can be used to estimate yields of directly produced $^{12}_{\Lambda}B^{*}$ and $^{7}_{\Lambda}He^{*}$ hypernuclei in coincidence with forward produced kaons detected in HKS.

4.2 Indirect production mechanism

On the other hand, it is known from old emulsion experiments [1] that various hypernuclei, including proton or neutron rich ones, can be produced as hyperfragments by K^{-} induced reactions (see previous Table 2). Formation probabilities of $^{4}_{\Lambda}H$ hypernuclei in the K^{-} absorption at rest on ^{4}He, ^{7}Li, ^{9}Be, ^{12}C, ^{16}O, and ^{40}Ca targets have been measured with the aid of the characteristic π^{-} (133 MeV/c) from the two-body decay of $^{4}_{\Lambda}H$, ($^{4}_{\Lambda}H \rightarrow {}^{4}He + \pi^{-}$), at KEK [36] as well. The production rates $^{4}_{\Lambda}H$ obtained by the KEK group [36] and by the European K^{-} Collaboration [1] are shown in Table 5. Similarly, the rates of production of $^{3}_{\Lambda}H$ and $^{5}_{\Lambda}He$ by stopping K^{-} mesons have been deduced [1] and are given in Table 6.

Table 5: Comparison of $^{4}_{\Lambda}H$ production rates by stopping K^{-} mesons.

KEK (Tokyo)		European K^{-} Collaboration	
Target	Rate ($\times 10^{-3}$)	Target	Rate ($\times 10^{-3}$)
^{7}Li	30		
^{9}Be	15.7		
^{12}C	10.0	C, N, O	7.3
^{16}O	4.7		
^{40}Ca	≤ 2.7	Ag, Br	2.4

Table 6: Production rates of $^{3}_{\Lambda}H$ and $^{5}_{\Lambda}He$ measured by the European K^{-} collaboration.

Target	$^{3}_{\Lambda}H$ rate ($\times 10^{-3}$)	$^{5}_{\Lambda}He$ ($\times 10^{-3}$)
C, N, O	1.62	21.6
Ag, Br	0.54	1.4

It is to be noticed that the ${}^{4}_{\Lambda}H/{}^{3}_{\Lambda}H$ production ratio is ≈ 5 for both light and heavy targets. The large drop in ${}^{5}_{\Lambda}He$ production in going from light to heavy targets is explained by the strong inhibtion of helium emission due to the high Coulomb barrier presented by silver and bromine nuclei.

From observations of neutral hyperon emission it has been shown that the overall hypernuclear production rates by stopping K^- mesons are 8 ± 2% from C, N, O and 58 ± 15% from Ag, Br.

The two body reactions for K^- absorption at rest, which produce strangeness (which finally results in a Λ hyperon) in the nucleus, are listed in Table 7.

Table 7: Two body reactions that produce strangeness (Λ hyperon) by K^- absorption at rest.

$K^- + p \rightarrow \Lambda + \pi^0$	$K^- + n \rightarrow \Lambda + \pi^-$
$K^- + p \rightarrow \Sigma^- + \pi^+$	$K^- + n \rightarrow \Sigma^- + \pi^0$
$K^- + p \rightarrow \Sigma^0 + \pi^0$	$K^- + n \rightarrow \Sigma^0 + \pi^-$
$K^- + p \rightarrow \Sigma^+ + \pi^-$	

The observed formation probabilities of hyperfragments per stopped K^- could be explained by a model in which a quasi-free produced Λ is trapped in the nucleus and forms a "Λ compound nucleus", which may decay into a hyperfragment such as ${}^{4}_{\Lambda}H$. In this model, which was proposed by Tamura et al. [37], the ${}^{4}_{\Lambda}H$ formation probabilities per produced Λ can be expressed in terms of three physical factors as:

$$P({}^{4}_{\Lambda}H) = \int P_{\Lambda}(E_{\Lambda}) F_C(E_{\Lambda}) D_C({}^{4}_{\Lambda}H, E_X) dE_{\Lambda} \ ,$$

where, $P(E_\Lambda)$ represents the energy distribution of produced Λ. $F_C(E_\Lambda)$ stands for the formation probability of a Λ compound nucleus, when a Λ with a kinetic energy E_Λ is produced. $D_C({}^{4}_{\Lambda}H, E_X)$ is the probability of forming ${}^{4}_{\Lambda}H$ from the Λ compound nucleus with excitation energy E_X. The calculated values in case of stopped K^- are shown in Fig. 15. According to this model, formation probabilities of ${}^{4}_{\Lambda}H$ hyperfragments are higher for higher energy Λ hyperons. The momentum transferred to the produced Λ hyperon with K^- at rest is about 250 MeV/c. Therefore, one can expect that about the same or even more abundant hyperfragments must be produced in the electromagnetic production of a Λ hyperon, where the momentum transfer to the Λ hyperon is in the range of 250-450 MeV/c for photons in the energy range of 1-2 GeV.

The formation probability of ${}^{4}_{\Lambda}H$ from K^- absorption at rest on light nuclear targets was also investigated by employing anti-symmetrized molecular dynamics (AMD) combined with multi-step binary statistical decay [38]. The calculated hyperfragment isotope distribution of a ^{12}C target is shown in Fig. 16. The total probability of *excited* hyperfragment formation amounts to about 29%. Mass distribution of $A \leq 10$ hyperfragments produced in AMD is about one-third of the total yield of the

hyperfragments and the rest is the contribution of hyperon compound nuclei with mass number A = 11 and 12. Calculated result shows good agreement with the data of ${}^{4}_{\Lambda}H$ formation (~ 1%).

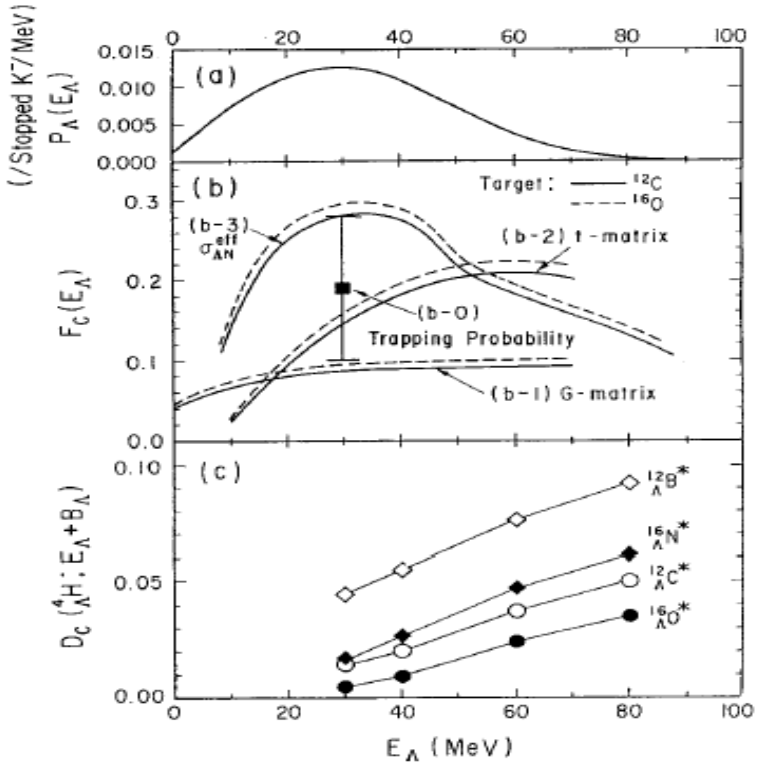

Figure 15: (a) The calculated energy distribution of Λ produced from K^- absorption at rest. (b) The formation probabilities of the Λ compound nucleus on C and O targets, $F_c(E_\Lambda)$, estimated in four different ways, from the experimental hyperon trapping probability (b-0), from the imaginary part of the Λ potential calculated by the G-matrix (b-1) and by the t-matrix (b-2), and estimated by Yazaki from the ΛN cross section with the Pauli suppression effect (b-3). (c) The fragmentation probabilities of ${}^{4}_{\Lambda}H$ from the Λ compound nucleus, D_C (${}^{4}_{\Lambda}H$, $E_X = E_\Lambda + B_\Lambda$) calculated for ${}^{12}_{\Lambda}C^*$, ${}^{12}_{\Lambda}B^*$, ${}^{16}_{\Lambda}O^*$, and ${}^{16}_{\Lambda}N^*$ (taken from Ref. [37]).

These investigations demonstrate that as the target mass number decreases from ^{16}O, ^{12}C to ^{9}Be, the main formation mechanism varies from statistical decay, followed by dynamical fragmentation, to direct formation in the nuclear environment. As a result different excited parent hyperfragments are produced. To clarify the formation mechanism of ${}^{4}_{\Lambda}H$, it is worthwhile, following Nara [38] to examine the parent hyperfragment distribution of ${}^{4}_{\Lambda}H$ in the statistical decay. In Fig. 17, we show the parent hyperfragment distribution of ${}^{4}_{\Lambda}H$. We note from Fig. 17 that the sources of ${}^{4}_{\Lambda}H$ are dynamically produced neutron rich hyperfragments, and their mass numbers widely range from 6 to 12. This result gives a slightly different picture from the *hyperon compound nucleus* proposed in Ref. [37]. In Tamura's work, the sources of ${}^{4}_{\Lambda}H$ are limited to hyperon compound nuclei with mass number 11 and 12, and they have estimated the formation probability of ${}^{4}_{\Lambda}H$ to be about 0.24~0.67%. In this work, although the contribution from these hyperon compound nuclei amounts to about 0.6%, it is found that hyperfragments with A ≤ 10 make non negligible contributions to the formation rates of ${}^{4}_{\Lambda}H$ (~0.5%), and their sum becomes the total yield (~1%). Thus the dynamical fragmentation or nucleon emission in

the primary stage due to multi-step processes is indispensable for quantitative arguments, which means that due to this mechanism various exotic hypernuclei can be produced as hyperfragments that are impossible to produce by direct population.

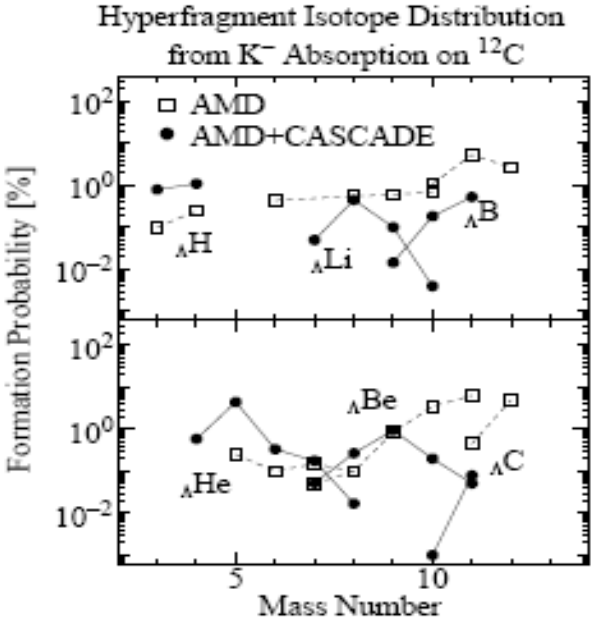

Figure 16: Hyperfragment isotope distribution from *K*⁻ absorption at rest on ^{12}C (from [38]). Boxes are the results of AMD calculation and black circles are the results after the multi-step statistical decay calculation.

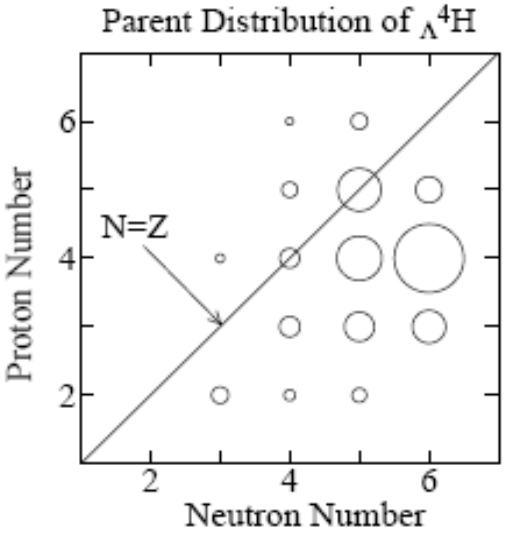

Figure 17: Parent hyperfragment distribution of $^{4}{}_{\Lambda}H$ from *K*⁻ absorption at rest on ^{12}C. The area of the circle is proportional to the probability from that hyperfragment (from [38]).

The kinematics of strangeness production processes in case of photon interactions (Table 8) are very similar to K^- induced reactions at rest, especially for photons in the 2 GeV energy range.

Table 8: Two body reactions that photon produce strangeness (Λ hyperon).

1	$\gamma + p \rightarrow \Lambda + K^+$	4	$\gamma + n \rightarrow \Lambda + K^0$
2	$\gamma + p \rightarrow \Sigma^0 + K^+$	5	$\gamma + n \rightarrow \Sigma^- + K^+$
3	$\gamma + p \rightarrow \Sigma^+ + K^0$	6	$\gamma + n \rightarrow \Sigma^0 + K^0$

All these 6 reactions are potential sources of the hyperfragment formation. The hyperfragment formation cross section in case of K^- photo-production can be expressed as:

$$d\sigma(\gamma + A \rightarrow hyperfragment + K^+ + X)/d\Omega = A^{0.8} \times d\sigma(\gamma + N \rightarrow \Lambda(\Sigma) + K^+)/d\Omega \times \varepsilon_\Lambda \times \varepsilon_{hyp}^i ,$$

where $d\sigma(\gamma + N \rightarrow \Lambda(\Sigma) + K^+)/d\Omega$ is the K^+ elementary photo-production cross section from nucleon and is equal to the sum of the cross sections of 1, 2 and 5 reactions in Table 8, ε_Λ is the Λ "sticking probability", and ε_{hyp}^i is the i-th hyperfragment formation weight. Here, for crude estimation, we assume $d\sigma(0^o, \gamma + N \rightarrow \Lambda(\Sigma) + K^+)/d\Omega \approx 1$ $\mu b/sr$, with $\varepsilon_\Lambda = 0.20$, and for ε_{hyp}^i we take the same weights which have been observed in emulsion (Table 2). For the K^+ photo-production cross section on ^{12}C we have:

$$d\sigma(0^\circ, \gamma + A \rightarrow K^+ + X)/d\Omega = A^{0.8} \times d\sigma(\gamma + N \rightarrow \Lambda(\Sigma) + K)/d\Omega \cong 4.2 \text{ μb/sr.}$$

The indirect hyperfragment photoproduction cross section on ^{12}C can be then defined as:

$$d\sigma(\gamma + A \rightarrow hyperfragment + K^+ + X)/d\Omega \cong 4.2 \times \varepsilon_\Lambda \times \varepsilon_{hyp}^i \text{ μb/sr.}$$

The resulting cross sections for the most probable hyperfragments are shown in Table 9. In addition to hyperfragment photo-production cross sections, relative weights of hyperfragments observed in emulsion, and available experimental [1] and theoretical [13] values for π^--decay widths are listed in Table 9 as well.

The Fig. 18 taken from Majling [39] shows clearly why the highly excited states of $^7{}_\Lambda He^*$ in which the "inner proton" is substituted by Λ ($Ps \rightarrow \Lambda$ transition) by means of $^7Li(\gamma,K^+)^7{}_\Lambda He^*$ reaction are the

source of hyperfragments ${}^{4}_{\Lambda}H$ and ${}^{6}_{\Lambda}H$. The thresholds for these decay channels are rather high, but large changes in the structure of these states prevent the neutron or Λ emission.

Table 9: Photo-production cross sections of light hyperfragments on ${}^{12}C$ target. In addition the relative weights and π^--decay widths are presented.

Hypernuclide	Photoproduction cross section (nb/sr)	Relative weight	π^--decay width $\Gamma_\pi / \Gamma_\Lambda$
${}^{3}_{\Lambda}H$	42	0.05	0.3
${}^{4}_{\Lambda}H$	33.6	0.04	0.5
${}^{5}_{\Lambda}He$	420	0.45	0.34
${}^{7}_{\Lambda}Li$	50.4	0.056	0.304
${}^{8}_{\Lambda}Li$	165.5	0.197	0.368
${}^{8}_{\Lambda}Be$	14.3	0.017	0.149
${}^{9}_{\Lambda}Be$	46.2	0.055	0.172
${}^{10}_{\Lambda}B$	2.1	0.0025	0.215
${}^{11}_{\Lambda}B$	15.1	0.018	0.213
${}^{12}_{\Lambda}B$ direct production	170	0.03	0.286

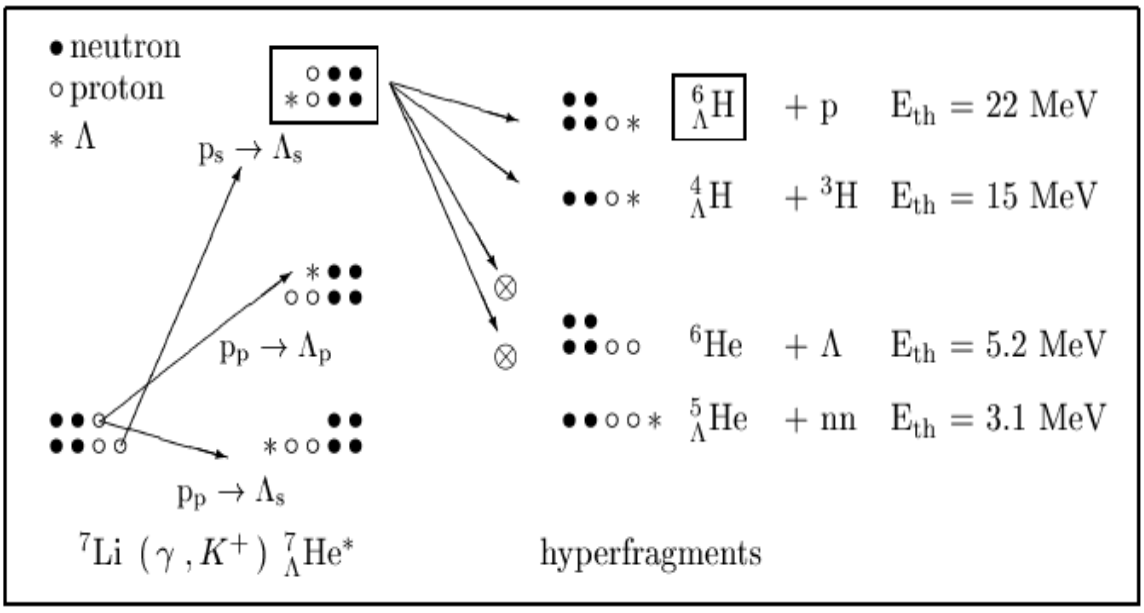

Figure 18: Different decay channels of excited ${}^{7}_{\Lambda}He^{*}$ hypernucleus (taken from [39]).

The probability of a compound residual hot hypernuclear formation at the end of pre-equilibrium phase of high-energy photo-nuclear reactions was calculated recently [40] with a time dependent Monte Carlo Multi-collisional Cascade (MCMC) approach. The obtained results for the probabilities (Fig.

19), mass and charge distributions (Fig. 20) of the formed hot hypernucleus, demonstrate that the γ-nucleus interactions in the 1 GeV energy region is a rich source of Λ hyperfragments.

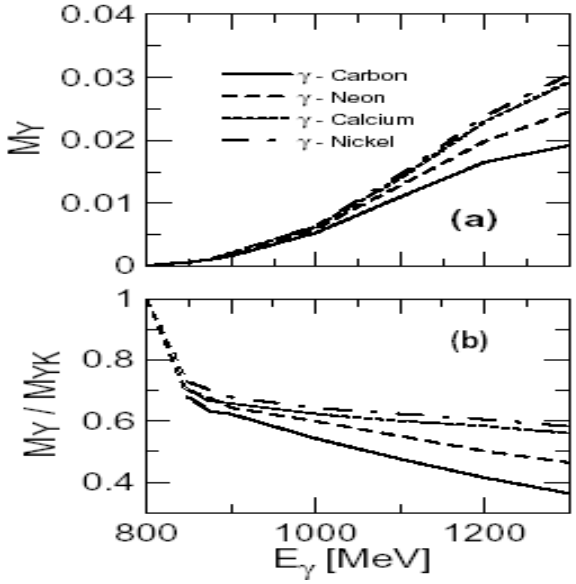

Figure 19: Hypernucleus multiplicity (a) and M_Y/M_{YK+} ratio (b) as functions of incident photon energy for $^{12}C(\gamma, K^+)$ (solid lines), $^{20}Ne(\gamma, K^+)$ (dashed lines), $^{40}Ca(\gamma, K^+)$ (dotted lines), and $^{58}Ni(\gamma, K^+)$ (dot-dashed lines) reactions (from [40]). In (b) the short dashed lines linking the curves to the vertical axis do not result from calculation (see [40] for more details).

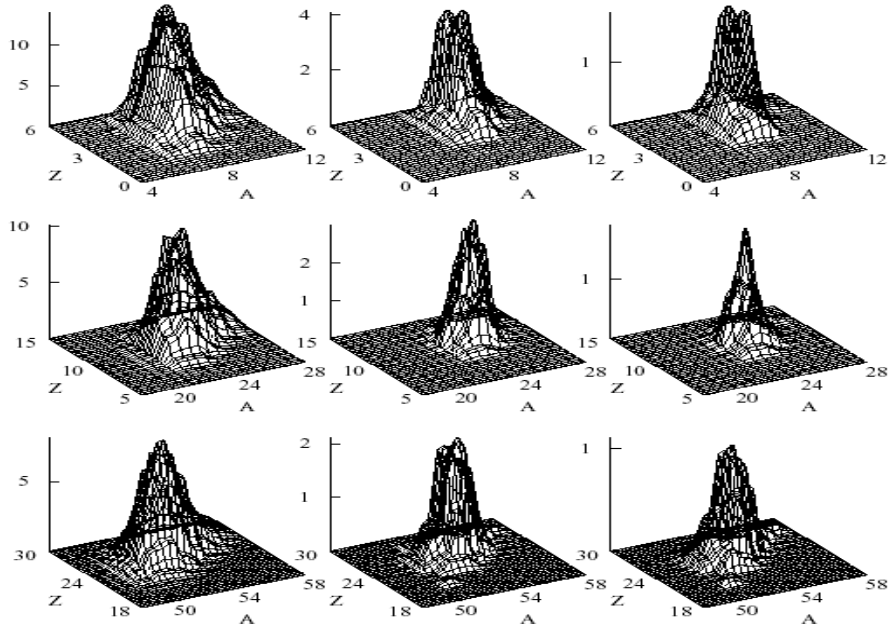

Figure 20: Residual nucleus mass and charge distributions for γ-Carbon (first row), γ-Aluminum (second row), and γ-Nickel (last row) at 1.2 GeV incident photon energy [40]. In the first column results for events inclusive in meson production (either a pion or a kaon) are displayed. In the middle column

distributions of mass and charge considering only events with hyperon production in the primary interaction, however disregarding if the hyperon is kept bound or not, are shown. The last column is the distribution for events having a bound hyperon formed at the end of pre-equilibrium phase of the residual hot nucleus. The results in columns are multiplied, respectively, by 10^2, 2 x10^4, and 2 x 10^4.

The large momentum transfer of the (π^+, K^+) reaction, which has been intensively used for production of hypernuclel recently, makes the quasi-free (QF) process dominant in the highly excited region where a Λ is knocked out from a nucleus. Some fraction of Λ produced in this region, however, trapped in the nucleus to form a hypernucleus through a finite probability of the ΛN scattering in nuclei. By using (π^+, K^+) reaction on ^{12}C target it was experimentally demonstrated that light Λ hypernuclei are produced followed after ΛN scattering [41]. The obtained probabilities (~20% of QF Λ) for the hypernuclear formation, suggests that there is a rich source of Λ hypernuclei in the QF regions of the (π^+, K^+), stopped K^-, and (γ, K^+) reactions.

From these discussions we can conclude that K^+ detection in the γ-nuclear interactions can serve as an effective (~20%) tag for different hypernuclear productions, which can be used to perform hypernuclear studies, e.g. weak decay π^- spectroscopy of hypernuclei with electron beam.

5. Proposed Project

We propose a new experiment for investigation of Λ hypernuclei by using the pionic decay. The project aims to determine precisely the binding energies of light hypernuclei, investigate production of exotic hypernuclei, and study impurity nuclear physics and the medium effect of baryons.

These investigations will fully utilize the unique features of the CEBAF beam and the newly developed experimental equipment (the HKS and Enge systems) dedicated for hypernuclear physics, as listed in the introduction chapter. These features make possible for the highest ever resolution and precision in using decay π^- to access the rich physics that hypernuclei can offer. All the equipment exists and is ready. Two production targets ^{12}C and ^{7}Li will be used to produce wide range of hypernuclei at ground states (or possible low lying states). We propose to run it in Hall C but it can be run in Hall A also by moving all the equipment to Hall A.

5.1 Experimental setup and expected performance

The experimental setup is rather similar to the HKS experiment (E01-011) completed in 2005. However, the beam lines will use the same design as that for the next experiment HKS-HES (E05-115) for easier beam handling. The general layout of the proposed experiment is illustrated in Fig. 21.

The incident electron beam hits the target which will be moved upstream by ~15 cm with respect to the HKS normal target position to avoid decay pions experiencing the Splitter field. The 25 mg/cm^2 target will be tilted ~60^o (30^o incline to the beam). Thus, the effective target thickness will be about 50mg/cm^2. Positively charged kaons will be detected by HKS as usual. The precisely measured kaons with high momentum resolution provide efficient tagging in coincidence of decayed pions to exclude nuclear pions as well as the precisely reconstructed production time. The produced hypernuclei predominantly at forward direction are stopped in the target and decays after some 200 ps inside of the target. Decay pions have a discrete momentum lying in the range ≤133 MeV/c and exit the target. For the measurements of momentum and outgoing angles of these monochromatic pions, we will use the existing Enge spectrometer as the high-resolution pion spectrometer ($H\pi S$). The central optical axis of

Enge will be normal to the target plane so that the target straggling energy loss uncertainty of the decayed pions will be minimized.

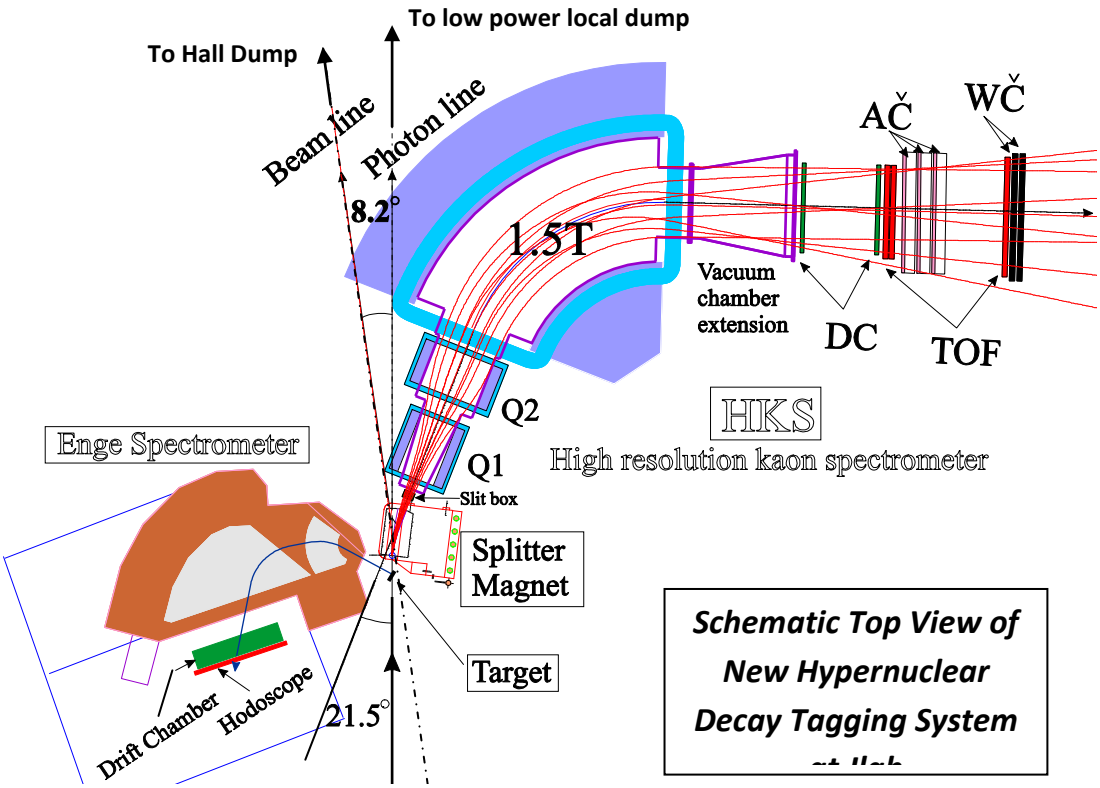

Figure 21: Schematic top view of the new hypernuclear decay tagging system.

5.2 High-resolution pion spectrometer - *HπS*

For the measurement of decay pions in the 100 MeV/c regions, we will use the existing Enge Split-Pole spectrometer and its detector package that were used in both the HNSS/E89-009 and HKS/E01-011 experiments to detect low energy scattered electrons. A new additional Lucite Čerenkov counter can be used in anti-coincidence with the Enge timing hodoscope to veto electrons ($\beta = 1$) from the trigger of pions ($\beta \approx 0.72$).

A Monte-Carlo simulation was carried out to determine its acceptance and resolution and to optimize the spectrometer setup. The optical features and acceptance of the spectrometer are studied by the RAYTRACE simulation. The optical model of Enge spectrometer used in the RAYTRACE simulation was based upon the data card from the HNSS/E89-009 experiment, in which the parameters have been tuned to reproduce the realistic acceptance of the experimental data. A GEANT Monte-Carlo simulation was used to study effects of multiple scattering and energy loss from target, as well as detector widows and materials. The expected parameters are summarized in Table 10.

Table 10: Parameters of the *HπS* spectrometer

Configuration	Enge Split-Pole spectrometer and detector package
Central momentum	115 MeV/c
Momentum acceptance	± 40%
Momentum resolution (r.m.s.)	10^{-4} without multiple scattering
Momentum resolution (r.m.s.)	4.9×10^{-4} with multiple scattering
Dispersion	1.28 cm/%
Time-zero precision	< 100 ps
Pion detection angle	~60 degree relative to the incident beam
Flight path length	309 c m
π^- survival rate	~ 60%
Solid angle	~20 msr
Total efficiency of the detector package	~80%

5.3 Momentum loss in the target

The energy resolution and the precision in determining the binding energies of hypernuclei are solely determined by the resolution and precision in analyzing the decayed pions. Due to ionization energy loss the monochromatic spectrum of decayed pions from a specific hypernuclear state is shifted as well as broadened. This is one of the two major sources contributed to the precision. Therefore the target thickness is selected to be thin enough to minimize target straggling effect to the decay pion spectra.

We have generated decay pion events and carried out a simulation study of decay pion spectra of hypernuclides by using the Monte Carlo method. The influence of the ionization energy loss has been calculated by using dedicated Monte Carlo code based on the individual collision method [42]. The dE/dx spectra of monochromatic pions (p = 115.8 MeV/c) from ${}^{12}_{\Lambda}B \rightarrow {}^{12}C + \pi^-$ decay randomly generated in the thickness of a 25 mg/cm^2 carbon target are shown in Fig. 22.

Fig. 22a shows that the average energy loss is about 40 keV which will introduce the binding energy shift and the energy broadening is also about 40 keV which contributes to the energy resolution. Fig. 22b shows the effect from the energy shift and broadening to the pion momentum. The corresponding momentum shift is about 100 keV/c while the contribution to the momentum reolusion id about 70 keV/c. These pions were further transported to the focal plane of the Enge spectrometer. With the position resolution achieved by the existing detector system and the multiple scattering from the existing detector materials, the momentum resolution of *HπS*(Enge) is about 4.9×10^{-4} rms. Fig. 22c shows the overall result from a combined simulation that includes target straggling and focal plane detection errors and multiple scatterings. The overall momentum resolution is σ = 92 keV/c, corresponding to a binding energy resolution of $\sigma \approx 55$ keV. These simulations have been confirmed

also by other independent GEANT simulation. Such energy resolution is capable to isolate structures separated by 120 keV or larger, such as the ground state doublet (1^- and 2^-) of $^{12}_{\Lambda}B$.

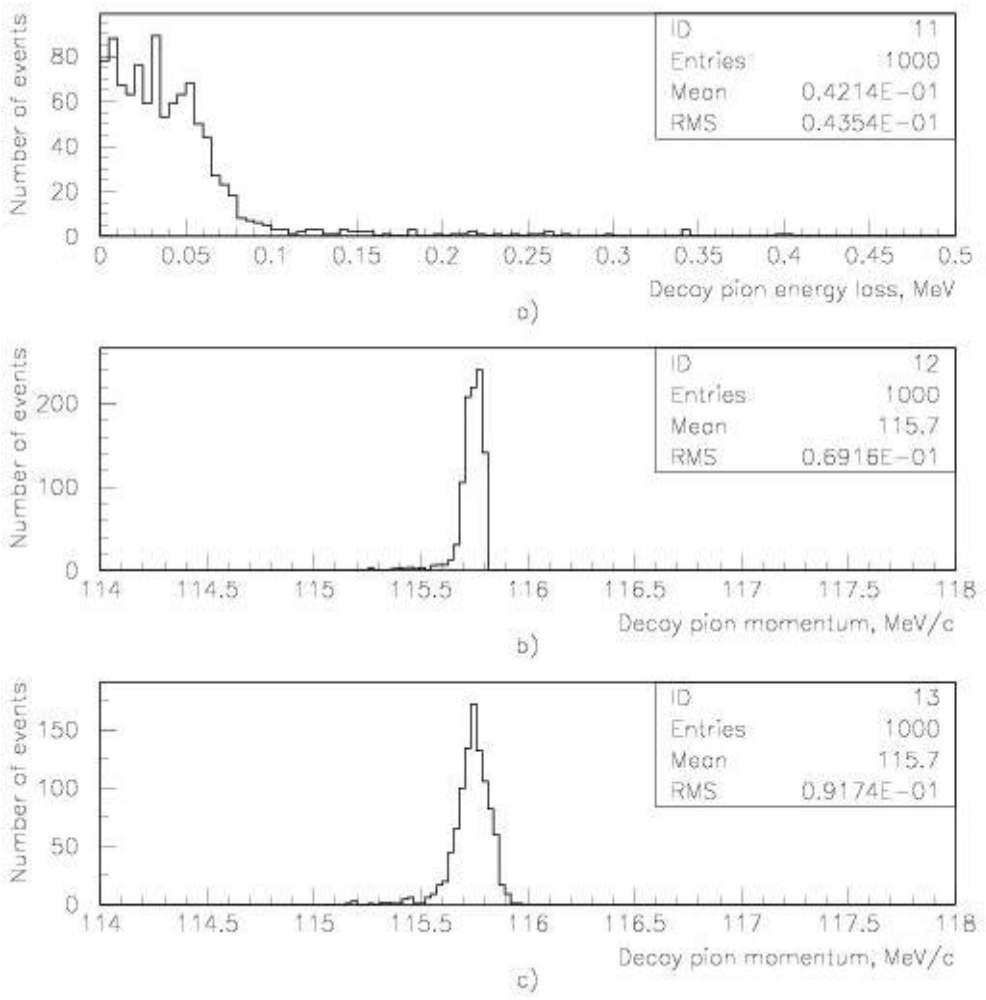

Figure 22: Simulated energy loss (a) and momentum (b) spectra for 115.8 MeV/c pions produced uniformly in the 25 mg/cm^2 carbon target; (c) is the momentum spectrum measured in the *HπS* with resolution $\sigma = 4.9 \times 10^{-4}$.

The binding energy determination precision ≤ ±10 keV will be achieved by two independent methods. The first method is a GEANT target energy loss simulation to extract the mean energy correction as a function of pion momentum. The second is the calibration using the monochromatic pions from decays of Λ produced by $\gamma p \rightarrow \Lambda K^+$ reaction. Water target can be used. The Doppler broadening to the pion momenta due to Λ recoil can be corrected by the kinematics reconstruction from the precise K^+ momentum and scattering angle reconstructions done by HKS. The mean of the "Λ" peak in terms of pion momentum will provide an absolute energy and momentum calibration in combination with the GEANT calculation of the target effect.

In addition, a δ scan by changing the Enge field setting can put the "Λ" peak at various momentum values across the focal plane. This in combination with Sieve Slit data will be used to calibrate the optics of *HπS*.

5.4 Expected yield of hypernuclei

The forward produced K^+ mesons detected in the HKS are a good trigger for hypernuclei production: about 3% of them are associated with "direct" and 20% with "indirect" production of hypernuclei. The remaining 77% of kaons are associated with quasi-free produced Λ particles, 64% of which decay through the $\Lambda \rightarrow \pi^- + p$ channel. The produced hypernuclei, besides light ($^3_\Lambda H$, $^4_\Lambda H$) ones, will stop in the target and decay after some 200ps with corresponding decay widths. The π^- decay widths for light hypernuclei ($A \leq 12$) lie in the range 0.15-0.5 (Table 11), e. g. the π^- decay width of the $^{12}_\Lambda B$ hypernucleus, which is produced directly through the $\gamma + ^{12}C \rightarrow ^{12}_\Lambda B + K^+$ reaction, is expected to be 0.286 [13]. Therefore, the π^- decay rate of $^{12}_\Lambda B$ from direct photo-production is expected to be:

$$R_{\pi^-}(^{12}_\Lambda B) = 0.03 \times 0.286 \times R_K = 0.0086 \times R_K ,$$

where R_K is the kaon single rate. For the "indirectly" produced hyperfragments, the corresponding π^- decay rates are determined as:

$$R^i_{\pi^-} = 0.2 \times \varepsilon^i_{hyp} \times \Gamma^i_{\pi^-} \times R_K ,$$

where ε^i_{hyp} and $\Gamma^i_{\pi^-}$ are population weights of hypernuclear isotopes and their π^- decay widths, respectively (see Table 11). The π^- decay rate from the quasi-free produced Λ particles is determined as:

$$R_{\pi^-}(\Lambda_{q.f.}) = 0.77 \times 0.64 \times R_K \cong 0.5 \times R_K .$$

Taking into account direct and indirect production mechanisms we can estimate the hyperfragment yields. The total π^- rate detected in the *HπS* in coincidence with HKS is then:

$$R_{\pi^-}(H\pi S) = [\Delta\Omega/(4\times\pi)] \times \varepsilon_s \times \varepsilon^t_{eff} \times [R_{\pi^-}(^{12}_\Lambda B) + \sum_i R^i_{\pi^-} + R_\pi(\Lambda_{q.f.})] \times R_K ,$$

where $\Delta\Omega \approx 20$ *msr*, $\varepsilon_s \approx 0.6$, and $\varepsilon^t_{eff} \approx 0.8$ are the solid angular acceptance of *HπS* (Enge), survival rate of the decayed pions, and total efficiency of the Enge spectrometer detector package, respectively. Thus alone the decay pion detection efficiency in *HπS* is:

$$\varepsilon^{H\pi S}_{eff} = [\Delta\Omega/(4\times\pi)] \times \varepsilon_s \times \varepsilon^t_{eff} = 0.88 \times 10^{-3} .$$

The hypernuclear decay pion "daily" yields detected in *HπS* in the case of 150 Hz K^+ rate in HKS for ^{12}C target (i.e. scaled from the E01-011 condition: 45μA beam and 50mg/cm^2 target) are listed in Table 11. Only the ground state of possible hypernuclei is listed as references. For $^{12}_\Lambda B$ we consider only the direct production mechanism. In Table 11, the relative weights evaluated from emulsion data and the

decay pion yield from quasi-free produced Λ are listed as well. The corresponding discrete pion spectrum detected in *HπS* without background is illustrated in Fig. 23.

Table 11: Hypernuclei (ground states only) and decay pion "daily" yields for ^{12}C target (t_{eff} = 50 mg/cm^2) with 150 Hz K^+ rate in HKS (Beam current: 45μA).

Hypernuclei	Relative yield	π^--decay width $\Gamma_\pi/\Gamma_\Lambda$	Decay π^-"daily" yield detected in *HπS*	π^- Mom. (MeV/c)
q. f. Λ	0.77	0.64	5.6×10^3	spread
$^{9}_{\Lambda}Be$	0.015	0.17	29	95.96
$^{8}_{\Lambda}Be$	0.01	0.15	17	97.17
$^{5}_{\Lambda}He$	0.09	0.34	349	99.14
$^{11}_{\Lambda}B$	0.01	0.21	24	105.9
$^{7}_{\Lambda}Li$	0.015	0.30	51	107.9
$^{3}_{\Lambda}H$	0.01	0.30	34	114.3
$^{12}_{\Lambda}B$ - direct production	0.03	0.29	100	115.8
$^{8}_{\Lambda}Li$	0.04	0.37	169	124.1
$^{4}_{\Lambda}H$	0.01	0.50	57	132.9

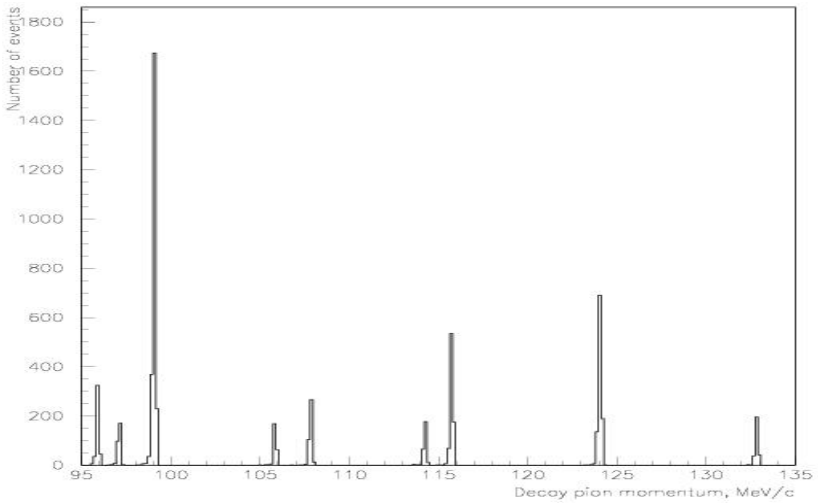

Figure 23: Demonstration of π^- decay spectra from different hyperfragments (*gs*) with their relative weights evaluated from emulsion data; the target straggling is taken into account with target thickness of 25 mg/cm^2; the *HπS* resolution is $\sigma = 4.9 \times 10^{-4}$; and total number of events is 6000. No background is included (see later discussion)

We must mention that the expected spectrum of hyperfragments will be different than the demonstrated one (see the last column of Fig. 20). This is connected to the fact that for identification purposes, in emulsion, events decaying into more than two particles were mainly considered. Thus there is selectivity for emulsion on the decay modes. In this experiment only the two body decay events

will be detected. So the weights relative between the presented hypernuclei in Table 11 may be different in the actual spectroscopy from this experiment. So the presented hyperfragment spectrum only demonstrates the sensitivity of the proposed experiment and its expected resolution. Background was not included and will be discussed next. In addition, no low lying states were considered in this illustration since their yields depend on the production cross sections and decay widths, thus varying case by case.

5.5 Background

In the real experimental conditions, we will have three sources of background:

a) The promptly produced pions;
b) The decay pions from quasi-free produced Λ particles;
c) Accidentals.

The promptly produced pions will be excluded by using coincidence requirement with the produced kaons. With tight 2ns coincidence window gate, all of them will be eliminated. However, this way does not allow excluding background from the decay of quasi-free produced Λ particles or from accidental coincidences. We carried out simulation studies of the decay pion spectrum from quasi-free produced Λ particles by using the Monte Carlo method. We took into account the following factors for the final distribution:

1. The momentum distribution of the "quasi-free" produced Λ particles. We assume isotropic production for the C.M. angular distribution with Gaussian momentum distribution (mean value is 200 MeV/c and σ = 100 MeV/c);
2. The full π^- spectrum are: 87% pions from "quasi-free" produced Λ particles, and 13% monochromatic pions from different hyperfragments with their relative weights, listed in the second column of Table 11;
3. The momentum resolution of the pion spectrometer; and
4. The ionization energy loss.

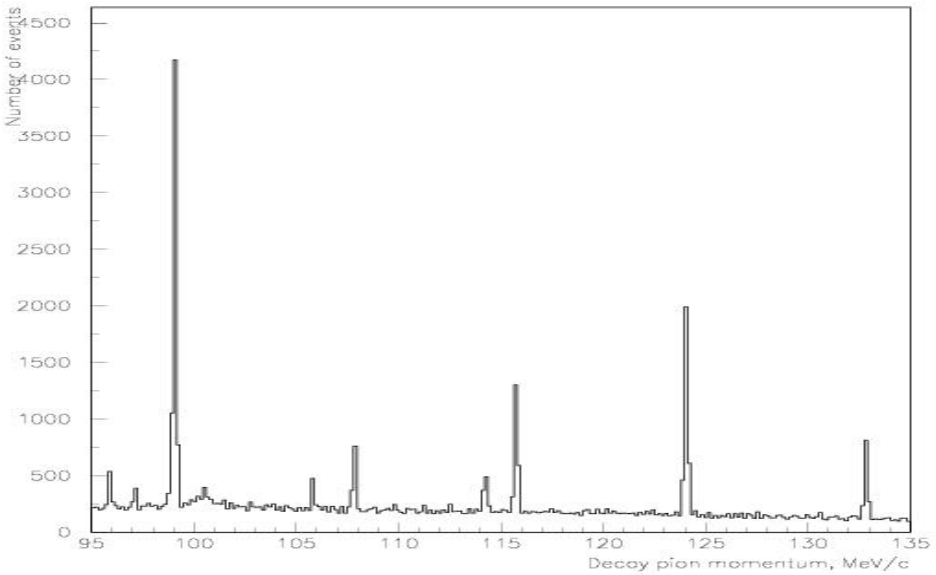

Figure 24: Simulated spectrum of the decayed pions (87% from quasi-free produced Λ particles, and 13% from different hyperfragments with their relative weights). Target thickness is 25 mg/cm^2; momentum resolution of $H\pi S$ is σ=4.9×10^{-4}; and total number of events is 10^5.

The simulated spectrum including background with total of 10^5 pions produced in the 25 mg/cm^2 carbon target (with energy loss) and measured in the $H\pi S$ with resolution $\sigma = 4.9 \times 10^{-4}$ is shown in Fig. 24. It demonstrates that monochromatic pion spectra are clearly seen even with a huge amount of quasi-free background.

5.6 Accidentals

The typical rate of kaons detected in HKS is about 200 count/s (with 30 μA beam current and a 100 mg/cm^2 C target). The simulations from the Radiation Control group (Pavel Degtiarenko) for a 30% momentum acceptance and 30 msr solid angle for the pion spectrometer show a 1.4×10^3/s rate for negatively charged pions. By scaling to the requested maximum luminosity (100 μA beam current and a 50 mg/cm^2 C target) and the realistic Enge acceptance, this implies an accidental rate of 1.65×10^{-3}/s within a 2 ns coincidence time window. This contribution to the overall background in the pion momentum spectrum is ~2.4%, thus negligible in comparison to the quasi free background.

5.7 Online trigger rate

The HKS online single rate with standard kaon trigger will be increased by a factor of 1.67 due to the increase of luminosity. However, the Enge spectrometer is at 60 degrees to detect the decay pions in low momentum. The electron single rate will be dramatically decreased in comparison to E01-011 (HKS) experiment. With the addition of a threshold Čerenkov detector with an online rejection rate of 90%, the online Enge single rate will be dominated by promptly produced pions and the online trigger rate is dominated by accidental coincidences. The anticipated trigger rate is in the order of ~50-100 Hz.

5.8 Requested beam time, energy, and current

In the proposed experiment we intend to measure precisely the decay π^- spectra of light hypernuclei which are produced in electron nuclear interactions "directly" or "indirectly". Our main goal is to measure precisely the binding energies and lifetimes of hypernuclei produced directly or indirectly through hyperfragments (see example in Table 11 from ^{12}C target), which will show up in $H\pi S$ with sufficient statistical significance. We propose to use two production targets: ^{7}Li, and ^{12}C. It is expected that by decreasing the target mass, the production rates of $^{3}_{\Lambda}H$ and $^{4}_{\Lambda}H$ are increased. The production of $^{3}_{\Lambda}H$ and $^{4}_{\Lambda}H$ from both targets provides important cross check on consistency as well as references to the other hypernuclei. Also, from the ^{7}Li target we are expecting formation of exotic $^{6}_{\Lambda}H$ hyperfragment (see Fig. 18 and reference [39]).

We request 20 days of beam time for each production target. The requested data taking hours were calculated so that at least about 1000 counts for $^{3}_{\Lambda}H$ and $^{4}_{\Lambda}H$ each can be accumulated. Thus, the total required data acquisition time is 40 days. In addition, we require 2 weeks commissioning to setup and calibrate the two spectrometer systems.

The requested electron beam energy is in the range of 1.8-2.4 GeV. The effective production thickness of our target will be 50 mg/cm^2. The nominal beam current will be 60 μA which is the same luminosity taken by the HKS (E01-011) experiment (30 μA beam with 50 mg/cm^2 target). However, if

the accidental rate between π^- and K^+ is as we expected and data acquisition rate allows high rate, we may request up to the maximum, 100μA, in order to explore the hypernuclei with small yield.

6 Summary

High resolution decay pion spectroscopy for light hypernuclei is proposed. The main goal of the present proposal postulates that we use the high resolution kaon spectrometer (HKS) and high resolution Enge spectrometer as the pion spectrometer (*HπS*) to carry out decay pion spectroscopy from two light production targets ^{7}Li, and ^{12}C and measure precisely binding energies and lifetimes of produced light hypernuclei or hyperfragments at about 2 GeV electron beam. The proposal is based on the successful operation of these magnetic spectrometers in Hall C at JLab and will fully take the advantage of the CEBAF high-quality high-power CW electron beam.

The physics subjects which can be investigated by means of decay pion spectroscopy include: (1) YN interactions, (2) study of exotic hypernuclei, and (3) impurity nuclear physics. This will be the most precise experiment for measuring of binding energies of light hypernuclei.

The proposed experimental program is a unique one and is not duplicated by any in the currently approved or planned experimental programs and can be performed only with the CEABF electron beam.

References

1. D. H. Davis, "50 years of hypernuclear physics, I. The early experiments", Nucl. Phys. A 754 (2005) 3c.
2. R. H. Dalitz, "50 years of hypernuclear physics, II. The later years", Nucl. Phys. A 754 (2005) 14c.
3. G. Keyes, M. Derrick, T. Fields et al., "Properties of the hypertriton", Phys. Rev. D1, 66 (1970).
4. O. Hashimoto, L. Tang, J. Reinhold (spokespersons), "Spectroscopic study of Λ hypernuclei up to medium-heavy mass region through the in the (e, e'K^+) reaction", JLAB Experiment E01-011.
5. O. Hashimoto, S. Nakamura, L. Tang, J. Reinhold "Spectroscopic investigation of Λ hypernuclei in the wide mass region using the (e, e'K^+) reaction", JLAB Experiment E05-115.
6. J-PARC Strangeness Nuclear Physics Group, Letter of intent for "New generation spectroscopy of hadron many body systems with strangeness S=-2 and -1", Letter of intent for nuclear and particle physics experiments at the J-PARC, J-PARC 03-6.
7. O. Hashimoto, H. Tamura, "Spectroscopy of Λ hypernuclei", Progress in Particle and Nuclear Physics 57 (2006) 564-653.
8. H. Tamura et al., "Gamma ray spectroscopy of light hypernuclei", J-PARC 50-GeV PS proposal E13 (2006), http://j-parc.jp/NuclPart/pac_0606/pdf/p13-Tamura.pdf
9. Th. Rijken, Y. Yamamoto, "Recent soft-core baryon-baryon interactions", Nucl. Phys. A 754 (2005) 27c.
10. A. Nogga, "Faddeev-Yakubovski calculations for A=4 hypernuclear system", Nucl. Phys. A 754 (2005) 36c.
11. Y. Fujimura, C. Nakamoto, M. Kohno, Y. Suzuki, K. Miyagawa, "Interactions between octet baryons and their applications to light hypernuclei", Nucl. Phys. A 754 (2005) 43c.
12. H. Nemura, Y. Akaishi, and Y. Suzuki, "Ab initio Approach to s-Shell Hypernuclei $^{3}_{\Lambda}H$, $^{4}_{\Lambda}H$, $^{4}_{\Lambda}He$, and $^{5}_{\Lambda}He$ with a $\Lambda N - \Sigma N$ Interaction", Phys. Rev. Lett. 89 (2002) 142504-1.

13. T. Motoba and K. Itonaga, “Pi-Mesonic Weak Decay Rates of Light-to-Heavy Hypernuclei”, Progress of Theoretical Physics Supplement, No. 117, (1994) p.477.
14. T. Motoba, “Mesonic weak decay of strange nuclear systems”, Proceedings of the IV International Symposium on Weak and Electromagnetic Interactions in Nuclei, 12-16 June 1995, Osaka, Japan. Edited by H. Ejiri, T. Kishimoto and T. Sato, World Scientific, 1995, p.504.
15. E. Hiyama, M. Kamimura, T. Motoba, T. Yamada, Y. Yamamoto, “Three-body model study of *A* = 6-7 hypernuclei: Halo and skin structures”, Phys. Rev. C53, (1996) 2075.
16. L. Majling et al., “Superheavy Hydrogen Hypernucleus $^{6}_{\Lambda}H$”, AIP Conference Proceedings Volume 831, (2006)p. 493.
17. P. K. Saha, T. Fukuda and H. Noumi, “Neutron-reach hypernuclei by the double-charge exchange reaction”, Letter of Intent for Nuclear and Particle Physics experiments at the J-PARC (LOI9), 2002.
18. E. Hiyama, M. Kamimura, K. Miyazaki, T. Motoba, “γ-transitions in *A*=7 hypernuclei and a possible derivation of hypernuclear size”, Phys. Rev. C59 (1999)2351.
19. K. Tanida, H. Tamura, D. Abe et al., “Measurement of the B(E2) of $^{7}_{\Lambda}Li$ and Shrinkage of the Hypernuclear Size”, Phys. Rev. Lett. 86 (2001) 1982.
20. H. Tamura, “High resolution spectroscopy of Λ hypernuclei: present status and perspectives”, Nucl. Phys. A691 (2001) 86c. “Impurity nuclear physics: Hypernuclear γ spectroscopy and future plans for neutron-reach hypernuclei” The European Physical Journal A-Hadrons and Nuclei, V13 (2002) 181.
21. R. H. Dalitz and A. Gal “The formation of, and the γ-radiation from, the shell hypernuclei”, Ann. Phys. 116 (1978) 167.
22. J. Pniewski and M. Danysz, “A note on the $^{7}_{\Lambda}He$ hypergragments”, Phys. Lett. V. 1, n. 4 (1962) 142.
23. D. J. Millener, Nucl. Phys. A754 (2005) 48c.
24. E. Oset, et al, Prog. Theor. Phys. 117 (1994).
25. T. Motoba, K. Itonoga and H. Bando, Nucl. Phys. A489 (1988) 683.
26. H. Tamura, et al, Nucl Phys A754 (2005) 58c.
27. R. E. Chrien, et al, Phys. Rev C41 (1990) 1062.
28. M. Juric, G. Bohm, J. Klabuhn et al., “A new determination of the binding-energy values of the light hypernuclei (A ≤ 15)”, Nucl. Phys. B 52 (1973) 1.
29. P. Dluzewski et al., “On the binding energy of the $^{12}_{\lambda}$C(g.s.) hypernucleus”, Nucl. Phys. A484 (1988) 520.
30. T. Yamazaki et al., “New aspects and new tools in hypernuclear studies: experiments with a superconducting toroidal spectrometer” INS-Rep.-728 (1988).
31. H. Outa et al., “Lifetime measurement of $^{4}_{\Lambda}H$ hypernucleus”, INS-Rep.-914 (1992).
32. The FINUDA Collaboration, “FINUDA A DETECTOR FOR NUCLEAR PHYSICS AT DAΦNE, LNF-93/021 (1993).
33. F. X. Lee, T. Mart, C. Bennhold, H. Haberzettl, L. E. Wright, ”Quasifree Kaon Photoproduction on Nuclei”, arXiv: nucl-th/9907119.
34. H. Yamazaki et al., “The ^{12}C(γ, K^{+}) reaction in the threshold region”, Phys. Rev. C 52, R1157–R1160 (1995).
35. M. Sotona et al., Proceedings of Mesons and Light Nuclei ’98, (1998) 207.
36. H. Tamura, T. Yamazaki, R. S. Hayano et al., “Formation of $^{4}_{\Lambda}H$ hypernuclei from K^{-}absorption at rest on light nuclei”, Phys. Rev. C 40 (1989) R479.
37. H. Tamura, T. Yamazaki, M. Sano et al., “Compound-hypernucleus interpretation on $^{4}_{\Lambda}H$ formation probabilities in stopped- K^{-} absorption”, Phys. Rev. C 40 (1989) R483.
38. Y. Nara, A. Ohnishi and T. Harada, “Target mass dependence of $^{4}_{\Lambda}H$ formation mechanism from K^{-}absorption at rest”, *Phys. Lett.* 346 *(1995)* 217.

39. L. Majling, "Hypernuclei ${}^{6}_{\Lambda}H$ and ${}^{8}_{\Lambda}H$ could be identified – so what?", IX International Conference on Hypernuclear and Strange Particle Physics, October 10-14, 2006, Mainz, Germany.
40. M. Goncalves, E.C. de Oliveira, E.L. Medeiros, S. de Pina, and S.B. Duarte, **"**Hot Hypernucleus Formation in High-Energy Photonuclear Reactions", Brazilian Journal of Physics, vol. 34, no. 3A, September, 2004, 919.
41. S. Ajimura et al., "Λ Hypernuclei by Quasifree (π^+, K^+) Reaction on ${}^{12}C$", Nuclear Physics A577 (1994) 271c-276c.
42. K. A. Ispirian, A. T. Margarian, A. M. Zverev "A Monte Carlo method for calculation of the distribution of ionization losses"**,** Nucl. Instr. and Meth.117 (1974) 125.